2012

Admicellar Polymerization Of Calcium Carbonate And Its Performance In Drilling Fluids

Poh Lee Cheah
University of Mississippi

ADMICELLAR POLYMERIZATION OF CALCIUM CARBONATE AND ITS PERFORMANCE IN DRILLING FLUIDS

A Thesis

presented in partial requirements

for the degree of Master of Science

in the Department of Chemical Engineering

The University of Mississippi

by

POH LEE CHEAH

August 2012

ABSTRACT

Admicellar polymerization using sodium dodecylsulfate (SDS) template to form ultrafilm polystyrene on commercial calcium carbonate ($CaCO_3$) of various particle sizes was studied. Adsorption isotherms of SDS decrease after the critical micelle concentration (CMC) of SDS was observed. This is explained by the phase behavior of SDS with calcium ion. The solubility product constants (K_{sp}) for calcium dodecylsulfate ($Ca(DS)_2$) were calculated as $1.55x10^{-9}M^3$ at 30^oC and $8.58x10^{-9}M^3$ at 50^oC. At SDS concentrations above the CMC, precipitation of $Ca(DS)_2$ was governed by the critical ratio of calcium ion concentration bound onto anionic micelles which was 0.22 at 30^oC and 0.20 at 50^oC. It was estimated that precipitates of $Ca(DS)_2$ formed between 5.12 to $6.85x10^{-3}M$ SDS at 30^oC. Adsolubilization of styrene and partition coefficient (K_{adm}) data showed initial partitioning of styrene at the core and only at higher concentrations in the palisade layer. However, no observation of polystyrene ultrathin films was observed using Fourier Transform Infra-red (FTIR) or Tapping mode Atomic Force Microscopy (AFM). Nevertheless, application testing of low-polymer content admicellar polymerized $CaCO_3$ in drilling fluids showed increase in mud viscosity and yield point with improved fluid loss control.

DEDICATION

This thesis is dedicated to my family and friends in Malaysia who give the strength and courage during the time of stress and anxiety. Not to forget my advisor Dr John O' Haver, Dr Wasan Saphanuchart and Dr Chun Hwa See who helped and guided me through the hardships and problems of my work. Finally, I would like to thank all my friends and colleagues in Ole Miss for their support.

LIST OF ABBREVATIONS AND SYMBOLS

SDS	Sodium dodecylsulfate
$CaCO_3$	Calcium carbonate
AIBN	Azoisobutylnitrile
BET	Brunanauer-Emmett-Teller
pzc	Point of zero charge
CMC	Critical micelle concentration
FTIR	Fourier transform infra-red spectroscopy
AFM	Atomic force spectroscopy
$Ca(DS)_2$	Calcium dodecylsulfate
K_{adm}	Partition coefficient in admicelle
K_{sp}	Solubility product
PV	Plastic viscosity
YP	Yield point

ACKNOWLEDGEMENTS

I express my deepest appreciation to my advisor, Dr. John O'Haver and my committee member, Dr. Paul Scovazzo and Dr. Peter Sukanek. I would like to thank to the Chair of the department Dr. Clint Williford, my advisor and BCI Chemical Corp. Sdn. Bhd. for given me the funding and assistantship in my studies and research. I would like to thank Dr. Wasan Saphanuchart and Dr. Chun Hwa See for providing advice and guidance.

I would also like to thank Dr. Wei-Yin Chen and Chemistry Department of University of Mississippi for the help in some of the instruments in this thesis work.

Lastly, I would like to thank Tiffany Hester, Samuel Apetuje and Olugbenga Ojo for helping out in the lab and experiment work.

TABLE OF CONTENT

LIST OF TABLES

LIST OF FIGURES

1.0 INTRODUCTION

1.1 Surfactant

Surfactants are widely used in various applications such as pharmaceuticals, food technology, detergency, agriculture, emulsion polymerization, flocculation and flotation, the petroleum industry, material science and other areas[1]. Surfactants are defined as "surface active agents" and exhibit characteristics such as the tendency to partition at the interface, altering (usually lowering) interfacial free energy or surface tension and forming aggregates in solution which are called micelles. Surface tension is the minimum amount of work required to create/ expand a unit of area of the interface: $\gamma = W_{min}/\Delta$ where γ is surface tension, W_{min} is the minimum work required, Δ is the interfacial area. Surfactant usually adsorbs at the interface and lowers the surface tension which decreases the work required to create/ expand these interfaces.

A surfactant molecule has an amphipathic nature (Figure 1.1) with both lyophobic (solvent-hating) and lyophilic (solvent-loving) groups. The term 'head' group is usually used to refer to the lyophilic group, while 'tail' usually refers to the lyophobic group. When the solvent is water, these terms become hydrophilic and hydrophobic.

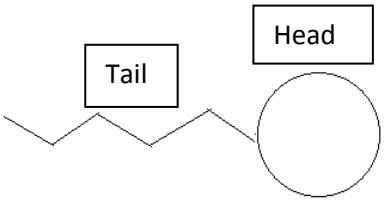

Figure 1.1: Amphipathic nature of a surfactant molecule

The presence of lyophobic groups in a solvent increases the free energy of a system and causes surfactant molecule to orient accordingly in a way to minimize the contact area of lyophobic groups with the solvent. For example, the orientation of the surfactant molecules at a water-air interface shown in Figure 1.2 has the lyophobic (hydrophobic) group oriented towards the air.

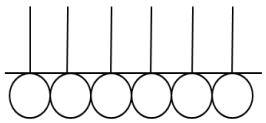

Figure 1.2: Orientation of the surfactant molecules in water phase

Surfactants can be classified into 4 types according to their hydrophilic or head group:

1. Anionic surfactants have negatively charged head groups. For example, $RCOO^-Na^+$ (soap), $RC_6H_4SO_3^-Na^+$ (alkylbenzene sulfonate).
2. Cationic surfactants have positively charged head groups. For example, $RNH_3^+Cl^-$ (salt of a long chain amine), $RN(CH_3)_3^+Cl^-$ (quaternary ammonium chloride).
3. Zwitterionic surfactant may have both positive and negative charged group. For example, $RN^+H_2CH_2COO^-$ (long chain amino acid), $RN^+(CH_3)_2CH_2CH_2SO_3^-$ (sulfobetaine).
4. Nonionic surfactant has no apparent ionically charged group. For example, $RCOOCH_2CHOHCH_2OH$ (monoglyceride long chain fatty acid), $RC_6H_4(OC_2H_4)_xOH$ (polyoxyethylenated alkylphenol), $R(OC_2H_4)_xOH$ (polyoxyethylenated alcohol).

When the interface has been saturated with surfactants molecules, further addition of surfactant molecules forms aggregates in the bulk called micelles. The concentration where micelle starts to formed is called critical micelle concentration (CMC). Micellization occurs at/near maximum interface coverage in order to minimize the free energy of the system. For the example of a

surfactant in water, hydrophobic groups directed inward while hydrophilic directed outwards to minimize the contact between hydrophobic group and water (Figure 1.3).

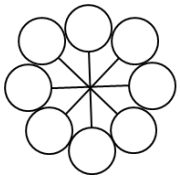

Figure 1.3: Micelle formation in water

Micelles can be classified into at least 4 types:

1. Small, spherical micelles (aggregation number < 100)
2. Elongated cylindrical, rodlike micelles with hemispherical ends
3. Large, flat lamellar micelles
4. Vesicles, bilayer lamellar micelles in concentric spheres

A typical surface tension vs log concentration plot is shown in Figure 1.4. The value of the CMC can be observed from the change in electrical conductivity, surface tension, light scattering, or fluorescence spectroscopy.

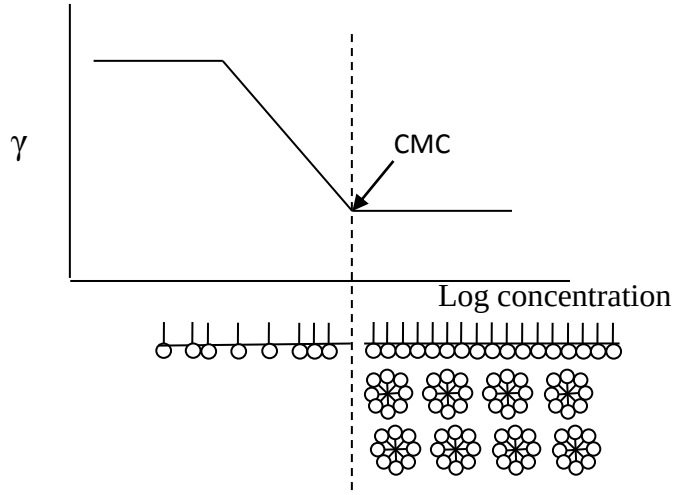

Figure 1.4: Surface tension vs log concentration plot.

1.2 Surfactant Adsorption At Solid-liquid Interface

Surfactant tends to adsorb at interfaces in order to minimize the free energy of the system and maximize the entropy. Among the factors that influenced solid/liquid interface adsorption process are the surface charge of the solid, the structure of the surfactant and the nature of the solvent.

Surface charge of a solid can be determined by zeta potential measurement. Zeta potential is the potential of a charged surface at the shear plane between the solid and the surrounding solution as the solid and the solution move with respect to each other. Point of zero charge (pzc) is defined as the electrolyte's pH when a solid surface exhibits zero net electrical charge when submerged in an electrolyte. Below the pzc, the surface is positively charged (attracts anions) while above the pzc, the surface is negatively charged (attracts cations).

Surfactant molecules tend to partition at interfaces due to several mechanisms such as ion exchange, ion pairing, acid-base interaction, polarizable π electrons, London dispersion force, hydrophobic bonding etc. Surface aggregates called hemimicelles/ admicelles form on the surface when sufficient amounts of adsorbed surfactant are present. The orientation of the adsorbed surfactant may cause changes in the surface properties of the solid.[2-4]

From the Gibbs adsorption equation,

$$\Gamma_{ad} = -\frac{1}{4.606\,RT}\frac{\partial\gamma}{\partial log C} \qquad (1.1)$$

where Γ_{ad} is the surface excess concentration of adsorbed component for 1:1 ionic surfactant, dγ is the change of solid/liquid interfacial tension, C is the molar concentration of the component,

R is the gas constant, T is the temperature. In the presence of swamping amount of electrolytes, the surface excess concentration of adsorbed component is:

$$\Gamma_{ad} = -\frac{1}{2.303\,RT}\frac{\partial\gamma}{\partial log C} \quad (1.2)$$

Experiments can be done to quantify the amount of adsorbed surfactant per gram of adsorbent (mol/g) using the change of concentration method, given in functional form below where

$$n_{ad} = \frac{(C_o - C_1)V}{m} \quad (1.3)$$

n_{ad} is the amount of adsorbed surfactant per gram of adsorbent (mol/g), C_o-C_1 is the difference of surfactant concentration before adsorption and after adsorption, V is the volume of the liquid phase and m is the mass of adsorbent. Adsorption isotherm can be plotted as n_{ad} against C_1.

Adsorption can also be expressed in the form of surface concentration (mol/cm^2),

$$\Gamma_{ad} = \frac{(C_o - C_1)V}{a_s\, m} \quad (1.4)$$

where a_s is the surface area per unit mass of adsorbent. An adsorption isotherm can be plotted as Γ_{ad} against C_1.

Surface area per adsorbate molecule can be calculated as follows where a^s_1 (angstroms square),

$$a_1^s = \frac{10^{16}}{N\Gamma_{ad}} \quad (1.5)$$

where N is the Avogadro's number.

The typical adsorption isotherm of ionic surfactants on strongly charged sites is a S-shaped (Figure 1.5). Initially, there is ion exchange at region 1, increase adsorption at region 2 due to hydrophobic interaction when more aggregates adsorbed on the surface, slope at region 3 decreases because the adsorbent starts to get saturated with surfactant and has the same charge as surfactant. Maximum adsorption at region 4 is obtained when the surface is saturated with surfactant.

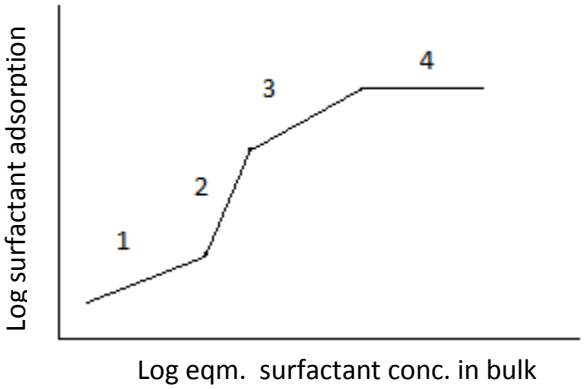

Figure 1.5: S-shaped adsorption isotherm

Examples of surfactant adsorption on charged surface by inonic surfactants include anionic surfactant adsorbed on alumina[5-9], cationic surfactants on silica[10-20] and nonionic surfactant adsorption on alumina[21] and on apatite[2].

1.3 Adsolubilization

Micelles featured a very useful property called micellar solubilization. Micellar solubilization is a phenomenon of solute addition on or into micelles. This effect is the main contribution of surfactants to oil removal in detergency, micellar catalysis of organic reactions, emulsion polymerization, waste treatment in separation process and emulsion interaction in enhanced oil recovery etc. An analogy to micellar solubilisation, one can expect an admicelle

(adsorbed micelle) to behave similarly. Solubilization at the surface by an admicelle is called adsolubilization. Adsolubilization has provided a novel application for the formation of ultra-thin films on surfaces by in-situ polymerization. Admicellar polymerization (Figure 1.6) has been widely used for various applications such as the enhancement of filled rubber[10,22], surface modification of glass fibers[23,24] and production of hydrophobic cotton[25].

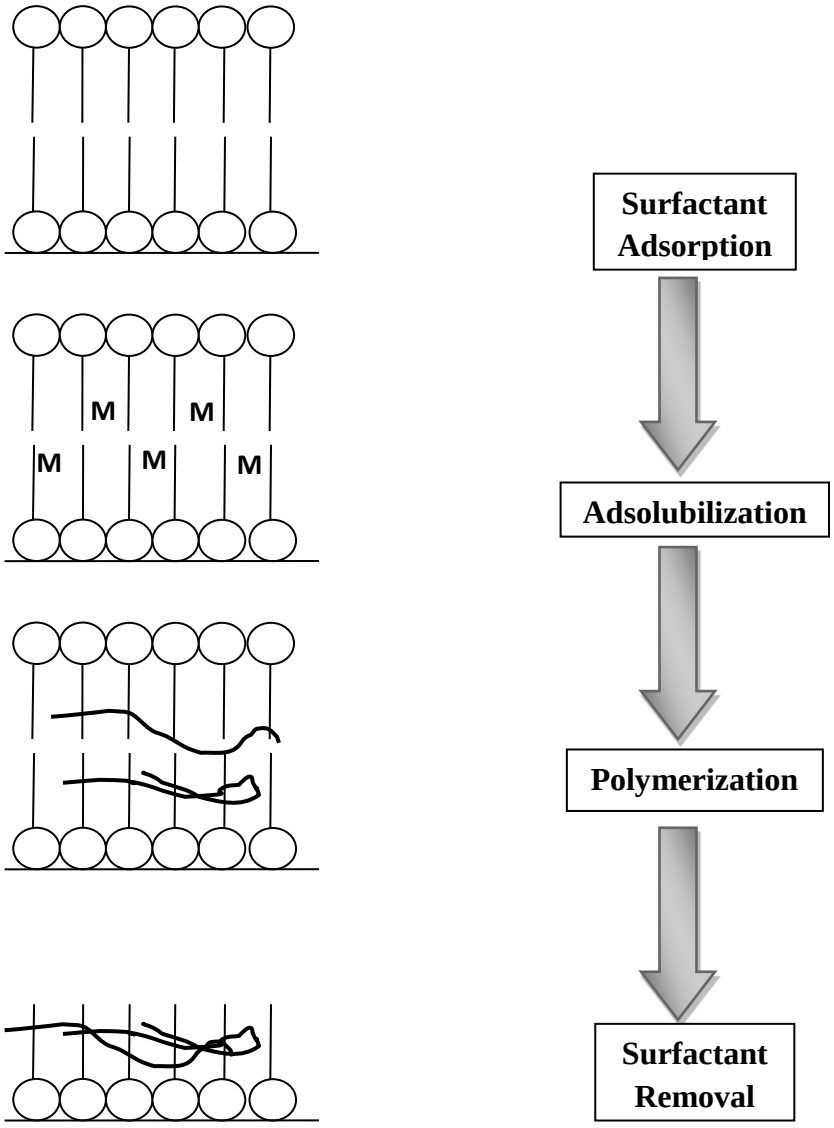

Figure 1.6: Process for admicellar polymerization

List of References

1.4 References

1 "Handbook of Applied Surface and Colloid Chemistry", John Wiley and Sons, 2002.

2 H.Sis and S.Chander, "Adsorption and Contact Angle of Single and Binary Mixtures of Surfactants in Apatite ", Minerals Engineering 16, 839-48, 2003.

3 V.Monticone, P.Favoriti, D.Lemordant, and C.Treiner, "Effect of pH on the Coadsorption of Weak Acids to Silica/Water and Weak Bases to Alumina/Water Interfaces as Induced by Inonic Surfactants" Langmuir 16, 258-264, 2000.

4 C.L.Lai, J.H.Harwell, E.A.O'Rear, S.Komatsuzaki, J.Arai, T.Nakakawaji and Y.Ito, "Adsorption Isotherms of perfluorocarbon Surfactant from Aqueous and Non-aqueous Solutions & Friction Measurements of perfluorosurfactant-adsorbed Alumina" Colloid and Surfaces A: Physicochemical and Engineering Aspects 104, 231-241, 1995.

5 Yeskie, MA, "Various Aspects of Surfactant Aggregates Adsorbed on an Oxide Surface: The Hemicelle/Admicelle Transition and the Interaction of Alcohols and Alkanes", PhD, Dissertation, University of Oklahoma, 1988.

6 J.Wu, J.H.Harwell, E.A.O'Rear, "2-Dimensional Solvents: Kinetics of Styrene Polymerization in Admicelles at or near Saturation", J. Phys. Chem. 91, 623-634, 1987.

7 J.H.O'Haver, J.H.Harwell, "Adsolubilization: Some expected and Unexpected Results", ACS Symposium Series No.615 Surfactant Adsorption and Surface Solubilization Chapter 4 Ravi Sharma Editor 1995.

8 K.T.Valsaraj, P.M.Jain, R.R.Kommalapati, J.S.Smith, "Reusable Adsorbates for Dilute Solution Separation: Adsorption of Phenanthrene in Surfactant-modified Alumina", Separation and Purification Technology 13,137-145, 1998.

9 S.P.Nayyar, D.A.Sabatini, J.H.Harwell, “Surfactant Adsolubilization and Modified Admicellar Sorption of Nonpolar, Polar, and Ionizable Organic Contaminants”, Environ. Sci. Technol. 28, 1874-81, 1994.

10 P. Nontasorn et al, “Admicellar polymerization modified silica via a continuous stirred-tank reactor system: Comparative properties of rubber compounding”, ChE Journal, 108, 213-218, 2005.

11 P.Asvapathanagul et.al., “Adsolubilization of toluene and acetophenone as a function of surfactant adsorption”, J.Colloid and Interface.Sci. 292, 305-311, 2005.

12 T.Pradubmook et al., “Effect of pH on adsolubilization of toluene and acetophenone into adsorbed surfactant on precipitated silica”, Colloid and Surfaces A: Physicochem Eng Aspects 224, 93-98, 2003.

13 J.H.O'Haver et.al, “In-situ Formation of polystyrene in adsorbed surfactant bilayers on precipitated silica”, Langmuir Vol.10, 8, 2558-2593, 1994.

14 B. Kitiyanan et.al., “Adsolubilization of styrene and isoprene in CTAB admicelle on Precipitated Silica”, Langmuir Vol.12, 9, 2162-2168, 1998.

15 J.Dickson, J.O'Haver, “Adsolubilization of Napthalene and αNapthol in CnTAB admicelles”, Langmuir18, 9171-9176, 2002.

16 T.Behrends, R.Herrmann, “Adsolubilization of anthracene on surfactant covered silica in dependence on pH: indications for different adsolubilization in admicelles anf hemimicelles”, Colloids and Surfaces A: Physicochemical and Engineering Aspects 162,15-23, 2000.

17 K.Esumi, “Interactions between Surfactants and Particles: Dispersion , Surface Modification and Adsolubilization”, J.Colloid and Interface 241, 1-17, 2001.

18 K.Hayakawa, Y.Miyamoto, J.Kurawaki, Y.Kusumoto, I.Satake, M.Sakai, "Thermodynamics of the Adsolubilization Equilibrium of RhodamineB by Surfactant-Modified Zeolites", Bulletin Chem.Soc. Japan 73, 1777-1782, 2000.

19 I.Cherkaoui V.Monticone C.Vaution C.Treiner, "Coadsorption of Sodium Salt of Two Steroid Molecuels at a Silica/Interface as Induced by the Adsorption of a Cationic Surfactant", Int'l . Of Pharmaceutics 201, 71-77, 2000.

20 P.Favoriti V.Monticone Ctreiner, "Coadsorption of Napthalene Derivatives and CTAB on Alumna/water, TiO2/water, SiOH/water", J.Colloid And Interface Sci 179, 173-80, 1996.

21 Y.Tan e.al., "Lipophilic linker impact on adsorption of and styrene adsolubilization in polyethoxylated octylphenols", Physichem Eng Aspect 232,101-111, 2004.

22 V. Thamm., "Comparison of Rubber Reinforcement Using Various Surface-modified Prepicitated Silica", J. Appl. Phy. Sci. 59, 1742-50, 1996.

23 S.S.Sakhalkar, D.E.Hirt, "Admicellar polymerization of polystyrene on glass fibers", Langmuir11, 3369-73, 1995.

24 U.Somnuk, N.Yanumet, J.W.Ellis, B.P.Grady, E.A.O'Rear, "Adhesion Improvement in Glass Fiber Reinforced Polyethylene Composite via Admicellar Polymerization", Polymer composites, V.24, 1, 171-80, Feb2003.

25 T.Pongrayoon et al, "Wettabulity of cotton modified by admicellar polymerization", Langmuir 19, 3770-3778, 2003.

2.0 REVIEW: ADMICELLAR POLYMERIZATION

Admicellar polymerization on rubber fillers: Alumina/ aluminium

Admicellar polymerization was first published by J. Wu et.al. in 1987[1,2] where a polystyrene ultrathin film was successfully formed on alumina using sodium dodecyl sulfate (SDS) surfactant. It was proven that polymerization was indeed taking place in the admicelle. In 1988[3], they furthered their study onto alumina powder. Film thickness on the powder calculated was comparable to the SDS bilayer adsorption. In addition, washing steps after admicellar polymerization was found to affect final surface properties.

D.V. Le (2004)[4] managed to show corrosion control of aluminium alloys by forming a thin film of poly(2,2,2-trifluoroethyl acrylate) (PTFEA) and polymethyl methacrylate (PMMA) via admicellar polymerization. PTFEA showed higher hydrophobicity and better corrosion control over PMMA.

S. Wang (2006)[5] found that styrene monomer enhanced sodium dodecylsulfate (SDS) adsorption onto alumina. Ratios of 2.5-2.9:1 of SDS:styrene was obtained. Characterization of styrene on alumina after admicellar polymerization showed positive results with tetrahydrofuran (THF) extraction but direct observation was found to be insensitive in attenuated total reflectance (ATR) and diffuse reflectance infrared Fourier Transform (DRIFT). Extraction of polymer was found to be difficult because a more tightly bound polystyrene cross-linked divinylbenzene (PS-co-DSB) cannot be extracted. However, hydrophobic properties can be achieved to resist water

for up to 90 min. Scanning electron microscopy (SEM) showed changes in topography after polymerization but failed to differentiate among different coatings. On the other hand, Thermogravimetric analysis (TGA) provided strong evidence of the presence for residual SDS and PS-co-DSB.

P.M. Karlsson (2009)[6] successfully polymerized polymethylmethacrylate (PMMA) and polystyrene (PS) onto the surface of aluminum pigment to inhibit the oxidation process. Formation of PS was less than PMMA due to the lower solubility of styrene in the bulk solution. Hydrophobic initiator was preferred because of the hydrophobicity of the tail region in the admicelle for polymerization. Inhibition test on the susceptibility of the aluminum pigments to alkaline water for PMMA-modified aluminium pigment powder was stable (no visible changes) up to 110 days.

C.Attaphong (2010)[7] tested the effectiveness of anionic polymerizable surfactant adsorbed on positively charged alumina surface after admicellar polymerization. It was concluded that the admicelle layer as well as the adsolubilization capacity of that layer remained stable after washing.

Admicellar polymerization on rubber fillers: Silica

J.H.O'Haver (1994)[8] first started the work of admicellar polymerization on amorphous silicas using different surfactant types: water soluble cationic cetyltrimethyl ammonium bromide (CTAB), water insoluble cationic surfactant methyltri(C_8-C_{10}) ammonium chloride (ADOGEN 464) and nonionic surfactant octylphenoxypoly(ethoxy)ethanol (MACOL OP10SP). Maximum adsorption of surfactant on silica is the highest for ADOGEN, followed by CTAB and MACOL. This is explained by larger hydrophobic group of nonionic surfactant hence lower adsorption

onto silica. However, for the case of water insoluble cationic surfactant ADOGEN has the highest adsorption even with sterically 4-alkyl chains head group is explained by formation of multiple layers on the surfaces because of Van der Waals forces and water insolubility. Ratio of adsorbed CTAB to adsolubilized styrene was 2. Thin film of polystyrene was proved to form on the surface using different initiation schemes for polymerization: thermally initiated polymerization using 2,2-azobis(2-methylpropionitrile) (AIBN) initiator or redox polymerization using ferrous sulfate. High initiator to monomer concentration was necessary when using AIBN because of the ethanol used to dissolve AIBN participated in adsolubilization and may consume free radicals that were formed. Slower rate of conversion was observed in redox polymerization due to the small amount of ferrous sulfate. Very low amount and low molecular weight polymers extracted by boiling products in refluxed tetrahydrofuran (THF) were explained by the entrapment of polymer chains in highly porous silica surface and only shorter chains or polymer on or near the surface can be extracted. Further explanation which suggested that monomers diffuse into admicelle during the polymerization reaction may form polymer near the surface with higher molecular weight while monomers which diffuse into admicelle before initiation of polymerization may form lower molecular weight polymer.

V. Thammathadanukul et. al. (1996)[9] compared properties of rubber after reinforcement of two different surface-modified silicas, one silane-coupled and the other modified by admicellar polymerization. Cetyltrimethyl ammonium bromide (CTAB) was used to form the admicelle, styrene–isoprene or styrene-butadiene were used as co-monomers for thin film formation. Overall, rubber properties were improved after reinforcement of modified silicas with both techniques especially for admicellar polymerized silicas which provided a better flex-

cracking resistance. They observed that the higher the surface area of admicellar polymerized silicas, the better the rubber physical properties.

In 2005, P.Nontasorn[10] successfully performed admicellar polymerization in a continuous stirred tank reactor to produce modified silicas. Reinforcement into rubber proved to improve the physical properties and rubber testing results were consistent with those obtained from batch systems.

P. Rangsunvigit (2008)[11] used cetyltrimethyl ammonium bromide (CTAB) and polyoxyethylene octylphenol ether ($OPEO_{10}$) to modify silica surfaces. Co-monomers of styrene and isoprene were used to form the polymer coating. Increases in the ratio of $OPEO_{10}$: CTAB would decrease surfactant maximum adsorption because of less interaction and steric effect of the bulky head group of nonionic surfactant on silica. From the result, $OPEO_{10}$ was used to reduce the total amount of CTAB required to form a monolayer. Specific surface area was reported to reduce and mean agglomerate particle size was increased after surface modification. Polymer coating was further characterized using Thermogravimetric analysis (TGA) and Scanning electron microscope (SEM). It was found that rubber compound with modified silica using CTAB: $OPEO_{10}$ ratio of 1:3 has the best mechanical properties of those tested in this study.

T. Pongprayoon (2012)[12] compared different methods of admicellar polymerization to modify silica surface for the rubber reinforcement application, thermal or radiation-induced admicellar polymerization. Cationic surfactant C_{12}-, C_{14}-, C_{16}- trimethyl ammonium bromide (DTAB, TTAB, CTAB) were used to obtain admicelle layer and isoprene was used as the monomer. It was reported that 40phr (phr = parts per hundred rubber) of silica was the optimum ratio for the reinforcement of a model rubber compound. Rubber compound with modified silica

showed improved mechanical properties. Among the systems tested, modification of silica with CTAB via radiation-induced admicellar polymerization had the best performance, which is consistent with previous work done by N. Yooprasert et.al. (2010)[13]. CTAB has the longest hydrophobic chain length with closer packing and adsolubilized the highest amount of monomer and hence had the best film formation. Scanning electron microscopy (SEM) images further confirmed the better dispersion in rubber compound with modified silica.

Surface modification on other hydrophilic mineral surfaces

X.Wei et. al. (2003)[14] studied the effect of washing steps on admicellar polymerized titanium dioxide and alumina. Polystyrene was proven to form on the surface using ignition loss measurement. Soxhlet extraction with toluene however did not remove any polymer. X-ray photoelectron spectroscopy (XPS) showed that admicellar polymerization takes place both on internal and external surfaces. They believed that water washing removed surfactant on the surfaces but not those in the interior surfaces or below the polymer film.

M. Marquez et. al. (2005)[15] discussed different methods to surface modify on sand samples. Three different methods studied were: (1) in-situ graft polymerization of vinyl monomers (acrylamide or acrylic acid with vinyl acetate) onto an organosilane sublayer chemically bonded to the sand surface, (2) admicellar polymerization using Cetyltrimethylammonium bromide (CTAB) surfactant and various monomers (acrylic acid, vinyl acetate and acrylamide) and (3) grafting preformed using water soluble polymers onto an organosilane sublayer which was also chemically bonded to the sand surface. γ-Methacryloxypropyl-trimethyoxysilane (MPS) was used as the silane coupling agent during the silanation process. Among the 3 methods, grafting preformed polymers has the highest amount

of polymer coating followed by in-situ grafting polymerization and admicellar polymerization. They observed that the monomer's solubility affected the amount of admicellar-polymerized on sand surface. The higher the solubility of monomer in water, the lesser the monomer will participate in the admicelle resulting in easy removal after washing.

Surface modification of other composite fillers

S. Das (2011)[16] surface modified graphene with nylon 6-10 and nylon 6-6 polymer films and proved that the modification prevented aggregation and showed better dispersibility in a bulk nylon matrix. Sodium dodecylbenzene sulfate (SODS) was used to generate admicelle template and organic solvent carbon tetrachloride (CCl_4) was used to swell the admicelle surfactant to provide a better environment at the interface for polymerization. They showed nylon film can be noncovalently bonded onto a graphene surface and remained stable in low pH (1.7-2.5) conditions or after being freeze dried.

Y. Zhao (2011)[17] successfully formed polymethyl methacrylate (PMMA) nanofilm on rice straw fiber (RSF) surface. PMMA-modified rice straw showed good miscibility with polylactic acid (PLA). Modified RSF can be stably dispersed in PLA with less agglomeration. As the result, reinforcement of modified RSF into PLA composite showed improved tensile strength, increased elongation and increased thermal stability.

Admicellar polymerization on cotton fibers

X. Ren et. al. (2008)[18] used admicellar polymerization to obtain antimicrobial N-halamines polymer coatings on cotton fibers. FTIR and SEM proved the presence of N-halamines polymer coatings on the fabrics. The polymer-coated cotton after chlorination showed high efficiency in inactivating Staphylococus aureus and Escherichia coli. They also proved that

the polymer coating was stable and chlorine can be rechargeable despite 50 machine washing cycles.

A. Siriviriyanun et. al. (2009)[19] utilized admicellar polymerization to make a flame retardant cotton fabric coated with phosphorus-containing thin film poly(acryloyloxyethyldiethyl phosphate) (PADEP). Cationic surfactant hexadecyl/dodecyltrimethylammonium bromide (HTAB or DTAB) were used for admicelle layer. HTAB has larger hydrophobic core hence more ADEP adsolubilized and showed higher phosphorous content. FTIR further confirmed the formation of thin film PAEDP. They observed the higher the ADEP concentration, the lower the degradation temperature and the higher the char formation. All PADEP-coated cotton fabrics have less intense burning compared to untreated cotton. In addition, PADEP-coated cotton treated with HTAB has a self-extinguishing feature due to higher phosphorous coating.

J. Maity et. al. (2010)[20] admicellar polymerized fluoropolymer thin layers on cotton fabric and compared with direct fluorination method. Both methods successfully showed cotton surface with great hydrophobicity after modification. They discussed the advantages and disadvantages of both methods and found admicellar polymerization was more compatible with existing textile processing methods.

S. Tragoonwichian et. al. (2011)[21] produced cotton fabric with water repellent properties by admicellar polymerization silicon compounds as the hydrophobic surface. Point of zero charge was reported to affect surfactant adsorption while structure of silicon-based monomer had affected monomer adsolubilization. Hydrophobic coatings were proven by analysis from wetting time, Scanning Electron Microscopy (SEM), Fourier Transform Infrared Spectroscopy (FTIR), Energy Dispersive Spectroscopy (EDS), X-ray Photoelectron Spectroscopy (XPS) and contact

angle. Cotton fabric with better water repellency was produced by using cationic surfactant and less bulky silicon compound to form a thick and uniform hydrophobic film. In 2008[22], they worked on polymerizing UV-absorbing agent 2-hydroxy-4-acryloxybenzophenone (HAB) on cotton fabric. They observed closer packing of adsorbed surfactant sodium dodecylbenzene sulfate (DBSA) in the presence of NaCl electrolytes. Increase in temperature increased adsorption rate but slightly decreased adsorption amount of surfactant. In the monomer adsolubilization study, adsolubilized HAB constrained and hence reduced surfactant adsorption. It was reported that mole ratio of HAB to DSAB was about 1:2. FTIR and SEM images showed the presence of poly(HAB) and the fabric exhibited great UV protection properties with stability up to 24 hours. In his paper published in 2009[23], a bifunctional cotton fabric with both great UV-protective and water repellency was made. HAB-treated fabric was made initually and silicon-compound methacryloxymethyltrimethylsilane (MSi) was polymerized later using admicellar polymerization. Both process used DBSA as surfactant admicelle layer.

List of References

References

1. J. Wu, J. H. Harwell, E. A. O'Rear, "Two-Dimensional Reaction Solvents: Surfactant Bilayers in the Formation of Ultrathin Films", Langmuir 3 (1987) p531-37
2. J. Wu, J. H. Harwell, E. A. O'Rear, "Two-Dimensional Solvents: Kinetics of Styrene Polymerization in Admicelles at or near Saturation", J. Phys. Chem. (1987) p623-34
3. J.Wu, J. H. Harwell, E. A. O'Rear, S. D. Christian, "Applicatio n of Thin Films to Porous Mineral Oxides Using Two-Dimensional Solvents", AlChE Journal 34, 9 (1988) p1511-18
4. D.V. Le, M. M. Kendrick, E. A. O'Rear, "Admicellar Polymerization and Characterization of Thin Poly(2,2,2-trifluoroethyl acrylate) Film on Aluminium Alloys for In-Cervice Corrosion Control", Langmuir 20 (2004) p7802-10
5. S. Wang, T. Russo, G. G. Qiao, D. H. Solomon, R. A. Shanks, "Admicellar Polymerization of Styrene with Divinyl Benzene on Alumina Particles: The Synthesis of White Reinforcing Fillers ", J. Mater. Sci 41 (2006) p7474-82
6. P.M. Karlsson, N. B. Esbjornsson, K. Holmberg, "Admicellar Polymerization of Methyl Methacrylate on Aluminum Pigments", J. Colloid and Interface Science 337 (2009) p364-368
7. C.Attaphong, E. Asnachinda, A. Charoensaeng, D. A. Sabatini, S. Khaodhiar, "Adsorption and Adsolubilization of Polymerizable Surfactants on Aluminium Oxide", J. Colloid and Interface Science 344 (2010) p126-131
8. J. H. O'Haver, J. H. Harwell, E. E. O'Rear, L. J. Snodgrass, W. H. Waddell, "In Situ Formation of Polystyrene in Adsorbed Surfactant Bilayers on Precipitated Silica", Langmuir 10 (1994) p2588-93

9. V. Thammathadanukul, J. H. O'Haver, J. H. Harwell, S. Osuwan, N. NaRanong, W. H. Waddell, "Comparison of Rubber Reinforcement Using Various Surface-Modified Precipitated Silicas", J. Applied Polymer Science, 59 (1996) p1741-50
10. P. Nontasorn, S. Chavadej, P. Rangsunvigit, J. H. O'haver, S. Chaisirimahamorakot, N. Na-Ranong, "Admicellar Polymerication Modified Silica Via a Continuous Stirred-Tank Reactor System: Comparative Properties of Rubber Compounding", Chemical Engineering Journal 108 (2005) p213-18
11. P. Rangsunvigit, P. Imsawatgul, N. Na-ranong, J. H. O'Haver, S. Chavadej, "Mixed Surfactants for Silica Surface Modification by Admicellar Polymerization Using a Continuous Stirred Tank Reactor", Chemical Engineering Journal 136 (2008) p288-94
12. T. Pongprayoon, N. Yooprasert, P. Suwanmala, K. Hemvichian, "Rubber Products Prepared from Silica Modified by Radiation-induced Admicellar Polymerization", Radiation Physics and Chemistry 81 (2012) p541-46
13. N. Yooprasert, T. Pongprayoon, P. Suwanmala, K. Hemvichian, G. Tumcharern, "Radiation-induced Admicellar Polymerization of Isoprene on Silica: Effects of Surfactant's Chain Length", Chemical Engineering Journal 156 (2010) p193-99
14. X. Wei, A. D. W. Carswell, W. Alvarez, B. P. Grady, "X-ray Photoelectron Spectroscopic Studies of Hydrophilic Surfaces Modified via Admicellar Polymerization", J. Colloid and Interface Science 264 (2003) p296-300
15. M. Marquez, B. P. Grady, I. Robb, "Different Mwthods for Surface Modification of Hydrophilic Particulates with Polymers ", Colloids and Surfaces A: Physiochem. Eng. Aspects 266 (2005) p18-31

16. S. Das, A. S. Wajid, J. L. Shelburne, Y. Liao, M. J. Green, “Localized In Situ Polymerization on Graphene Surfaces for Stabilized Graphene Dispersions ”, ACS Appliied Materials and Interfaces 3 (2011) p1844-51
17. Y. Zhao, J. Qiu, H. Feng, M. Zhang, L. Lei, X. Wu, “Improvement of Tensile and Thermal Properties of Poly(lactic acid) Composites with Admicellar Polymerization ”, Chemical Engineering Journal 173 (2011) p659-66
18. X. Ren, L. Kou, H. B. Kocer, C. Zhu, S. D. Worley, R. M. Broughton, T. S. Huang, “Antimicrobial Coating of an N-halamine Biocidal Monomer on Cotton Fibers via Admicellar Polymerization”, Colloids and Surfaces A: Physiochem. Eng. Aspects 317 (2008) p711-16
19. A. Siriviriyanun, E. A. O’Rear, N. Yanumet, “The Effect of Phosphorous Content on the Thermal and the Burning Properties of Cotton Fiber Coated with an Ultrathin Film of a Phosphorous- Containing Polymer ”, Polymer Degradation and Stability 94 (2009) p558-65
20. J. Maity, P. Kothary, E. A. O’Rear, C. Jacob, “Preparation and Comparison of Hydrophobic Cotton Fabric, Obtained by Direct Fluorination and Admicellar Polymerization of Fluoromonomers ”, Ind. Eng. Chem. Res. 49 (2010) p6075-79
21. S. Tragoonwichian, P. Kothary, A. Siriviriyanun, E. A. O’Rear, N. Yanumet, “Silicon-Compound Coating for Preparation of Water Repellent Cotton Fabric by Admicellar Polymerization”, Colloid and Surfaces A: Physiochem. Eng. Aspects 384 (2011) p381-87
22. S. Tragoonwichian, E. A. O’Rear, N. Yanumet, “Admicellar Polymerization of 2-hydroxy-4-acryloyloxybenzophenone: The Production of UV-Protective Cotton”, Colloid and Surfaces A: Physiochem. Eng. Aspects 329 (2008) p87-94

23. S. Tragoonwichian, E. A. O'Rear, N. Yanumet, "Double Coating via Repeat Admicellar Polymerization for Preparation of Bifunctional Cotton Fabric: Ultraviolet Protection and Water Repellence", Colloid and Surfaces A: Physiochem. Eng. Aspects 349 (2009) p170-75

3.0 REVIEW: SURFACE MODIFICATION of $CaCO_3$

In 1980, S. Chibowski[1] investigated the adsorption of SDS on $CaCO_3$ surface in the presence of polyacrylamide (PAA) using radiotracer technique tracing for SDS labeled with ^{35}S. The effect of pH and electrical surface charge were studied. The presence of PAA on the surface of $CaCO_3$ increased SDS adsorption especially when pH is greater than the pzc. PAA-SDS complexes were assumed to be formed at $CaCO_3$ interface and therefore basic bonding was less sensitive to pH. It was found that PAA-SDS complexes formed in the bulk when premixing high concentration SDS and PAA solutions which contributed to the decrease in SDS adsorption.

In one application study on rheology for oil dispersion properties of silanated $CaCO_3$ done by R. D. Kurkarni (1982)[2], it was found that silanes reduced the particle- particle interaction and decreased the dissipation energy under shear.

K. A. Rezaei Gomari et. al. (2005)[3] showed that the wettability of calcite surface can be modified by long chain fatty acid adsorption. Effect of structure of fatty acids, water composition and pH were studied by contact angle measurement. Napthenic acid with two rings had greater contact angle (more oil-wet) than napthenic acids with one ring. Presence of magnesium and sulfate ions in water at pH 7 increased water wettability of calcite. While magnesium ions remained to increase water wettability at pH above 7, sulfate ions convert calcite surface to become oil-wet.

Surface modification of $CaCO_3$ particles using admicellar polymerization technique to apply as isotatic polypropylene filler was done by P. Ruangruang et.al. (2006)[4]. The point of zero charge (pzc) for $CaCO_3$ used was reported to be at pH 11.4. Sodium dodecylsulfate (SDS) was used as the surfactant. Equilibrium time for SDS adsorption on $CaCO_3$ can be achieved after 18 hours. The effect of increasing sodium ions provided shielding to surfactant head group repulsion and increased the amount of adsorbed SDS. An SDS adsorption isotherm was obtained and admicellar polymerization was run using propylene gas monomer. FTIR characterization analysis, gravimetric weight loss analysis, increased diameter of particles showed the presence of thin film of polypropylene on $CaCO_3$. The isopropylene (iPP) treated $CaCO_3$ composite was tested for non-isothermal crystallization studies. Crystallization temperature and the melting endotherm of iPP filled with modified $CaCO_3$ was lower than those for untreated $CaCO_3$ composite samples, which indicated reduced nucleation of filler particles. Decreases in Wide Angle X-ray Diffraction (WAXD) crystallinity were also observed. Mechanical properties testing on iPP filled with modified $CaCO_3$ showed reduced yield stress, increased yield strain, reduced flexural strength and increased impact resistance because the thin film acted as a lubricant between particles and the polymer matrix. Better dispersion and distribution of modified $CaCO_3$ was confirmed in Scanning Electron Microscopy (SEM) study.

Several studies have been done to modify the calcium carbonate ($CaCO_3$) mineral surface. H. Ding (2007)[5] modified $CaCO_3$ by grinding $CaCO_3$ with SDS in an ultrafine stirred mill and used this as filler in polyethylene (PE). They measured active rate which defined as ratio of floated product over overall mass of sample after mixing in water and aeration. The higher the active rate, the higher the hydrophobicity. Analysis with Infrared (IR) and X-ray photoelectron energy spectroscopy (XPS) were also performed. Decreases in particle size or

increases in specific surface area of the particles improved modification effect which means a more hydrophobic surface. Optimum experimental conditions were studied such as concentration of SDS, mass ratio of grinding media to feeding, and grinding forces and duration. Modified $CaCO_3$ was incorporated into PE as filler showed improved mechanical and physico-chemical properties. IR and XPS show SDS adsorption on the surface of $CaCO_3$.

J. Zhang et. al. (2010)[6] synthesized maleic anhydride grafting polyethylene wax (MA-g-PEW) by mixing melted polyethylene wax, maleic anhydride and free radical initiator di-tert-butyl peroxide (DTBP). Purified MA-g-PEW was prior dissolved in toluene and mixed with $CaCO_3$ by mechanical stirring. Fourier transform infrared spectroscopy (FTIR) characterization showed the presence of MA-g-PEW in modified $CaCO_3$. Transmission emission microscopy (TEM) showed less agglomeration and increases in $CaCO_3$ thickness after the modification. 100% active ratio (ratio of floated product over overall dispersed sample used to check for hydrophobicity) was able to be achieved at 2.5% MA-g-PEW or above. Decrease in shear forces and viscidity (less agglomeration) with increase weight ratio of MA-g-PEW to modified $CaCO_3$ indicated reduction in resistance forces. Overall, the optimum weight ratio of MA-g-PEW to modified $CaCO_3$ in order to completely surface modify $CaCO_3$ from hydrophilic to hydrophobic was reported as 2.5%.

Z. Hu et.al. (2010)[7] have used stearic/oleic acid to fabricate the surface of laboratory-synthesized or commercial precipitated $CaCO_3$. Both commercial and laboratory precipitated $CaCO_3$ (PCC) were chemically modified. Hydrophobicity analysis of the modified PCC's was determined by water contact angle analysis. PCC's were stirred with fatty-acids in water/hexane solution. Modified PCC showed increases in advancing and receding contact angle (increase hydrophobicity) and nearly no hysteresis at the optimum conditions. Commercial PCC with

hierarchical structure (lotus leaf-like surface) proved to be more hydrophobic with self-cleaning function (low wetting, water rolled-off easily) after modification compared to laboratory-synthesized PCC with flat structure. PCC modified with stearic acid had smaller advancing and receding contact angle than PCC modified with oleic acid. It was explained that calcium stearate salt aggregates were formed instead of a uniform hydrophobic layer. Both PCC modified with oleic/stearic possessed self-cleaning properties.

G. G. Wang et. al. (2011)[8] synthesized $CaCO_3$ by crystallization in geothermal water and fabricated monolayers of sodium stearate on the mineral by immersion. Continuous cactus-like $CaCO_3$ fouling was obtained after 48 hours of crystallization which provide the desired roughness surface for superhydrophobicity. FTIR analysis showed the long-chain aliphatic groups on modified $CaCO_3$. A large increase in water contact angle proved the superhydrophobicity properties after modification.

List of References

References

1. S. Chibowski, “Investigation on Interactions of Sodium Dodecyl Sulfate and Polyacrylamide Molecules on Calcium Carbonate Surfac Using Radiotracer Technique”, J. Colloid and Interface Science 76, 2, p371-74, 1980.
2. R.D. Kurkarni, P.S. Leung, E.D. Goddard, “Oil Dispersion properties of Silanated Calcium Carbonate: A Rheological Study”, Colloid and Surfaces 5, p321-32, 1982.
3. K.A. Razaei Gomari, A.A. Hamouda, “Effect of fatty acids, water composition and pH on the wettability alteration of calcite surface”, J. Petroleum Science and Engineering 50.P140-50, 2006.
4. P. Rungruang, B.P. Grady, P. Supaphol, “Surface-modified calcium carbonate particles by admicellar polymerization to be used as filler for isotactic polypropylene”, Colloids and Surfaces A: Physicochem. Eng. Aspects 275, p114-25, 2006.
5. H. Ding, S. Lu, Y. Deng, G. Du,“Mechano-activated surface modification of calcium carbonate in wet stirred mill and its properties”,Trans. Nonferrous Met. Soc. China7, p1100-04, 2007.
6. J. Zhang, J. Guo, T. Li, X. Li, “Chemical Surface Modification of Calcium Carbonate Particles by Maleic Anhydride Grafting Polyethylene Wax”, International Journal Green Nanotechnology: Physics and Chemistry 1, p65-71, 2010.
7. Z. Hu and Y.Deng, “Superhydrophobic Surfae Fabricated from Fatty Acid-Modified Precipitated Calcium Carbonate”, Ind. Eng. Chem. Res. 49, p5425-30, 2010.
8. G.G.Wang, L.Q. Zhu, H.C. Liu, W.P. Li, Langmuir dx.doi.org/10.1021/la202613r, 2011.

4.0 PRECIPITATION OF SDS BY CALCIUM IONS

4.1 Introduction

Precipitation of ionic surfactant in hard water is a drawback in many applications, detergency being the major one. Precipitation of surfactant is a concern during enhanced oil recovery process in which minimum mineral-surfactant interactions are desired. In contrast, precipitation of surfactant can be useful in waste water treatment or some separation process.

In this study, phase behavior of sodium dodecylsulfate (SDS) in calcium chloride ($CaCl_2$) solution has been studied. In the presence of sufficient calcium ion (Ca^{2+}), precipitation of calcium dodecyl sulfate $Ca(DS)_2$ takes place. A model was developed to predict the precipitation phase boundary.

4.2 Solubility of Calcium Dodecylsulfate $Ca(DS)_2$

In a system of SDS with calcium ions, $Ca(DS)_2$ will precipitate when the solubility product (K_{sp}) is exceeded. This is expressed mathematically in the equation below:

$$Ca^{2+}(aq) + 2DS^{-}(aq) \leftrightarrow Ca(DS)_2(s) \quad (4.1)$$

$$K_{sp} = [Ca^{2+}]_{un} [DS^{-}]^2_{mon} f_{Ca} f_{DS}^2 \quad (4.2)$$

$[Ca]^{2+}_{un}$ is the concentration of free calcium ions while $[DS^{-}]_{mon}$ is the monomeric concentration of the anionic surfactant. f_{Ca} and f_{DS} are the activity coefficients of the unbound calcium ion and anionic monomer respectively.

According to the Debye Huckel theory[1], activity coefficients of the ions can be calculated by:

$$log\ f_{Ca} = \frac{-0.5139(2)^2(I)^{0.5}}{1+1.9782(I)^{0.5}} \quad (4.3)$$

$$log\ f_{DS} = \frac{-0.5139(-1)^2(I)^{0.5}}{1+2.3079(I)^{0.5}} \quad (4.4)$$

where $I = \sum 0.5(c_i)(z_i)^2$ (4.5)

In our study, we calculated I as:

$$I = 0.5[Ca^{2+}](2)^2 + 0.5[Cl^-](-1)^2 + 0.5[Na^+](1)^2 + 0.5[DS^-](-1)^2$$

$$I = 3[CaCl_2] + [SDS] \quad (4.6)$$

The K_{sp} can be determined by studying the phase boundary of SDS over a range of calcium concentrations before SDS micelles are formed when all Ca^{2+} ions are unbound and all DS^- ions are free monomer. After micelles are formed, most of the anionic monomer exists as micelles with Ca^{2+} ion bound onto the micelles. As a result, the precipitation boundary after the CMC is determined by the ratio of Ca^{2+} ion concentration bound onto anionic micelles. One Ca^{2+} ion can neutralize charges of two DS^- micelles. This can be expressed as counterion binding of calcium, β_{Ca}:

$$\beta_{Ca} = \frac{2[Ca^{2+}]_b}{[DS^-]_{mic}} \quad (4.7)$$

$[Ca]^{2+}_b$ is the concentration of bound calcium ion on the micelles while $[DS^-]_{mic}$ is the surfactant concentration in the micelles.

4.3 Experimental Materials

Sodium dodecyl sulfate (SDS) was purchased from Amresco. SDS was recrystallized twice with 50/50 water/methanol mixture. $CaCl_2$ was obtained from Fisher Scientific. Distilled water was obtained from Great Value. Fiber optic illuminator (Fiber-Lite Model 190) from Dolan-Jenner Industries Inc, (Woburn Massachusetts) was used as the light source. A water bath was used to provide constant temperature.

4.4 Experimental Procedures

1M SDS and 1M $CaCl_2$ stock solutions were prepared in deionized water. SDS solution were prepared over a range of concentration (0 to 0.5M) and added with fixed amount of Ca^{2+} concentration (10^{-4}, 10^{-3}, 10^{-2}, 10^{-1}M). Solutions were made in 10mL vials and kept in the chiller at 4^{o}C to force the precipitation process. The solutions were then allowed to equilibrate at 30^{o}C for 4 days before observation. Observation were done by directing a light source to the sample in the dark in order to observe any presence of $Ca(DS)_2$ precipitate. Samples were transferred back to the water bath and equilibrated at 50^{o}C for another 4 days. The same procedures were done to observe for any precipitate formed.

4.5 Result and Discussion

4.5.1 Phase behavior of SDS with calcium ion

Phase behavior of SDS in different concentration of Ca^{2+} at 30^{o}C and 50^{o}C was studied (Figure 4.1 & 4.2). Experimental solubility product values of calcium dodecylsulfate $Ca(DS)_2$ and the critical ratio of Ca^{2+} counter ions binding to micelles were obtained.

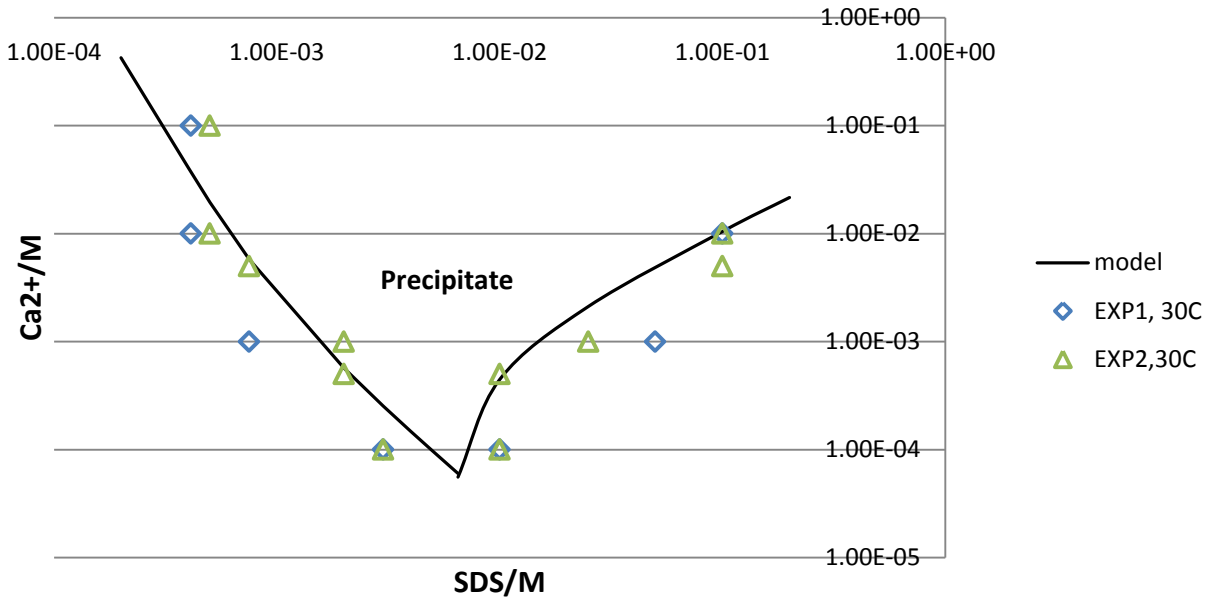

Figure 4.1: Precipitation phase boundary of SDS with calcium ion at 30°C

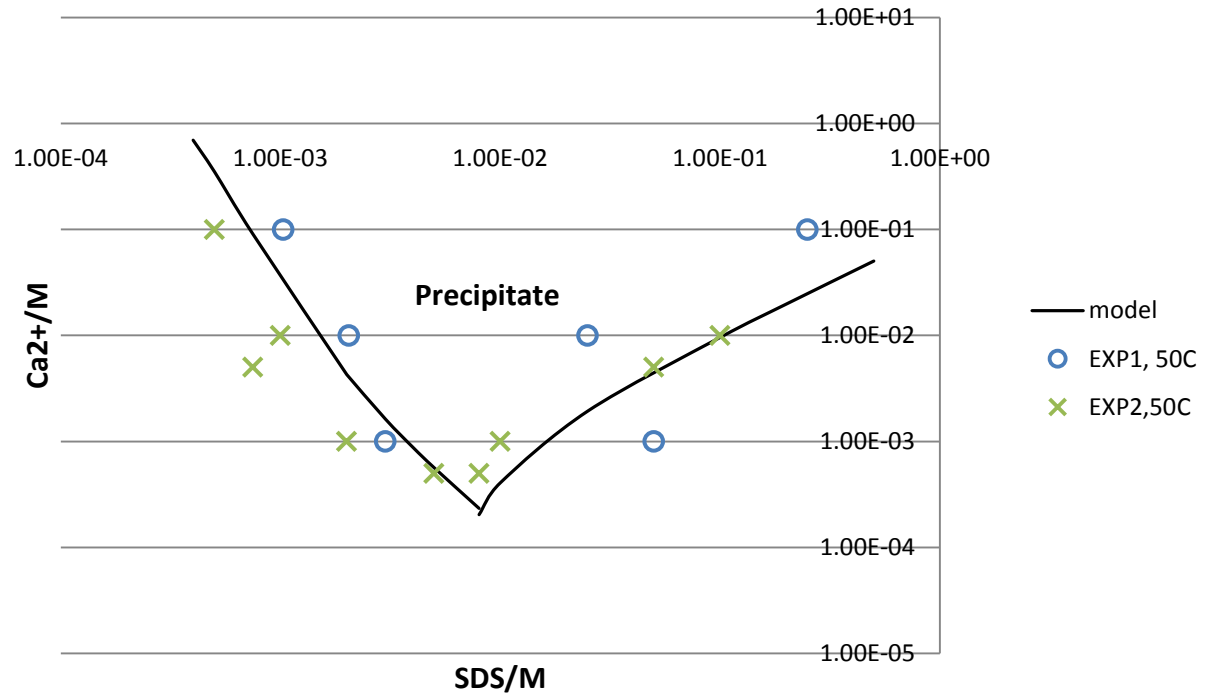

Figure 4.2: Precipitation phase boundary of SDS with calcium ion at 50°C

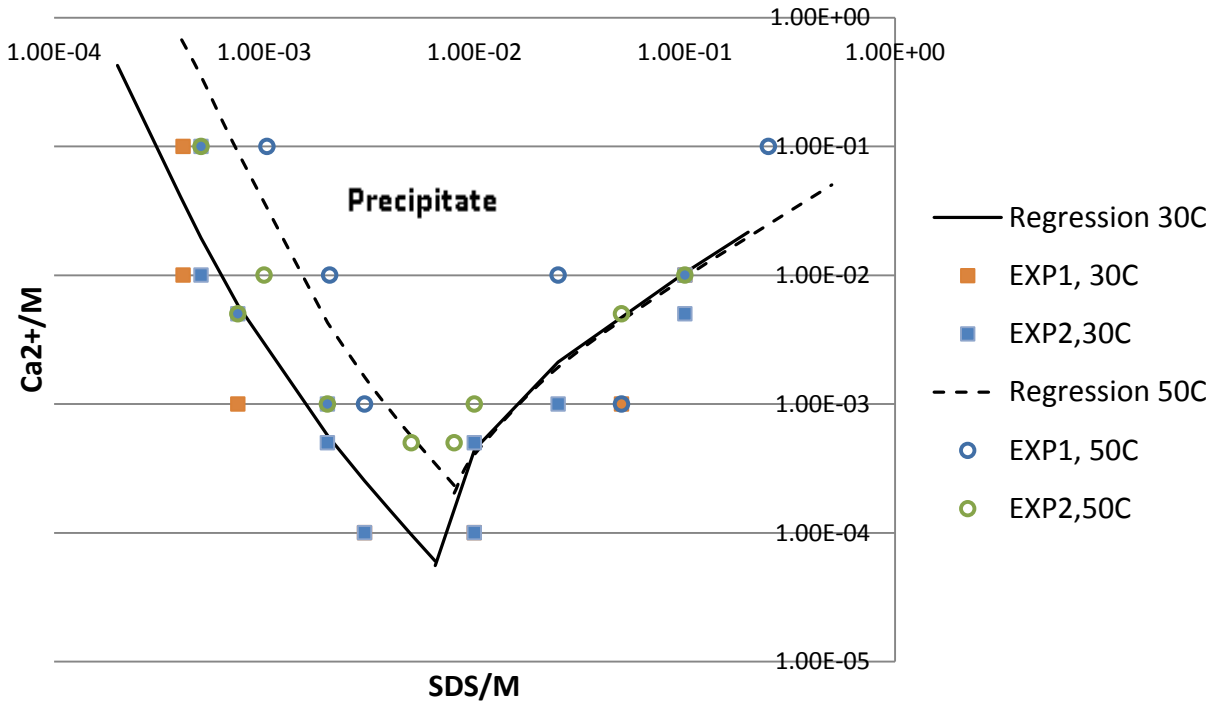

Figure 4.3 Temperature effect on precipitation phase boundary of SDS with calcium ion.

At SDS concentrations below the CMC, $[Ca]^{2+}_{un} = [CaCl_2]$ and $[DS^-]_{mon} = [SDS]$. The K_{sp} can be calculated by fitting the known concentration of $[CaCl_2]$ and [SDS]. Calculation of K_{sp} by minimizing the sum of error $\Sigma(K_{sp} - [Ca^{2+}]_{un} [DS^-]^2_{mon} f_{Ca} f_{DS}^2)$ is shown in Appendix A6 & A9. Value calculated for K_{sp} was 1.55×10^{-9} M^3 at 30°C and $8.58 \times 10^{-9} M^3$ at 50°C. At SDS concentrations above the CMC, the ratio of Ca^{2+} ion concentration bound onto anionic micelles was determined. $\beta_{Ca} = 2[Ca^{2+}]_b/[DS^-]_{mic} = 0.22$ at 30°C and 0.20 at 50°C. Stellner (1989)[1], reported a K_{sp} value of = $5.02 \times 10^{-10} M^3$, and a counter ion binding constant β_{Ca} of = 0.20 and β_{Na}= 0.45 at 30°C. Maneedaeng (2010)[2] showed that the K_{sp} for $Ca(DS)_2$ increases exponentially with temperature:

$$K_{sp} = (1.9369 \times 10^{-10}) + (2.1101 \times 10^{-14}) exp(0.2289T) \quad (4.8)$$

where T is in ^{o}C. From his result, K_{sp} of $Ca(DS)_2$ is calculated as 2.14 x $10^{-10}M^3$ at 30^{o}C and 2.17x$10^{-9}M^3$ at 50^{o}C.

From the figure, we can observe a sudden change in the slope after the CMC. This can be explained by the ability of micelles to compensate for higher concentration of Ca^{2+} counter ion. The higher degree of DS^- ions bound in the micelles, the higher the Ca^{2+} concentration needed to cause precipitation.

4.5.2 Precipitation of SDS by calcium carbonate ($CaCO_3$)

The solubility product for this system was determined to see if any precipitation occurred in the system SDS/$CaCO_3$. The solubility product of $CaCO_3$ at 30^{o}C was reported[3] as 8.7x$10^{-9}M^2$. Thus, constant Ca^{2+} ion concentration is calculated as square root of $K_{sp}(CaCO_3)$ which is 9.33x10^{-5}M. The ionic strength in the solution was expressed as

$$I = 0.5[Ca^{2+}](2)^2 + 0.5\left[{CO_3}^{2-}\right](-2)^2 + 0.5[Na^+](1)^2 + 0.5[DS^-](-1)^2$$

$$I = 4[CaCO_3] + [SDS] = 4\sqrt{Ksp(CaCO_3)} + [SDS] \qquad (4.9)$$

The ionic strength, I, was used to calculate the activity coefficients f_{Ca} and f_{DS}. Before the CMC, $[Ca^{2+}]_{un}\,[DS^-]^2_{mon}\,f_{Ca}\,f_{DS}{}^2$ was computed and compared with experimental K_{sp}. Above the CMC, we compared the critical ratio $2[Ca^{2+}]_b/[DS^-]_{mic}$ with experimental values of β_{Ca}. If $[Ca^{2+}]_{un}\,[DS^-]^2_{mon}\,f_{Ca}\,f_{DS}{}^2 > K_{sp}$ or $2[Ca^{2+}]_b/[DS^-]_{mic} > \beta_{Ca}$, precipitate formed, otherwise the solution was clear. It was calculated that precipitate formed in the range of 5.12 to 6.85x10^{-3}M SDS concentration at 30^{o}C.

4.6 Conclusion

In conclusion, SDS precipitated in the presence of calcium ions forming $Ca(DS)_2$. The phase behavior was shown, and the solubility product K_{sp} and critical ratio of calcium ion to dodecylsulfate anion in the micelles β_{Ca} were obtained by regression fitting. As the result, the model we applied was able to predict the precipitation phase boundary.

List of References

4.7 References

1 K.L. Steller and J.F. Scamehorn, "Hardness Tolerance of Anionic Surfactant Solutions. 1. Anionic Surfactant with Added Monovalent Electrolyte", Langmuir 5, 70-77, 1989

2 Maneedaeng, "Measurement and Modeling of the Solubility of Calcium Dodecylsulfate in Aqueous Solution", 17th TIChE Meeting 2007, Chiang-Mai, Thailand

3 "CRC Handbook of Chemistry and Physics" 53rd Edition, CRC Press: Cleveland Ohio 1972

5.0 SURFACE MODIFICATION OF CALCIUM CARBONATE BY ADMICELLAR POLYMERIZATION

5.1 Introduction

Calcium carbonate ($CaCO_3$) has wide application as mineral filler for polymers, and as an additive in rubber, adhesives, paint and paper, oil and gas drilling fluids etc. $CaCO_3$ usually has a high energy hydrophilic surface which limits the usage in the above mentioned applications. Hence, efforts had been made to modify the surface of $CaCO_3$ including direct methods such as immersion in sodium stearate solution[1], mechanical mixing with hydrophobic compounds[2-4], mechano-activated surface modification in wet ultra-fine grinding systems[5], pH dependent adsorption[6] and by silanation[7]. In this study, the formation of a thin polymer film using admicellar polymerization was attempted in order to modify the $CaCO_3$ surface. Previous work has used admicellar polymerization to obtain ultrathin polypropylene film on $CaCO_3$ surface[8]. In our study, we used sodium dodecyl sulfate (SDS) surfactant and adsolubilized and polymerized styrene to get a polystyrene thin film on the surface.

5.2 Experimental Materials

Different size grades of $CaCO_3$ with average diameter d(0.5) of 8, 26 and 105 µm were obtained from BCI Chemical Sdn. Bhd. SDS biotechnology grade was purchased from Amresco, Solon, Ohio. Styrene 99% was obtained from Acros Organics, New jersey, USA. Azoisobutylnitrile (AIBN) 98% initiator was purchased from Sigma Aldrich, St. Louis, MO.

Preliminary testing of the $CaCO_3$ surface area was obtained using Laser Diffraction method (by supplier) and Brunauer-Emmett-Teller (BET) theory analysis. Results were summarized in Table 5.1. The data observed had very high deviation between the two methods for fine and extra fine $CaCO_3$, up to 41% difference. The deviation contributed may be due to the difference in data interpretation for both method and also the different treatment during the analysis.

	Extra Fine	**Fine**	**Coarse**
Particle size, d(0.5) µm	8.3	26.2	105.0
Specific surface area, m^2/g (Laser Diffraction)	1.74	1.00	0.22
Specific surface area, m^2/g (Nitrogen BET)	1.09/1.776	0.59/0.987	0.28/0.498
Difference %	37	41	27

Table 5.1: Specific surface area of different grade of calcium carbonate: extra fine, fine, and coarse by Laser Diffraction Method and Nitrogen BET analysis.

The $CaCO_3$ particle's surface potential behavior was examined at different pH's and the "point of zero charge" (pzc) determined for the various grades of $CaCO_3$. It was concluded that the pH_{pzc} falls in the range of 10.5-13 (Figure 5.1). Solution with $CaCO_3$ in water exhibited buffer characteristics with an equilibrium pH_{eqm} of ~9. Surface charge on calcium carbonate will be positive at equilibrium and hence anionic surfactant SDS is suitable for achieving admicelle adsorption.

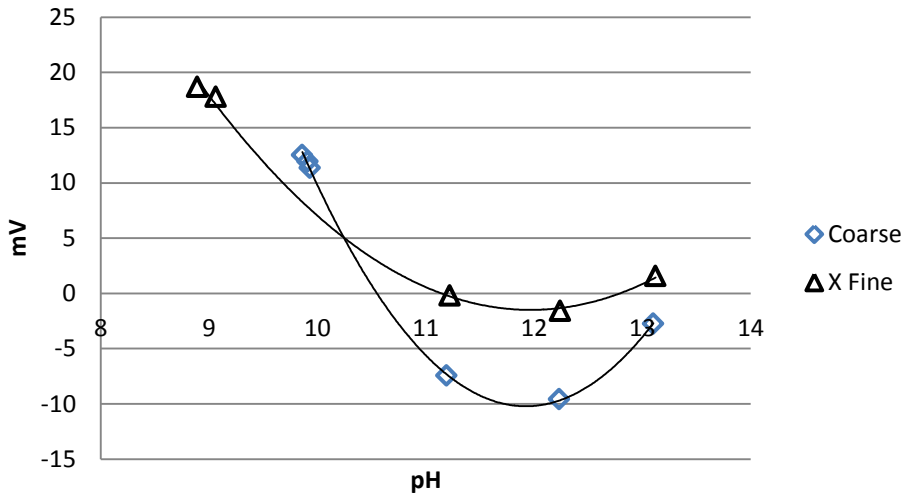

Figure 5.1: Point of zero charge (pzc) measurement of extra fine, coarse $CaCO_3$.

The critical micelle concentration (CMC) of SDS in $CaCO_3$ saturated water was determined to be ~4mM, which is 51% lower than that of pure SDS (Literature data: 8.1mM)[9]. From the slope of surface tension vs. log [SDS] and applying the Gibbs equation, one can also calculate a surface area per molecule (a^s_1) for SDS at saturation of 18.1 $Å^2$/molecule. With both the value for specific surface area of calcium carbonate and surface area per molecule for SDS, the amount of surfactant necessary for monolayer coverage was calculated for each size category of substrate and is summarized in Table 5.2.

Gibbs equation for (1:1) ionic surfactant in swamping electrolyte:

$$\Gamma = -1/(2.606RT) *(\delta\gamma/\delta \log C_1) \quad (5.1)$$

$$a^s_1 = 10^{23}/N\Gamma_1 \quad (5.2)$$

Monolayer calculation (μmol/g)

$$= \frac{\text{Specific surface area of calcium carbonate } \left(\frac{\text{m}^2}{\text{g}}\right)}{\text{Surface area per molecule SDS } \left(\frac{\text{Å}^2}{\text{molecule}}\right)} \times \frac{(10^{10})^2\ \text{Å}^2}{\text{m}^2} \times \frac{10^6 \mu\text{mols}}{6.02 \times 10^{23}\text{molecule}}$$

(5.3)

$\delta\gamma/\delta\log C_1$ is the slope of surface tension vs log SDS concentration plot, γ is in mN/m, R is the gas constant 8.31 J/mol-K, T is the temperature in Kelvin, Γ is in unit of mmol/m^2. N is the Avogrado number 6.02x10^{23}. a^s_1 gives unit of $Å^2$/molecule.

	Extra Fine	Fine	Coarse
Particle size, d(0.5) μm	8.3	26.2	105.0
Monolayer, μmol/g (Laser Diffraction)	32.00	18.39	4.05
Monolayer, μmol/g (Nitrogen BET)	20.71	10.91	4.71
Difference %	35	41	16

Table 5.2: Calculated monolayer coverage (μmol/gm) for extra fine, medium, coarse calcium carbonate.

5.3 Experimental Procedures

In the section mentioned previously (Section 5.2), particle size analysis was done using Malvern Zetasizer and NOVA B.E.T. Surface area analyzer. Malvern Zetasizer Nano ZS was used in PZC measurement. CMC measurements were obtained using the standard ring method in a KSV 70 tensiometer.

Surfactant adsorption experiments were started by preparing increasing concentration of SDS solution via a dilution method on 1 g of $CaCO_3$ solid. Samples were shaken vigorously and left overnight. Solution in the bulk was withdrawn and filtered the next day and the SDS concentration determined by a two-phase titration method described in T. Barr et. al.[10]. The

amount of adsorbed SDS can therefore be obtained by the change in concentration method,

$$n_{ad} = \frac{(C_o - C_1)V}{m} \quad (5.4)$$

n_{ad} is the amount of adsorbed surfactant per gram of adsorbent (mol/g), C_o-C_1 is the difference of surfactant concentration before adsorption and after adsorption, V is the volume of the liquid phase and m is the mass of adsorbent. The adsorption isotherm can then be plotted as adsorbed surfactant versus equilibrium surfactant concentration (Appendix B1 to B3).

Similar steps were used for determining styrene adsolubilization. A series of samples with increasing styrene concentration but constant SDS concentration (equilibrium concentration ~90% CMC) were added to 1g of $CaCO_3$. Samples were shaken vigorously and left overnight. The bulk solution was obtained by syringe filtration and analyzed by Shidmazu UV-VIS spectrophotometer analysis at 281nm. Similarly, the amount of adsolubilized styrene was computed by the change in the concentration method, using a calibration curve to determine the bulk concentration from the UV readings (Appendix B4 to B9).

Once adsorption and adsolubilization data are available, a ratio of SDS:Styrene for polymerization runs was determined. Polymerizations were carried out at various ratio of SDS:Styrene and a ratio of 10:1 for Styrene:AIBN. The solid was dispersed in a solution containing SDS and styrene for 3 hours initially. Next, AIBN was added and left for another 3 hours. Samples were shaken once every hour during these 6 hours. Then, samples were transferred to a 70^{o}C water bath to start polymerization and were allowed to stay in the bath for 3 hours. After polymerization, samples were washed with distilled water at least 5 times to remove accessible surfactant. Samples were dried in the oven at 100^{o}C for overnight and the final product obtained.

Characterization of modified $CaCO_3$ was carried out by Fourier Transform Infrared Spectroscopy (FTIR) and Atomic Force Microscopy (AFM) analysis.

5.4 Result and Discussion

Adsorption isotherm results for SDS on different grades $CaCO_3$ is shown in Figure 5.2. From the figure, we observed the saturated adsorption for extra fine, fine and coarse $CaCO_3$ were 35, 65, 13μmols/gm. It was noted that fine $CaCO_3$ has the highest SDS adsorption even though extra fine $CaCO_3$ has the highest specific surface area. Table 5.3 showed a comparison to the calculated bilayer adsorption with the experimental value from adsorption isotherm. The experiment value showed comparable result to bilayer adsorption calculated from BET specific surface area result except for fine grade $CaCO_3$. A very high deviation from calculated and experimental value (up to 66% difference) was observed for fine $CaCO_3$ for which we have found no explaination.

From the adsorption isotherm (Figure 5.2), we observed SDS adsorption decreases after CMC. We suspected SDS was being precipitated by some calcium ions (Ca^{2+}) and forming calcium dodecylsulfate $Ca(DS)_2$. However, in our of our study on $Ca(DS)_2$ solubility (Chapter 4),

	Extra Fine	Fine	Coarse
Bilayer, μmol/g (Laser Diffraction)	64.00	36.78	8.10
Bilayer, μmol/g (Nitrogen BET)	41.42	21.82	9.42
SDS saturated adsorption, μmol/g	35	65	13

Table 5.3: Comparison between calculated and experimental amount of SDS adsorption on different grade $CaCO_3$.

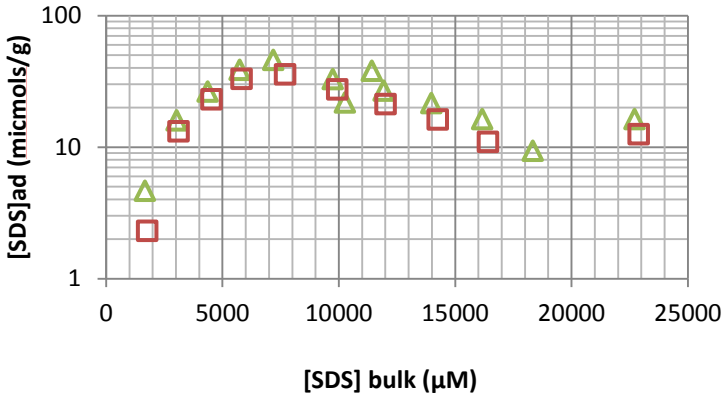

Figure 5.2a: Adsorption isotherm of SDS on extra fine $CaCO_3$.

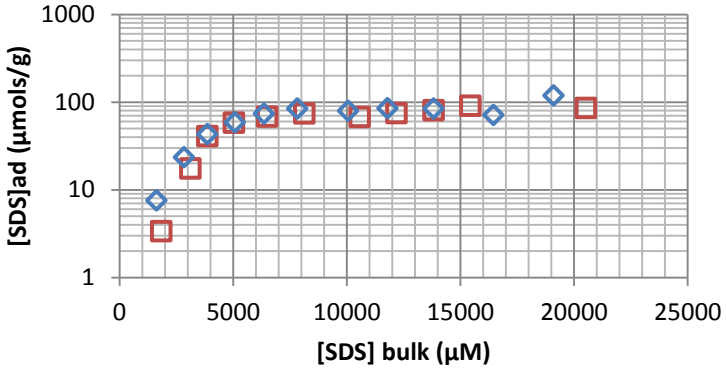

Figure 5.2b: Adsorption isotherm of SDS on fine $CaCO_3$.

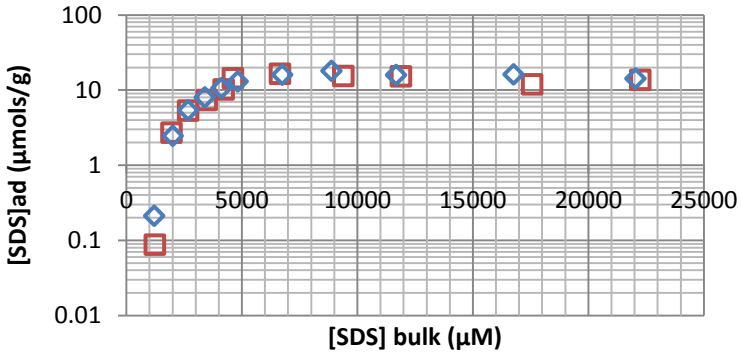

Figure 5.2c: Adsorption isotherm of SDS on coarse $CaCO_3$.

we showed that in fact that the $Ca(DS)_2$ precipitate phase boundary changed dramatically after reaching SDS CMC. The presence of SDS micelles takes up Ca^{2+} ions and reduces precipitation. Thus, the trend observed in adsorption isotherm can be explained to be precipitation and dissolution of $Ca(DS)_2$ which contributed to the adsorption maxima.

After getting saturated amount of SDS on each different calcium carbonate, styrene adsolubilization was obtained (Figure 5.3). Saturated styrene adsolubilization for extra fine, fine, and coarse $CaCO_3$ observed were 20, 20, 7μmol/g. The ratio of adsorbed SDS to styrene (mol/mol) was around 2 except for fine grade $CaCO_3$ which is 3.25. The partition coefficient, K_{adm} for each grades of $CaCO_3$ was calculated and plotted against styrene bulk concentration (Figure 5.4).

$$K_{adm} = \frac{X_{adm}}{C_{eq}} \tag{5.5}$$

$$X_{adm} = \frac{C_{ad}}{C_{ad} + C_{surfad}} \tag{5.6}$$

C_{ad}- styrene concentration in admicelle

C_{eq}- styrene concentration in bulk

C_{surfad}- surfactant adsorbed

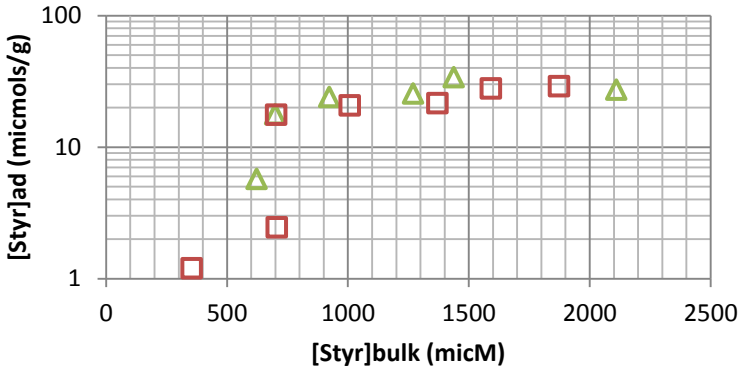

Figure 5.3a: Styrene adsolubilization on extrafine $CaCO_3$ at 35µmols SDS/g.

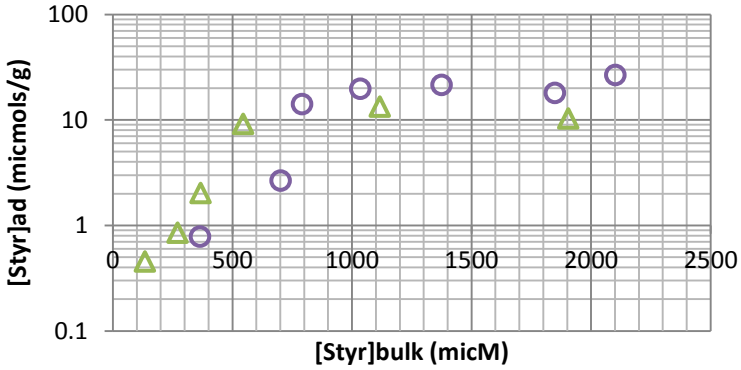

Figure 5.3b: Styrene adsolubilization on fine $CaCO_3$ at 65µmols SDS/g.

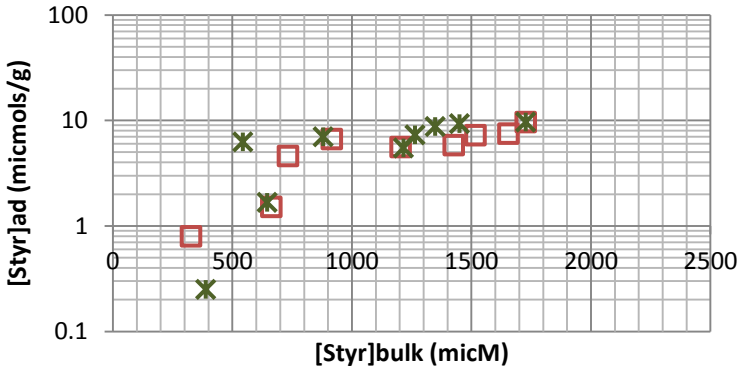

Figure 5.3c: Styrene adsolubilization on coarse $CaCO_3$ at 13µmols SDS/g.

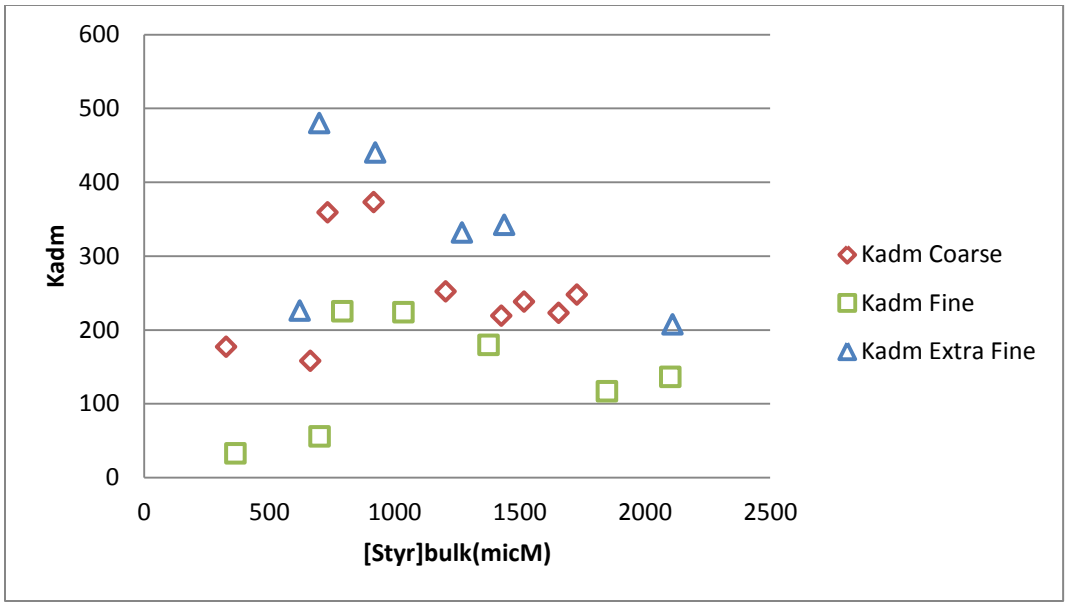

Figure 5.4: Partition coefficient K_{adm} against styrene bulk concentration.

For all three different grades $CaCO_3$, K_{adm} increases when styrene bulk concentration increases suggesting that styrene initially partitioned at the core of the admicelle while at higher styrene bulk concentrations the K_{adm} decreases with styrene bulk concentration, suggesting styrene partitioning into the palisade of the admicelle.[11]

From both the result of adsorption and adsolubilization, admicellar polymerization experimental runs were planned as below (Table 5.4) with the corresponding ratio of SDS adsorbed: Styrene adsolubilized.

	Extra Fine	Fine	Coarse
SDS adsorbed: Styrene adsolubilized (HH)	1.75	3.25	1.86
SDS adsorbed: Styrene adsolubilized (HM)	3.50	6.50	-
SDS adsorbed: Styrene adsolubilized (HL)	5.25	-	-
SDS adsorbed: Styrene adsolubilized (MH)	0.53	0.67	0.31
SDS adsorbed: Styrene adsolubilized (MM)	1.06	1.34	0.62
SDS adsorbed: Styrene adsolubilized (ML)	1.59	2.01	-

Table 5.4: Ratio of SDS adsorbed: Styrene adsolubilized in admicellar polymerization experiment run. (H:high, M:medium, L:low)

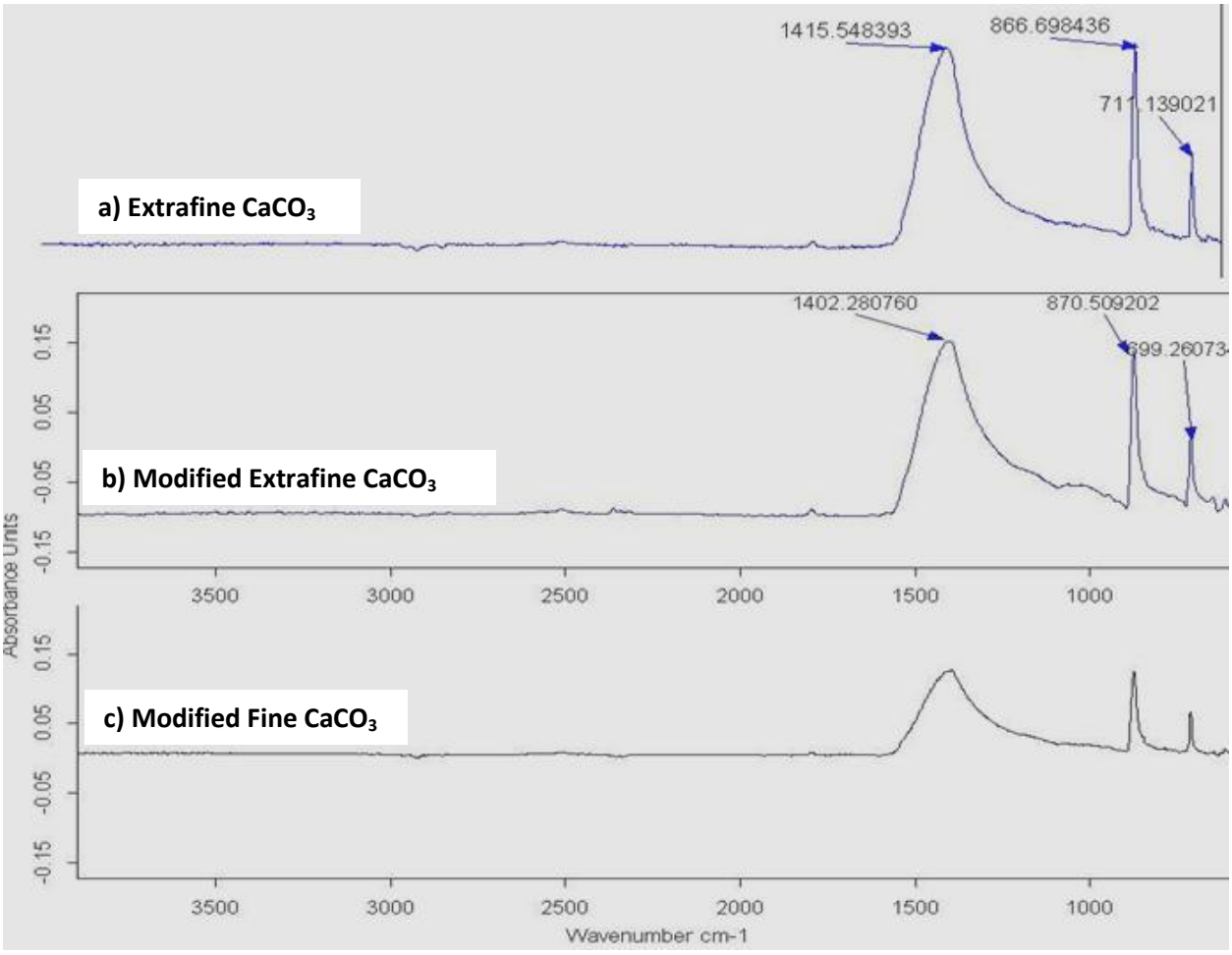

Figure 5.5: FTIR spectrum for $CaCO_3$ before and after admicellar polymerization.

Subsequent characterization by FTIR was done to compare the unmodified and modified calcium carbonate (Figure 5.5). Fundamental bands of calcite were observed at 708 cm^{-1} (ν4 -in-

plane bend), 883 cm^{-1} (ν2 -out-of-plane bend) and at about 1400 - 1500 cm^{-1} (ν3 –asymmetric stretch). Some changes shown at 1060cm^{-1} can be contributed from S-O stretching due to the SDS residue. Overall, no polystyrene absorption in spectrum could be found after admicellar polymerization.

Tapping mode AFM imaging was also performed to check for polystyrene thin film (Figure 5.6 & 5.7). However, no soft polymer phase was observed.

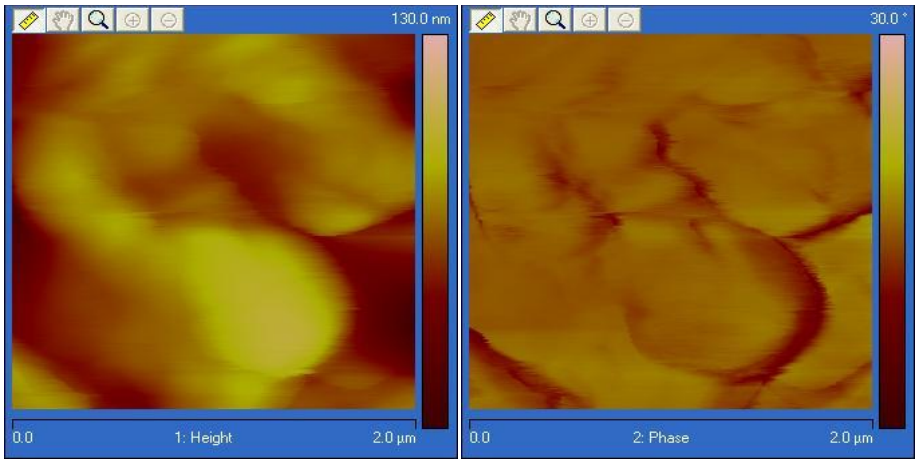

Figure 5.6: AFM image of extrafine $CaCO_3$ after polymerization.

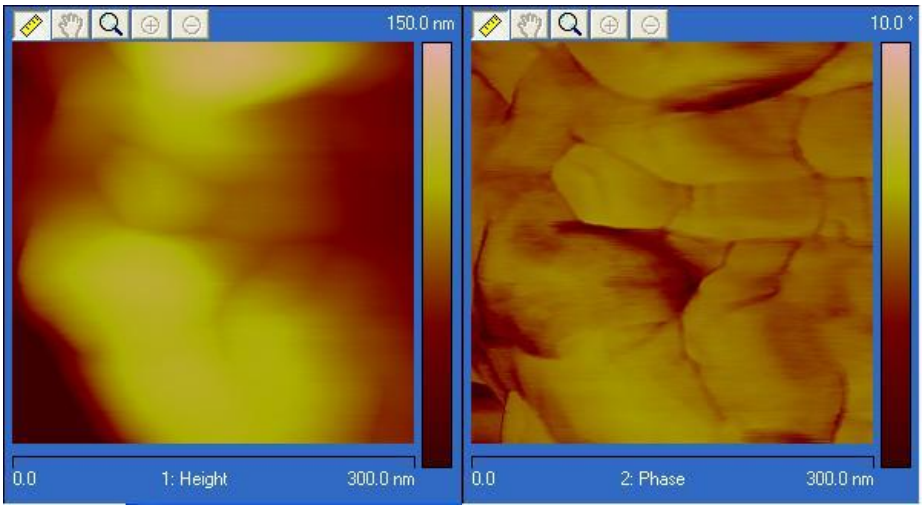

Figure 5.7: AFM image of fine $CaCO_3$ after polymerization.

5.5 Conclusion

SDS adsorption and styrene adsolubilization were observed from adsorption and adsolubilization isotherm. However, attempts to form polystyrene thin films on $CaCO_3$, a relatively soluble and non-porous mineral surface, using admicellar polymerization was found to be unsuccessful. This was in contrary with the result obtained by P. Ruangruang et. al.[8] because the concentration of SDS used in their studies were relatively low and therefore no precipitation issue (discussed in Chapter 4). Negative result shown in final product required further investigation such as using nonionic surfactant (avoid precipitation).

List of References

5.6 References

1. G.G.Wang, L.Q. Zhu, H.C. Liu, W.P. Li, Langmuir dx.doi.org/10.1021/la202613r, 2011.
2. J. Zhang, J. Guo, T. Li, X. Li, "Chemical Surface Modification of Calcium Carbonate Particles by Maleic Anhydride Grafting Polyethylene Wax", International Journal Green Nanotechnology: Physics and Chemistry 1, p65-71, 2010.
3. Z. Hu and Y.Deng, "Superhydrophobic Surface Fabricated from Fatty Acid-Modified Precipitated Calcium Carbonate", Ind. Eng. Chem. Res. 49, p5425-30, 2010.
4. S. Chibowski, "Investigation on Interactions of Sodium Dodecyl Sulfate and Polyacrylamide Molecules on Calcium Carbonate Surfac Using Radiotracer Technique", J. Colloid and Interface Science 76, 2, p371-74, 1980.
5. H. Ding, S. Lu, Y. Deng, G. Du,"Mechano-activated surface modification of calcium carbonate in wet stirred mill and its properties",Trans. Nonferrous Met. Soc. China7,p1100-04,2007.
6. K.A. Razaei Gomari, A.A. Hamouda, "Effect of fatty acids, water composition and pH on the wettability alteration of calcite surface", J. Petroleum Science and Engineering 50.P140-50,2006.
7. R.D. Kurkarni, P.S. Leung, E.D. Goddard, "Oil Dispersion properties of Silanated Calcium Carbonate: A Rheological Study", Colloid and Surfaces 5, p321-32, 1982.
8. P. Rungruang, B.P. Grady, P. Supaphol, "Surface-modified calcium carbonate particles by admicellar polymerization to be used as filler for isotactic polypropylene", Colloids and Surfaces A: Physicochem. Eng. Aspects 275, p114-25, 2006.
9. R.Sowada,"Tenside Surfavtants Detgts. 31" 195 (1994).

10. T. Barr, J. Oliver, W.V. Stubbings, “The determination of surface active agents in solutions”, JSCI 67, p45-48, Feb 1948.
11. J.D. Rouse, D.A. Sabatini, N.E. Deeds, R.E. Brown, J.H Harwell, “Micellar solubilization of unsaturated hydrocarbon concentrations as evaluated by semiequilibrium dialysis”, Environ. Sci. Technol. 29, p2484-89, 1995.

6.0 DRILLING FLUIDS TESTING

6.1 Introduction[1]

Petroleum consists of organic materials derived from animals and plants over millions of years ago. Oil and gas migrated within the permeable strata and became trapped in reservoirs. Oil and gas might be found near sedimentary rocks which consist of carbonate rocks, limestone or dolomites. They can be found in salt domes which result from the deformation of upward rising of salt that trap and accumulate the oil. Many of the reservoirs were found beneath horizontal salt layers. Oil and gas trapped in reservoirs can be categorized as structural (deformation by folding of rock layers) or stratigraphic (geological process due to difference in rock properties).

6.1.1 Drilling methods

An early traditional way in petroleum drilling is called cable tool drilling. An impact tool is dropped to crush the rocks which are retrieved later as cuttings using a bailer. The process is simple but works only for shallow wells and is not time efficient. Another way of drilling is rotary drilling. This type of drilling uses continuous circular motion of drills bits to break rocks and removed cuttings from the bottom of the wellbore up to the surface through an annulus. Here, drilling mud is used to lubricate and keep the bit cool, and to suspend, remove and release cuttings from the wellbore. Drilling mud can be circulated back after removal of cuttings using separation devices such as shale shaker. This process is more advanced with enhanced efficiency. A third method of drilling is called coiled-tubing drilling. This method features

continuous drill string made of steel or composite that is flexible and can be run in and pulled out easily compared to conventional drill pipe which requires assembling and dismantling .

6.1.2 Function of drilling fluids

Drilling fluid has the important functions as below:

- Suspension, removal, and release of cuttings
- Pressure control
- Seal permeable formations
- Well bore stability and minimizing formation damage
- Lubrication, cooling and support of bit and drilling assembly
- Transmit hydraulic energy to tools and bit
- Facilitate cementing and completion
- Minimize impact on environment

6.1.3 Composition of drilling fluids

Drilling fluid can be classified into 3 different types according to its base fluid and constituents[2]:

- Water-based (Fresh water)
    - Solution: True and colloidal, i.e., solids do not separate from water on prolonged standing. Solids in solution with water include: salts (e.g., sodium

chloride, calcium chloride), surfactants (e.g., detergents, flocculants), organic colloids (e.g., cellulosic and acrylic polymers)

  - Emulsion: An oily liquid maintained in small droplets in water by an emulsifying agent (e.g., diesel oil and a film-stabilizing surfactant)
  - Mud: A suspension of solids (e.g., clays, barite, small cuttings) in any of the above liquids, with chemical additives as required to modify properties

- Non-aqueous (Oil: Diesel or crude)
  - Oil mud: A stable oil-base drilling fluid contains: 1. Water-emulsifying agents 2. Suspending agents 3. Filtration-control agents
  - Contains cuttings from the formations drilled. May contain barite to raise density

- Gaseous (Dry gas: Air, natural gas, exhaust gas, combustion gas)
  - Mist: Droplets of water or mud carried in the air stream
  - Foam: Air bubbles surrounded by a film of water containing a foam stabilizing surfactant
  - Stable foam: Foam containing film-strengthening materials, such as organic polymers and bentonite

6.2 Additives in drilling fluids: Review on Calcium Carbonate

Drilling fluid additives play a major role in their applications. Types of additives can be categorized according to their functionality such as: viscosity control, weighting agents, corrosion inhibitors, bacteria control, shale stabilizers, clay stabilizers, formation damage prevention, lost circulation materials, lubricants, surfactants, emulsifiers, defoamers and more.

Our target material calcium carbonate falls into the category of weighting agent and lost circulation material (LCM)/ bridging agent. Often barite is the most common weighting agent but calcium carbonate is preferable when a high density drilling fluid is not required. Calcium carbonate is much cheaper and less abrasive. It is readily soluble in hydrochloric acid which is commonly used to stimulate a production well.

Some review on bridging theory in the past:

- A. Abrams (1977)[3] claimed two guides in selecting proper size and concentration of bridging materials.
    - Median particle size of the bridging materials has to be equal or slightly greater than 1/3 of the median pore size of the formation
    - The concentration of bridging materials has to be at least 5% of the total solids volume on the final mud
- M.A. Dick et. al. (2000)[4] proposed Ideal Packing Theory which can achieve a particle size range with optimum size distribution for improved bridging efficiency in drilling fluids. The theory was derived from $D^{1/2}$ rule by M. Kaeuffer (1973)[5] who proposed that ideal packing occurs when cumulative volume vs. square root of particle's diameter ($D^{1/2}$) has a linear relationship.
- S. Vickers et. al. (2006)[6] later claimed "The Vickers Method" which is an improved theory of Abrams Rule and Ideal Packing Theory. Five criteria that were to fulfill:
    - D90 = largest pore throat
    - D75 < 2/3 of largest pore throat
    - D50 +/- 1/3 of the mean pore throat
    - D25 1/7 of the mean pore throat

- D10 > smallest pore throat

Filtration control is one of the main criteria required in drilling fluids in order to minimize fluid loss, particles invasion and formation damaging. Bailey et. al. (1999)[7] concluded that quick formation of external filter cake and thin internal filter cake are important to avoid lost of solids that plug the surface pores and reduce formation permeability.

M. Aston et. al. (2002)[8] had detail studied the effect of common oil muds additives on fluid loss control. They found 3 major components that play the important role: an emulsified system, fine solids with platey structure (e.g. organophilic clay) and fluid loss control agent. They had pointed out that granular shaped lime or larger particles such as barite and calcium carbonate created filter cake with large void spaces and provide no fluid loss control in a non-viscosified system. Emulsion and solid materials give better performance when both were present. Despite the function of fluid loss additives, they cannot replaced clay solids and emulsion system. Low oil/water ratio was preferable with proper control on viscosity changes. They proposed the mechanism of oil flowing through the interfacial region between particles/droplets from the filter cake permeability.

M.C. Goud (2006)[9] studied the combined use of graphite and calcium carbonate to strengthen the oil-well formation. The group discussed the ability of graphite to seal the fractures and followed by calcium carbonate to hold the mouth of the fracture opening. The study showed the possibility to drill through challenging wellbore with small operational window of pore pressure and fracture pressure by well monitoring the use of bridging and sealing agents with the correct size and concentration accordingly.

Omland et. al. (2007)[10] optimized the particle concentration and size distribution using solids control equipment. The bridging particles used were mixtures of calcium carbonate, graphite and nutshells. They pointed out the importance of continuous control of correct concentration and size distribution upon using the solids control equipment in the field.

S. Vickers et.al. (2007)[11] verified that a fluid formulation with graphite, calcium carbonate and sulphonated asphalt reduced the risk of large filtrate invasion and minimized pore pressure transmission. The presence of graphite has the largest effect on fluid loss control and increasing return permeability. A fluid containing all three components proved to have the best return permeability in their studies.

Z. Li et. al. (2011)[12] tested on the effect of particle distribution and surface modification of calcium carbonate to the drill-in fluid's performance. Optimum blend of various sized calcium carbonate was achieved with design software based on $D^{1/2}$ theory of Ideal Packing Theory. Among the surface active agents and coupling agents used to modified calcium carbonate's surface, stearic acid provides the best modification effect. They claimed that the organophilic passageway in the filter cake formed by the modified calcium carbonate increases the permeability for oil and gas during production. They concluded that optimization of calcium carbonate particle size distribution according to Ideal Packing Theory and modified surface nature of calcium carbonate can lead to high performance drilling fluids with good fluid loss control and return permeability.

In our study, we tested the performances of our laboratory made admicellar polymerized $CaCO_3$ in drilling fluids. Modified and unmodified $CaCO_3$ were mixed in low and high content $CaCO_3$ mud formulation and the rheology and fluid loss properties were compared.

6.3 Experimental materials

Oil-based drilling fluids were made with: base oil (Escaid 110), primary emulsifier (LT3), secondary emulsifier (S-emul), lime, organophilic clay (BENTONE 38 and GELTONE), drill water, calcium chloride ($CaCl_2$), and calcium carbonate ($CaCO_3$) in range of particles sizes stated in Table 6.1. Complete formulations were summarized in Table 6.2 & 6.3.

	d(0.1)	d(0.5)	d(0.9)
$CaCO_3$ (C)	26.3	105.0	284.6
$CaCO_3$ (F)	2.3	26.2	66.2
$CaCO_3$ (XF)	1.2	8.3	17.6
Modified $CaCO_3$ (C)	8.9	74.5	324.6
Modified $CaCO_3$ (F)	2.9	23.5	74.0
Modified $CaCO_3$ (XF)	1.7	10.4	20.7

Table 6.1: Particle size distribution for $CaCO_3$ and modified $CaCO_3$ (as in Chapter 5) used in the mud testing.

Equipment used in the testing included: OFITE Metal Mud Balance (#115-00-10) for density measurement, OFITE Electrical Stability Meter, Hamilton Beach Mixers for mud mixing, Fann Series 35 Viscometer for rheology testing, OFITE aging cell, roll oven, and high-temperature high-pressure (HTHP) filter press for fluid loss measurement.

6.4 Experimental procedures

Mud was prepared according to standard formulation; one containing high $CaCO_3$ content and another low $CaCO_3$ content (Table 6.2 & 6.3). Mud was prepared using commercial available $CaCO_3$, (Control) or with modified $CaCO_3$, (Sample). Each mud testing involved the following steps:

1. Mix the mud appropriately. (Table 6.2 & 6.3)
2. Check mud density and viscosity before hot roll.

3. Pour the mud into aging cell and place in the hot rolling oven at 275^{o}F for 16 hours.
4. Cool the mud to room temperature and mud density and rheology are tested after hot roll. Measure electrical stability value (ESV) of the mud.
5. Perform HTHP filtration test with testing condition of 275^{o}F and 500psi differential pressure. Report fluid loss results as 2 times the volume of fluid obtained in 30mins and measure the filter cake thickness.

6.5 Results and discussions

Results for mud properties are collected in Table 6.4 and 6.5 and summarized in Figure 6.1. Plastic viscosity (PV) and yield point (YP) are the parameters of the Bingham plastic model. PV is the slope of the shear-stress/shear-rate curve when extrapolated to infinite shear rate. It is a measure of fluid's resistance to flow caused by mechanical friction between solids-solids, solids-liquids and shearing layers of the mud itself.[13] Hence, mud density is increased by the addition of weighting agent (eg. $CaCO_3$, barite), this in turn increases PV (viscous and high concentration of solids). However, high PV means a high frictional pressure at the annulus which might lead to formation damage. Therefore, PV is an indication of solids control in the mud system. YP is the yield stress extrapolated to zero shear rate. It is a measure of the electro-chemical attractive forces between particles within the mud under flowing conditions. It is a function of the surface properties and volume concentration of the mud solids.[13] It can be used to interpret the mud's carrying capacity to lift cuttings out from the annulus.

High density, high PV and high YP were observed in high $CaCO_3$ content formulation which is expected due to abundance of $CaCO_3$. PV reduced after hot roll showed the effect of temperature treatment to viscosity change in mud. Sample A showed a slightly higher PV (48cP) than Control A (38cP) but both have same YP. Higher PV may be due to increase in ultra-fine

drill solid content in the sample mud caused by friction during hotroll. Overall, both have rather the same properties (HTHP fluid loss= 3.6ml).

For low $CaCO_3$ content mud, lower mud density was obtained (mud weight for Sample B is 10.2 pounds per gallon). Both muds became thicker after temperature treatment. Both have the same PV, however Sample B has a higher YP (73 $lb/100ft^2$) compared to Control B (54 $lb/100ft^2$). This is due to Sample B has overall higher viscosity than Control B. Higher YP can be explained by neutralization of negative charges in clay particles and hydrophobic surface properties of modified $CaCO_3$ bringing the particles closer resulting in flocculation.[13] This indeed showed that the effect of surface modification $CaCO_3$ contributed to the rheology difference between Control B and Sample B. In addition, HTHP fluid loss proved to be improved from 4ml (Control B) to 3.2 ml (Sample B). Organophilic passageway discussed by Z. Li et. al.(2011)[12] can be used to better explain fluid loss control when hydrophobic surface- modified $CaCO_3$ formed a thin filter cake that restrict the water from passing through.

6.6 Conclusions

Based on the observation of low content $CaCO_3$ mud, we are able to compare readily available $CaCO_3$ and surface-modified $CaCO_3$. The hydrophobic surface properties of modified $CaCO_3$ indeed increase mud's viscosity and give higher YP. An organophilic passageway of filter cake was formed and provided good fluid loss control.

MIXING PROCEDURE									
PRODUCT NAME	**Mixing Procedure**	**S. G.**	**% Vol.**	**lb/bbl**	**350 mL**	**Scale down**	**Weight gram**	**Mixing Time**	**Mixer Speed**
Escaid 110	**1**	**0.800**	1.103	124.99	156.24	124.99	100.00	5	
LT3	**2**	**0.940**	0.400	10.00	56.70	53.30	50.10		Low
Lime	**3**	**2.200**	0.019	6.00	2.73	6.00	13.20	5	Low
BENTONE 38	**4**	**2.200**	0.013	4.00	1.82	4.00	8.80	5	Low
Drill Water	**5**	**1.000**	0.368	52.08	52.08	52.08	52.08	10	Low
GELTONE	**6**	**1.700**	0.025	6.00	3.53	6.00	10.20	10	Low
S-emulsifier	**7**	**0.940**	0.013	1.00	1.89	1.78	1.67		
$CaCl_2$	**8**	**1.700**	0.095	23.00	13.53	23.00	39.10	10	Low
$CaCO_3$(XF)	**9**	**2.700**	0.086	33.00	12.22	33.00	89.10	10	High
$CaCO_3$ (F)	**10**	**2.700**	0.261	100.00	37.04	100.00	270.00	10	High
$CaCO_3$ (C)	**11**	**2.700**	0.086	33.00	12.22	33.00	89.10	10	High
				393.08	141.68	**10.41**	**Mud weight**		
Remarks:				**Vol mL**	**350.00**	**1.25**			
				Low Speed				75	Low
				High Speed				10	High
				Total minutes				85	Min.
				Hot Static	-	°F	Formulation No.		
				Hot Rolling	275	°F	Date:		
				Hours Run	16	hours	Tested by:		

Table 6.2: Mud formulation with high $CaCO_3$ content

MIXING PROCEDURE									
PRODUCT NAME	**Mixing Procedure**	**S. G.**	**% Vol.**	**lb/bbl**	**350 mL**	**Scale down**	**Weight gram**	**Mixing Time**	**Mixer Speed**
Escaid 110	**1**	**0.800**	1.696	144.73	180.91	144.73	115.78	5	
LT3	**2**	**0.940**	0.499	50.09	53.29	50.09	47.08		Low
Lime	**3**	**2.200**	0.024	5.64	2.56	5.64	12.41	5	Low
BENTONE 38	**4**	**2.200**	0.024	5.64	2.56	5.64	12.41	5	Low
Drill Water	**5**	**1.000**	0.567	60.52	60.52	60.52	60.52	10	Low
GELTONE	**6**	**1.700**	0.041	7.52	4.42	7.52	12.78	10	Low
S-emulsifier	**7**	**0.940**	0.017	1.67	1.78	1.67	1.57		
$CaCl_2$	**8**	**1.700**	0.119	21.62	12.72	21.62	36.75	10	Low
$CaCO_3$(XF)	**9**	**2.700**	0.018	5.07	1.88	5.07	13.70	10	High
$CaCO_3$ (F)	**10**	**2.700**	0.053	15.22	5.64	15.22	41.11	10	High
$CaCO_3$ (C)	**11**	**2.700**	0.018	5.07	1.88	5.07	13.70	11	High
Barite	**12**	**4.200**	0.205	91.72	21.84	91.72	385.24	10	High
				414.52	106.68	**9.87**	**Mud weight**		
Remarks:				**Vol mL**	**350.00**	**1.18**			
				Low Speed				86	Low
				High Speed				10	High
				Total minutes				96	Min.
				Hot Static	-	°F	Formulation No.		
				Hot Rolling	275	°F	Date:		
				Hours Run	16	hours	Tested by:		

Table 6.3: Mud formulation with low $CaCO_3$ content

Mud Properties		Control A		Sample A	
		BHR	AHR	BHR	AHR
Mud Weight	**ppg**	10.8	10.9	11.1	11.1
600 rpm		256	201	239	221
300 rpm		192	163	170	173
200 rpm		157	140	141	146
100 rpm		115	112	102	113
6 rpm		47	56	39	58
3 rpm		41	51	34	53
Plastic Viscosity	**cp**	64	38	69	48
Yield Point	**lb/100ft^2**	128	125	101	125
Gel Strength	**10 sec**	39	46	35	48
Gel Strength	**10 min**	53	45	45	47
HTHP, 275^{o}F/600psi	**ml**		3.6		3.6
HTHP Filter Cake	**cm**		0.2		0.3
ESV, 120^{o}F	**volt**	1287	534	800	654

Table 6.4: Mud properties with high $CaCO_3$ content.
BHR= before hot roll, AHR= after hot roll 275^{o}F 16hrs.

Mud Properties		Control B		Sample B	
		BHR	AHR	BHR	AHR
Mud Weight	**ppg**	10.2	10.0	10.2	10.2
600 rpm		80	114	78	141
300 rpm		51	84	46	107
200 rpm		40	71	34	91
100 rpm		27	56	20	72
6 rpm		9	29	4	39
3 rpm		8	10	3	36
Plastic Viscosity	**cp**	29	30	32	34
Yield Point	**lb/100ft^2**	22	54	14	73
Gel Strength	**10 sec**	9	26	3	32
Gel Strength	**10 min**	11	29	8	32
HTHP, 275^{o}F/600psi	**ml**		4.0		3.2
HTHP Filter Cake	**cm**		0.2		0.2
ESV, 120^{o}F	**volt**	185	517	206	583

Table 6.5: Mud properties with low $CaCO_3$ content.
BHR= before hot roll, AHR= after hot roll 275^{o}F 16hrs

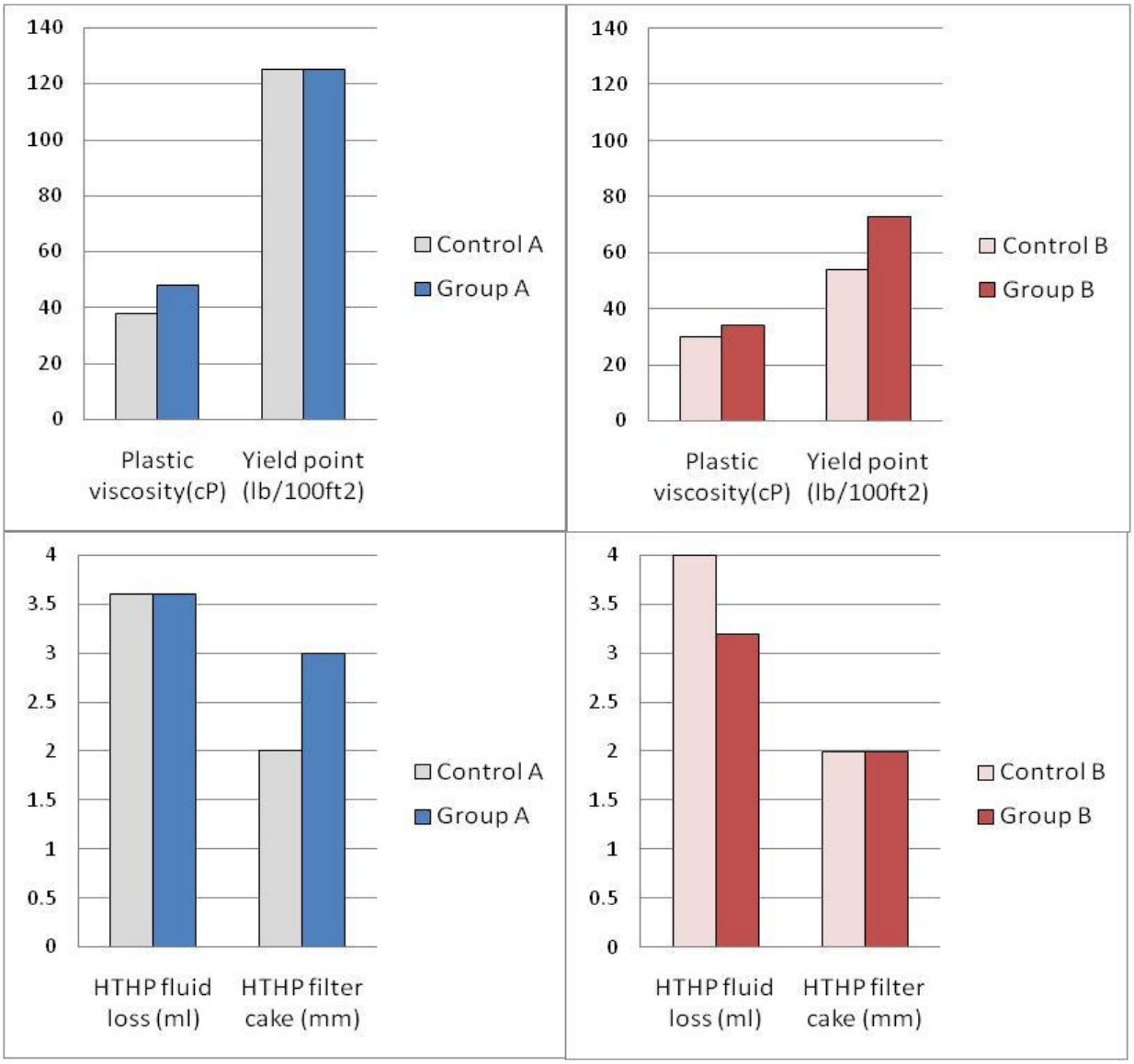

Figure 6.1: Comparison of mud properties (plastic viscosity/cP, yield point/(lb/100ft^2), HTHP fluid loss/ml, HTHP filter cake/mm) after hot roll 275^{o}F 16hrs.
A: High $CaCO_3$ content mud
B: Low $CaCO_3$ content mud

List of References

6.7 References

1. Magcobar, “Handbook of drill fluids”, 1998
2. C. Ryen, H.C.H. Darley, G. R. Gray, “Composition and Properties of Drilling and Completion Fluids” (6th Edition). Saint Louis, MO, USA: Gulf Publishing Company, (2011) p22
3. A. Abrams, “Mud Design to Minimize Rock Impairment due to Particle Invasion”, J. Petroleum Technology (1977) p586-92
4. Dick, M.A., Heinz, T.J., Svoboda, C.F., Aston, M., “Optimizing the Selection of Bridging Particles for Reservoir Drilling Fluids”, SPE 58793, 2000 SPE International Symposium on Formation Damage, Lafayette, LA, 23-24 February 2000.
5. Kaeuffer, M., Determination de L’Optimum deRemplissage Granulometrique et Quelques proprieties S’y Rattachant,: presented at Congres International de I’A.F.T.P.v., Rouen, Oct. 1973.
6. S. Vickers, M. Cowie, T. Jones, A. J. Twynam, “A new methodology that surpasses current bridging theories to efficiently seal a varied pore throat distribution as found in natural reservoir formations”, AADE-06-DF-HO-16 (2006)
7. L. Bailey, E.S. Boek, S.D>M. Jacques, T. Boassen, O.M. Selle, J-F. Argillier, D.G. Longeron, “Particulate Invasion From Drilling Fluids”, SPE Journal, V.5 No.4 (2000), p412-19
8. M. Aston, P. Mihalik, J. Tunbridge, BP Exploration, S. Clarke, BP Institute Cambridge, “Towards Zero Fluid Loss Oil Based Muds”, SPE 77446 (2002)
9. M.C. Goud, G. Joseph, “Drilling Fluid Additives and Engineering to Improve Formation Integrity”, SPE/IADC 104002 (2006)

10. T.H. Omland, B. Dahl, A. Saasen, K. Taugbol, P.A. Amundsen, “Optimization of Solids Control Opens Up Opportunities for Drilling of Depleted Reservoirs”, SPE 110544 (2007)
11. S. Vickers, M. Cowie, M. Burgess, D. Anderson, “The Application of Specifically Formulated Bridging Materials to Successfully Reduce Pore Pressure Transmission to Enable Depleted Fractured Reservoirs to be Drilled and Produces Without Incurring Formation Damage”, SPE 107753 (2007)
12. Z. Li, J. Yan, G. Jiang, S. Xie, Y. Fu, W. Zang, S. Yang, “The Research on Smart Drill-in Fluid Design”, Advanced Materials Research V.146-47 (2011) p1075-79
13. Bakers Hughes INTEQ, “Drilling Engineering Workbook”, Dec 1995, Chapter 1, p26-29

List of Appendices

Appendix A

A1: Phase boundary SDS-Ca^{2+} at 30°C (Test1)

Phase boundary SDS-Ca^{2+} at 30°C (Test1)

	M	Vol(mL)	MW	wt(g)
STOCK SDS	1	25	288.38	7.2095
10xdil SDS	0.1			
25xdil SDS	0.041096			
100xdil SDS	0.01			
STOCK CaCl2	1	250	110.98	27.745
10xdil CaCl2	0.1			
100xdil CaCl2	0.01			
1000xdil CaCl2	0.001			
10000xdil CaCl2	0.0001			
Total vol/ml	10			

clear
precipitate

				H	F	D	B	
				20	20	20	20	
			[Ca2+]stk/ml	1000xdil	100xdil	10xdil	STK CaCl2	
				1	1	1	1	ml
[SDS]/M		stk sds/ml	Dil/ml	1.00E-04	1.00E-03	**[SDS] in B&D** 1.00E-02	1.00E-01	M
0	100xdil SDS	0.00	9.00			0.00E+00		
1.00E-04		0.10	8.90			1.00E-04		
2.50E-04		0.25	8.75			2.50E-04		
5.00E-04		0.50	8.50			4.11E-04		
7.50E-04		0.75	8.25			1.03E-03		
1.00E-03		1.00	8.00			2.05E-03		
2.00E-03		2.00	7.00			3.08E-03		
3.00E-03		3.00	6.00			4.11E-03		
4.00E-03		4.00	5.00			8.22E-03		
5.00E-03		5.00	4.00			1.23E-02		
6.00E-03	10xdil SDS	0.60	8.40			1.64E-02		
7.00E-03		0.70	8.30			2.05E-02		
8.00E-03		0.80	8.20			...		
9.00E-03		0.90	8.10			...		
1.00E-02		1.00	8.00			...		
2.50E-02		2.50	6.50			2.50E-02		
5.00E-02		5.00	4.00			5.00E-02		
7.50E-02	STK SDS	0.75	8.25			7.50E-02		
1.00E-01		1.00	8.00			1.00E-01		
2.50E-01		2.50	6.50			2.50E-01		
5.00E-01		5.00	4.00			5.00E-01		

A2: Phase boundary SDS-Ca^{2+} at 30°C (Test2)

Phase boundary SDS-Ca^{2+} at 30°C (Test2)

	M	Vol(mL)	MW	wt(g)
STOCK SDS	1	100	288.38	28.838
10xdil SDS	0.1			
25xdil SDS	0.041096			
100xdil SDS	0.01			
STOCK CaCl2	1	250	110.98	27.745
10xdil CaCl2	0.1			
100xdil CaCl2	0.01			
1000xdil CaCl2	0.001			
10000xdil CaCl2	0.0001			
Total vol/ml	10			

					H	G	F	E	D	B	
					20	10	20	100	20	20	
				[Ca2+]stk/ml	**1000xdil**	**100xdil**			**10xdil**	**STOCK CaCl2**	
					1	**0.5**	**1**	**5**	**1**	**1**	**ml**
	[SDS]/M		stk sds/ml	Dil/ml	1.00E-04	5.00E-04	1.00E-03	5.00E-03	1.00E-02	1.00E-01	**M**
0	0	**100xdil SDS**	0.00	9.00							
1	1.00E-04		0.10	8.90							
2	2.50E-04		0.25	8.75							
3	5.00E-04		0.50	8.50							
4	7.50E-04		0.75	8.25							
5	1.00E-03		1.00	8.00							
6	2.00E-03		2.00	7.00							
7	3.00E-03		3.00	6.00							
8	4.00E-03		4.00	5.00							
9	5.00E-03		5.00	4.00							
			16.60								
10	6.00E-03	**10xdil SDS**	0.60	8.40							
11	7.00E-03		0.70	8.30							
12	8.00E-03		0.80	8.20							
13	9.00E-03		0.90	8.10							
14	1.00E-02		1.00	8.00							
15	2.50E-02		2.50	6.50							
16	5.00E-02		5.00	4.00							
			11.50								
17	7.50E-02		0.75	8.25							
18	1.00E-01		1.00	8.00							
19	2.50E-01		2.50	6.50							
20	5.00E-01		5.00	4.00							
			9.25								

A3: Phase boundary SDS-Ca^{2+} at 50°C (Test1)

Phase boundary SDS-Ca^{2+} at 50°C (Test1)

	M	Vol(mL)	MW	wt(g)
STOCK SDS	1	25	288.38	7.2095
10xdil SDS	0.1			
25xdil SDS	0.041096			
100xdil SDS	0.01			
STOCK CaCl2	1	250	110.98	27.745
10xdil CaCl2	0.1			
100xdil CaCl2	0.01			
1000xdil CaCl2	0.001			
10000xdil CaCl2	0.0001			
Total vol/ml	10			

clear
precipitate

				H	F		D	B	
				20	20		20	20	
				1000xdil	**100xdil**		**10xdil**	**STK CaCl2**	
			[Ca2+]stk/ml	**1** 1.00E-04	**1** 1.00E-03	**[SDS]/M in B&D**	**1** 1.00E-02	**1** 1.00E-01	**ml** **M**
[SDS]/M		stk sds/ml	Dil/ml						
0	**100xdil SDS**	0.00	9.00			0.00E+00			
1.00E-04		0.10	8.90			1.00E-04			
2.50E-04		0.25	8.75			2.50E-04			
5.00E-04		0.50	8.50			4.11E-04			
7.50E-04		0.75	8.25			1.03E-03			
1.00E-03		1.00	8.00			2.05E-03			
2.00E-03		2.00	7.00			3.08E-03			
3.00E-03		3.00	6.00			4.11E-03			
4.00E-03		4.00	5.00			8.22E-03			
5.00E-03		5.00	4.00			1.23E-02			
6.00E-03	**10xdil SDS**	0.60	8.40			1.64E-02			
7.00E-03		0.70	8.30			2.05E-02			
8.00E-03		0.80	8.20			…			
9.00E-03		0.90	8.10			…			
1.00E-02		1.00	8.00			…			
2.50E-02		2.50	6.50			2.50E-02			
5.00E-02		5.00	4.00			5.00E-02			
7.50E-02	**Stk SDS**	0.75	8.25			7.50E-02			
1.00E-01		1.00	8.00			1.00E-01			
2.50E-01		2.50	6.50			2.50E-01			
5.00E-01		5.00	4.00			5.00E-01			

A4: Phase boundary SDS-Ca^{2+} at 50°C (Test2)

Phase boundary SDS-Ca^{2+} at 50°C (Test2)

	M	Vol(mL)	MW	wt(g)
STOCK SDS	1	100	288.38	28.838
10xdil SDS	0.1			
25xdil SDS	0.04109589			
100xdil SDS	0.01			
STOCK CaCl2	1	250	110.98	27.745
10xdil CaCl2	0.1			
100xdil CaCl2	0.01			
1000xdil CaCl2	0.001			
10000xdil CaCl2	0.0001			
Total vol/ml	10			

					H	G	F	E	D	B	
					20	10	20	100	20	20	
				[Ca2+]stk/ml	**1000xdil**	**100xdil**			**10xdil**	**STOCK CaCl2**	
					1	**0.5**	**1**	**5**	**1**	**1**	**ml**
	[SDS]/M		stk sds/ml	Dil/ml	1.00E-04	5.00E-04	1.00E-03	5.00E-03	1.00E-02	1.00E-01	**M**
0	0	**100xdil SDS**	0.00	9.00							
1	1.00E-04		0.10	8.90							
2	2.50E-04		0.25	8.75							
3	5.00E-04		0.50	8.50							
4	7.50E-04		0.75	8.25							
5	1.00E-03		1.00	8.00							
6	2.00E-03		2.00	7.00							
7	3.00E-03		3.00	6.00							
8	4.00E-03		4.00	5.00							
9	5.00E-03		5.00	4.00							
			16.60								
10	6.00E-03	**10xdil SDS**	0.60	8.40							
11	7.00E-03		0.70	8.30							
12	8.00E-03		0.80	8.20							
13	9.00E-03		0.90	8.10							
14	1.00E-02		1.00	8.00							
15	2.50E-02		2.50	6.50							
16	5.00E-02		5.00	4.00							
			11.50								
17	7.50E-02		0.75	8.25							
18	1.00E-01		1.00	8.00							
19	2.50E-01		2.50	6.50							
20	5.00E-01		5.00	4.00							
			9.25								

A5: Precipitate boundarySDS-Ca^{2+} at 30^{o}C Test 1&2

Precipitate boundary at 30C (Exp1&2)

EXP1, 30C

Ca/M	SDS/M
1.00E-04	3.00E-03
1.00E-04	1.00E-02
1.00E-03	7.50E-04
1.00E-03	5.00E-02
1.00E-02	4.11E-04
1.00E-02	1.00E-01
1.00E-01	4.11E-04
1.00E-01	

EXP2,30C

Ca/M	SDS/M
1.00E-04	3.00E-03
1.00E-04	1.00E-02
5.00E-04	2.00E-03
5.00E-04	1.00E-02
1.00E-03	2.00E-03
1.00E-03	2.50E-02
5.00E-03	7.50E-04
5.00E-03	1.00E-01
1.00E-02	5.00E-04
1.00E-02	1.00E-01
1.00E-01	5.00E-04
1.00E-01	

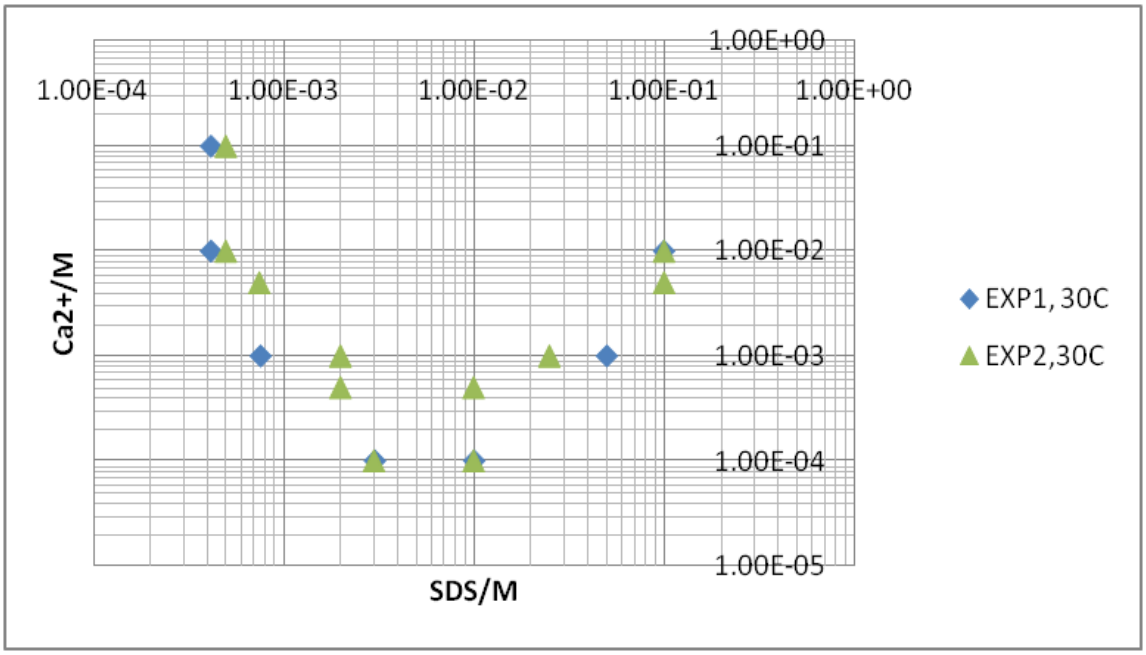

A6: Regression of $Ca(DS)_2$ K_{sp} (1.55E-9M^3) and β_{Ca} (0.22) at 30°C

Regression Ksp before and after CMC (30 C)

BEFORE CMC			
Ca/M	**logCa**	**SDS/M**	**logSDS**
1.00E-04	-4.00E+00	3.00E-03	-2.52E+00
1.00E-03	-3.00E+00	7.50E-04	-3.12E+00
1.00E-02	-2.00E+00	4.11E-04	-3.39E+00
1.00E-01	-1.00E+00	4.11E-04	-3.39E+00

1.00E-04	-4.00E+00	3.00E-03	-2.52E+00
5.00E-04	-3.30E+00	2.00E-03	-2.70E+00
1.00E-03	-3.00E+00	2.00E-03	-2.70E+00
5.00E-03	-2.30E+00	7.50E-04	-3.12E+00
1.00E-02	-2.00E+00	5.00E-04	-3.30E+00
1.00E-01	-1.00E+00	5.00E-04	-3.30E+00
1.00E-01	-1.00E+00		

REGRESSION 30C				
I	logfCa	logfDS	Ca*DS2*fca*fDS2	Ksp-Ca*DS2*fca*fDS2
3.30E-03	-1.06E-01	-2.61E-02	6.25E-10	9.22E-10
3.75E-03	-0.112278	-2.76E-02	3.83E-10	1.16E-09
3.04E-02	-0.266526	-6.39E-02	6.81E-10	8.66E-10
3.00E-01	-0.540564	-1.24E-01	2.74E-09	-1.20E-09

3.30E-03	-0.106035	-2.61E-02	6.25E-10	9.22E-10
3.50E-03	-0.10887	-2.68E-02	1.38E-09	1.71E-10
5.00E-03	-0.127516	-3.12E-02	2.58E-09	-1.04E-09
1.58E-02	-0.206668	-5.00E-02	1.39E-09	1.59E-10
3.05E-02	-0.266816	-6.40E-02	1.01E-09	5.40E-10
3.01E-01	-0.540603	-1.24E-01	4.06E-09	-2.51E-09
			Min Error	0.00E+00
			Ksp	1.55E-09
		Ref. 1	Stellner 1989	5.02E-10
				w swamping NaCl
		Ref. 2	Maneedaeng	2.13948E-10

	CMCsds	6.00E-03
AFTER CMC		
Ca/M	**SDS/M**	**SDSmic**
1.00E-04	1.00E-02	4.00E-03
1.00E-03	5.00E-02	4.40E-02
1.00E-02	1.00E-01	9.40E-02
	SLOPE	0.112869
	βCa	0.225738

Ca/M	**SDS/M**	**SDSmic**	
1.00E-04	1.00E-02	4.00E-03	
5.00E-04	1.00E-02	4.00E-03	
1.00E-03	2.50E-02	1.90E-02	
1.00E-02	1.00E-01	9.40E-02	
5.00E-03	1.00E-01	9.40E-02	outlier
	SLOPE	0.10963	
	βCa	0.219259	
	Average βCa	0.222498	

A7: Modeling of $Ca(DS)_2$ using K_{sp} (1.55E-9M^3) and β_{Ca} (0.22) at 30°C

BEFORE CMC			
Ca/M	**logCa**	**SDS/M**	**logSDS**
6.02E-05	-4.22E+00	6.50E-03	-2.19E+00
9.71E-05	-4.01E+00	5.00E-03	-2.30E+00
1.47E-04	-3.83E+00	4.00E-03	-2.40E+00
2.53E-04	-3.60E+00	3.00E-03	-2.52E+00
5.69E-04	-3.25E+00	2.00E-03	-2.70E+00
5.69E-04	-3.25E+00	2.00E-03	-2.70E+00
5.82E-03	-2.24E+00	7.50E-04	-3.12E+00
1.95E-02	-1.71E+00	5.00E-04	-3.30E+00
4.08E-02	-1.39E+00	4.00E-04	-3.40E+00
4.24E-01	-3.72E-01	2.00E-04	-3.70E+00

MODEL					
I	**logfCa**	**logfDS**		**Ca*fca*fDS**	**Ksp/DS2**
6.68E-03	-1.45E-01	-3.53E-02	3.18E-09	3.67E-05	3.67E-05
5.29E-03	-1.31E-01	-3.20E-02	0.00E+00	6.20E-05	6.20E-05
4.44E-03	-1.21E-01	-2.97E-02	-8.40E-09	9.69E-05	9.69E-05
3.76E-03	-0.112412	-2.76E-02	0.00E+00	1.72E-04	1.72E-04
3.71E-03	-0.111686	-2.74E-02	0.00E+00	3.88E-04	3.88E-04
3.71E-03	-0.111686	-2.74E-02	0.00E+00	3.88E-04	3.88E-04
1.82E-02	-0.218942	-5.29E-02	4.34E-09	2.76E-03	2.76E-03
5.89E-02	-0.337078	-7.99E-02	2.60E-08	6.20E-03	6.20E-03
1.23E-01	-0.425479	-9.96E-02	0.00E+00	9.69E-03	9.69E-03
1.27E+00	-0.717614	-1.61E-01	0.00E+00	3.88E-02	3.88E-02
				Set Ksp:	1.55E-09

AFTER CMC		
	CMCsds	6.00E-03
Ca/M	**SDS/M**	**SDSmic**
5.56E-05	6.50E-03	5.00E-04
4.45E-04	1.00E-02	4.00E-03
2.11E-03	2.50E-02	1.90E-02
1.05E-02	1.00E-01	9.40E-02
2.16E-02	2.00E-01	1.94E-01
SLOPE	0.11125	
Set βCa:	0.2225	

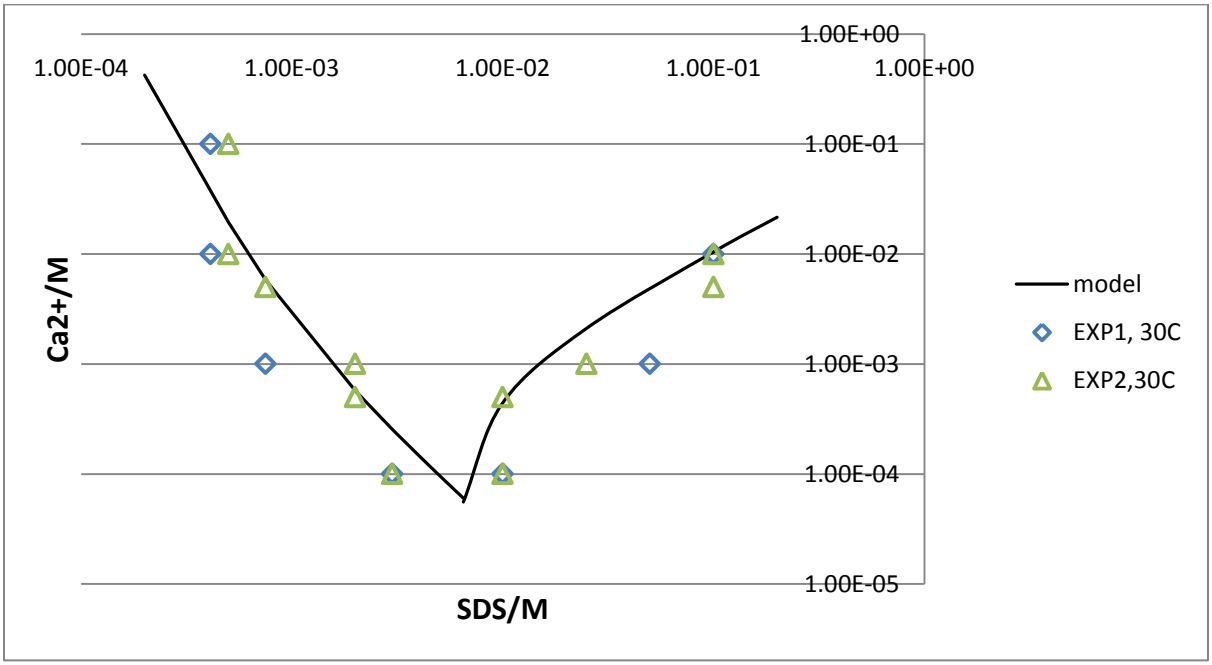

A8: Precipitate boundarySDS-Ca^{2+} at 50^{o}C Test 1&2

Precipitate boundary at 50C (Exp1&2)

EXP1, 50C

Ca/M	SDS/M
1.00E-04	
1.00E-04	
1.00E-03	3.00E-03
1.00E-03	5.00E-02
1.00E-02	2.05E-03
1.00E-02	2.50E-02
1.00E-01	1.03E-03
1.00E-01	2.50E-01

EXP2,50C

Ca/M	SDS/M
1.00E-04	
1.00E-04	
5.00E-04	5.00E-03
5.00E-04	8.00E-03
1.00E-03	2.00E-03
1.00E-03	1.00E-02
5.00E-03	7.50E-04
5.00E-03	5.00E-02
1.00E-02	1.00E-03
1.00E-02	1.00E-01
1.00E-01	5.00E-04
1.00E-01	

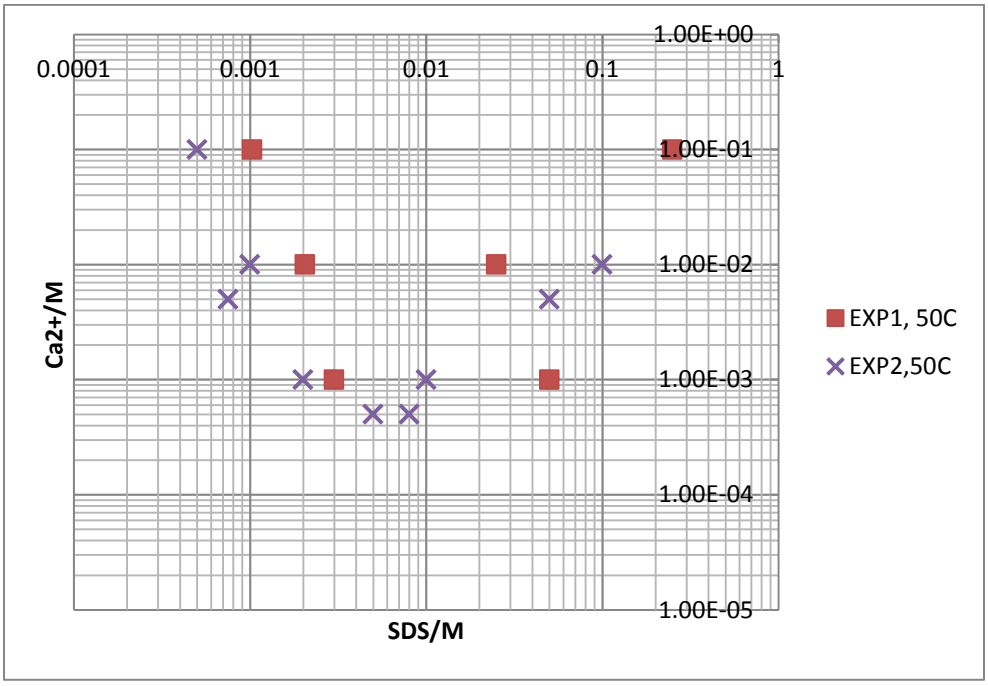

A9: Regression of $Ca(DS)_2$ K_{sp} (8.58E-9M^3) and β_{Ca} (0.20) at 50°C

Regression Ksp before and after CMC (50 C)

BEFORE CMC			
Ca/M	logCa	SDS/M	logSDS
1.00E-03	-3.00E+00	3.00E-03	-2.52E+00
1.00E-02	-2.00E+00	2.05E-03	-2.69E+00
1.00E-01	-1.00E+00	1.03E-03	-2.99E+00
5.00E-04	-3.30E+00	5.00E-03	-2.30E+00
5.00E-04	-3.30E+00	8.00E-03	-2.10E+00
1.00E-03	-3.00E+00	2.00E-03	-2.70E+00
5.00E-03	-2.30E+00	7.50E-04	-3.12E+00
1.00E-02	-2.00E+00	1.00E-03	-3.00E+00
1.00E-01	-1.00E+00	5.00E-04	-3.30E+00

REGRESSION 50C				
I	logfCa	logfDS	Ca*DS2*fca*fDS2	Ksp-Ca*DS2*fca*fDS2
6.00E-03	-1.38E-01	-3.38E-02	5.61E-09	2.97E-09
3.21E-02	-0.271761	-6.51E-02	1.67E-08	-8.08E-09
3.01E-01	-0.540831	-1.24E-01	1.72E-08	-8.64E-09
6.50E-03	-0.142932	-3.49E-02	7.66E-09	9.18E-10
9.50E-03	-0.167969	-4.09E-02	1.80E-08	-9.43E-09
5.00E-03	-0.127516	-3.12E-02	2.58E-09	5.99E-09
1.58E-02	-0.206668	-5.00E-02	1.39E-09	7.19E-09
3.10E-02	-0.268432	-6.43E-02	4.01E-09	4.57E-09
3.01E-01	-0.540603	-1.24E-01	4.06E-09	4.52E-09
			Min Error	0.00E+00
			Ksp	8.58E-09
		Ref. 1	Stellner 1989	5.02E-10
				w swamping NaCl, 30C
		Ref. 2	Maneedaeng	2.16522E-09

	CMCsds	6.00E-03
AFTER CMC		
Ca/M	SDS/M	SDSmic
1.00E-03	5.00E-02	4.40E-02
1.00E-02	2.50E-02	1.90E-02
1.00E-01	2.50E-01	2.44E-01
	SLOPE	0.436438
	βCa	0.872877 Bad regression

Ca/M	SDS/M	SDSmic
5.00E-04	8.00E-03	2.00E-03
1.00E-03	1.00E-02	4.00E-03
5.00E-03	5.00E-02	4.40E-02
1.00E-02	1.00E-01	9.40E-02
	SLOPE	0.101819
	βCa	0.203638

A10: Modeling of $Ca(DS)_2$ K_{sp} (8.58E-9M^3) and β_{Ca} (0.20) at 50°C

BEFORE CMC			
Ca/M	logCa	SDS/M	logSDS
2.33E-04	-3.63E+00	8.00E-03	-2.10E+00
5.64E-04	-3.25E+00	5.00E-03	-2.30E+00
8.79E-04	-3.06E+00	4.00E-03	-2.40E+00
1.62E-03	-2.79E+00	3.00E-03	-2.52E+00
4.27E-03	-2.37E+00	2.00E-03	-2.70E+00
4.27E-03	-2.37E+00	2.00E-03	-2.70E+00
8.97E-02	-1.05E+00	7.50E-04	-3.12E+00
3.51E-01	-4.55E-01	5.00E-04	-3.30E+00
6.94E-01	-1.59E-01	4.00E-04	-3.40E+00
4.38E+00	6.41E-01	2.00E-04	-3.70E+00

AFTER CMC		
	CMCsds	6.00E-03
Ca/M	SDS/M	SDSmic
2.04E-04	8.00E-03	2.00E-03
4.07E-04	1.00E-02	4.00E-03
1.93E-03	2.50E-02	1.90E-02
9.57E-03	1.00E-01	9.40E-02
1.97E-02	2.00E-01	1.94E-01
5.03E-02	5.00E-01	4.94E-01
SLOPE	0.1018	
Set βCa:	0.2036	

MODEL					
I	logfCa	logfDS		Ca*fca*fDS	Ksp/DS2
8.70E-03	-1.62E-01	-3.94E-02	2.69E-07	1.34E-04	1.34E-04
6.69E-03	-1.45E-01	-3.54E-02	8.67E-07	3.43E-04	3.43E-04
6.64E-03	-1.44E-01	-3.52E-02	7.36E-07	5.36E-04	5.36E-04
7.87E-03	-0.155096	-3.78E-02	2.71E-08	9.53E-04	9.53E-04
1.48E-02	-0.201679	-4.88E-02	7.37E-08	2.15E-03	2.15E-03
1.48E-02	-0.201679	-4.88E-02	7.37E-08	2.15E-03	2.15E-03
2.70E-01	-0.526652	-1.21E-01	4.34E-07	1.53E-02	1.53E-02
1.05E+00	-0.696067	-1.57E-01	4.86E-07	3.43E-02	3.43E-02
2.08E+00	-0.769568	-1.71E-01	7.63E-07	5.36E-02	5.36E-02
1.31E+01	-0.911904	-1.99E-01	2.78E-07	2.15E-01	2.15E-01
				Set Ksp:	8.58E-09

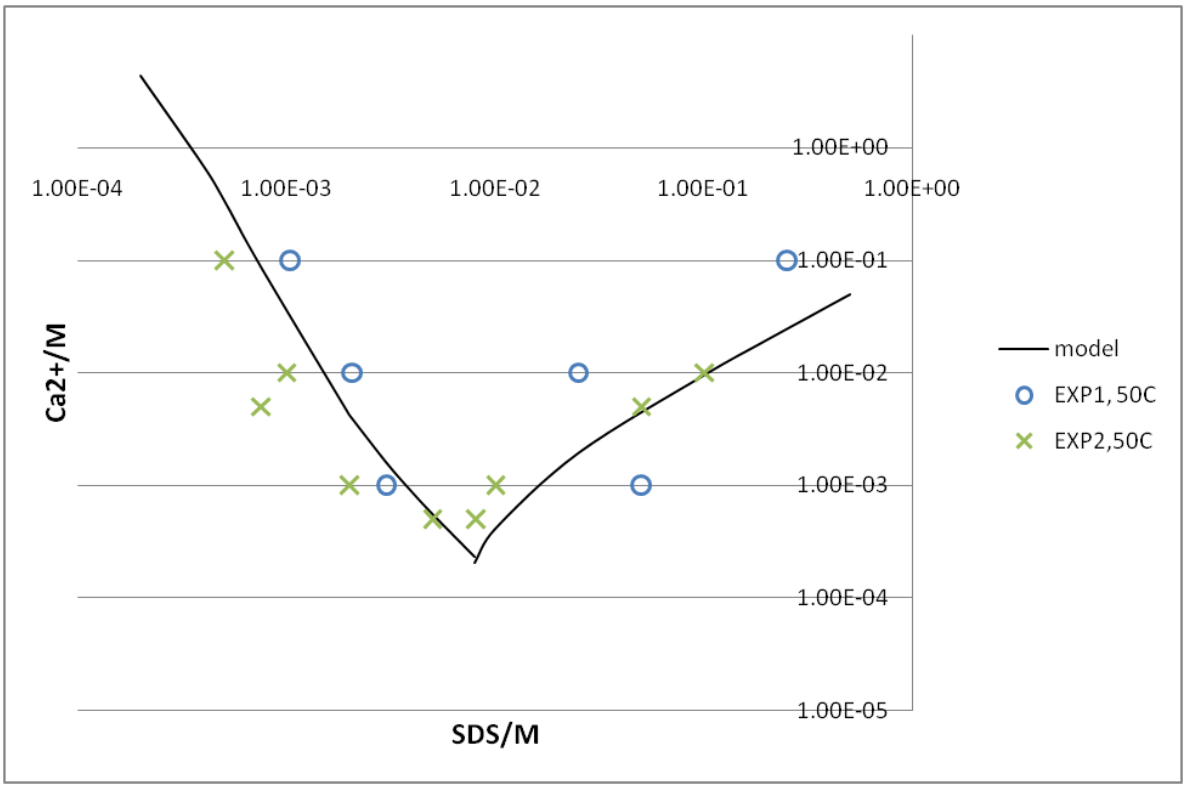

Appendix B

B1: Adsorption Isotherm SDS on coarse $CaCO_3$

Adsorption Isotherm SDS on CaCO3 (Experiment1):

						CPB titrant =			1016 µM		
Run	Stock mL	Dilution (DI)	[SDS] added (µM)	C CaCO3 wt(g)	SDS analyte supernatant (mL)	initial reading (mL)	final reading (mL)	total mL CPB	[CPB] = [SDS] bulk (µM)	[SDS]ad (µM)	[SDS]ad (µmols/g)
11	10	10	25000	4.0312	0.5	28.2	39.2	10.95	22250.4	2749.6	13.642
10	8	12	20000	4.071	0.5	39.7	48.4	8.65	17576.8	2423.2	11.905
9	6	14	15000	4.0833	0.5	22.3	28.2	5.85	11887.2	3112.8	15.246
8	5	15	12500	4.0203	1	30.4	39.7	9.25	9398	3102	15.432
7	4	16	10000	4.0812	1	23.8	30.4	6.55	6654.8	3345.2	16.393
6	3	17	7500	4.0065	1	17.7	22.3	4.55	4622.8	2877.2	14.363
5	2.5	17.5	6250	4.005	1	19.6	23.8	4.15	4216.4	2033.6	10.155
4	2	18	5000	4.1081	1.5	12.5	17.7	5.15	3488.267	1511.73	7.360
3	1.5	18.5	3750	4.0243	1.5	15.6	19.6	3.95	2675.467	1074.53	5.340
2	1	19	2500	4.0244	2	8.6	12.5	3.85	1955.8	544.2	2.705
1	0.5	19.5	1250	4.1299	4	10.7	15.6	4.85	1231.9	18.1	0.088
0	0	20	0	4	1	0	0.05	0.05	0	0	0

Adsorption Isotherm SDS on CaCO3 (Experiment2):

						CPB titrant =			1016 µM		
Run	Stock mL	Dilution (DI)	[SDS] added (µM)	CaCO3 wt(g)	SDS analyte supernatant (mL)	initial reading (mL)	final reading (mL)	total mL CPB	[CPB] = [SDS] bulk (µM)	[SDS]ad (µM)	[SDS]ad (µmols/g)
11	10	10	25000	4.1462	0.5	12.4	23.3	10.85	22047.2	2952.8	14.243
10	8	12	20000	4.024	0.5	39.2	47.5	8.25	16764	3236	16.083
9	6	14	15000	4.1816	0.5	23.3	29.1	5.75	11684	3316	15.860
8	5	15	12500	4.0241	1	29.1	37.9	8.75	8890	3610	17.942
7	4	16	10000	4.0633	1	9.6	16.3	6.65	6756.4	3243.6	15.965
6	3	17	7500	4.1194	1	37.9	42.7	4.75	4826	2674	12.982
5	2.5	17.5	6250	4.0315	1	16.3	20.4	4.05	4114.8	2135.2	10.593
4	2	18	5000	4.0274	1	20.4	23.8	3.35	3403.6	1596.4	7.928
3	1.5	18.5	3750	4.0122	1.5	23.8	27.8	3.95	2675.467	1074.53	5.356
2	1	19	2500	4.0128	2	42.7	46.7	3.95	2006.6	493.4	2.459
1	0.5	19.5	1250	4.1273	4	27.8	32.6	4.75	1206.5	43.5	0.211
0	0	20	0	4	1	0	0.05	0.05	0	0	0

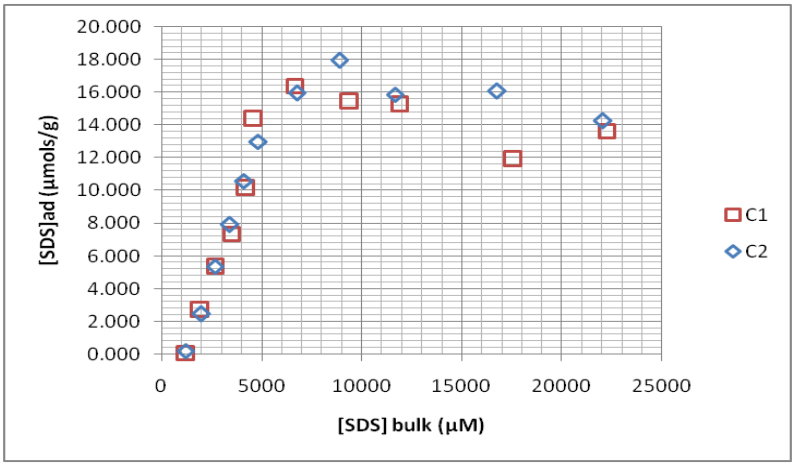

B2: Adsorption Isotherm SDS on fine $CaCO_3$

Adsorption Isotherm SDS on CaCO3 (Exp1)

						CPB titrant =			1016 µM		
Run	Stock mL	Dilution (DI)	[SDS] added (µM)	F CaCO3 wt(g)	SDS analyte supernatant (mL)	initial reading (mL)	final reading (mL)	total mL CPB	[CPB] = [SDS] bulk (µM)	[SDS]ad (µM)	[SDS]ad (µmols/g)
11	25	25	25000	1.0502	0.5	11.8	22	10.1	20523.2	4476.8	85.256
10	20	30	20000	1.0049	0.5	22	29.7	7.6	15443.2	4556.8	90.692
9	18	32	18000	1.0366	0.5	29.7	36.6	6.8	13817.6	4182.4	80.695
8	16	34	16000	1.019	0.5	36.6	42.7	6	12192	3808	74.740
7	14	36	14000	1.0196	0.5	42.7	48	5.2	10566.4	3433.6	67.352
6	12	38	12000	1.0503	0.5	7.1	11.2	4	8128	3872	73.731
5	10	40	10000	1.0321	1	11.2	17.7	6.4	6502.4	3497.6	67.776
4	8	42	8000	1.0235	1	25.8	30.85	4.95	5029.2	2970.8	58.052
3	6	44	6000	1.0479	1	21.9	25.8	3.8	3860.8	2139.2	40.828
2	4	46	4000	1.0079	1.4	30.9	35.3	4.3	3120.571	879.429	17.451
1	2	48	2000	1.0197	2	12.3	16	3.6	1828.8	171.2	3.358
0	0	20	0	1	1	0	0.1	0.1	0	0	0

Adsorption Isotherm SDS on CaCO3 (Exp2)

						CPB titrant =			1016 µM		
Run	Stock mL	Dilution (DI)	[SDS] added (µM)	F CaCO3 wt(g)	SDS analyte supernatant (mL)	initial reading (mL)	final reading (mL)	total mL CPB	[CPB] = [SDS] bulk (µM)	[SDS]ad (µM)	[SDS]ad (µmols/g)
11	25	25	25000	1	0.5	11.6	21.1	9.4	19100.8	5899.2	117.984
10	20	30	20000	1	0.5	31.5	39.7	8.1	16459.2	3540.8	70.816
9	18	32	18000	1	0.5	21.1	28	6.8	13817.6	4182.4	83.648
8	16	34	16000	1	0.5	28.1	34	5.8	11785.6	4214.4	84.288
7	14	36	14000	1	0.5	39.8	44.85	4.95	10058.4	3941.6	78.832
6	12	38	12000	1	0.5	1.8	5.75	3.85	7823.2	4176.8	83.536
5	10	40	10000	1	1	29.8	36.15	6.25	6350	3650	73.000
4	8	42	8000	1	1	20.4	25.5	5	5080	2920	58.400
3	6	44	6000	1	1	12.1	16	3.8	3860.8	2139.2	42.784
2	4	46	4000	1	1.4	34	38	3.9	2830.29	1169.71	23.394
1	2	48	2000	1	2	26.5	29.8	3.2	1625.6	374.4	7.488
0	0	20	0	1	1	0	0.1	0.1	0	0	0

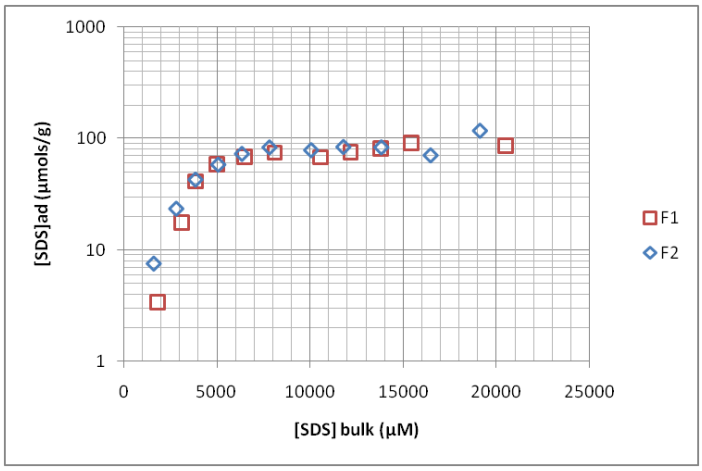

B3: Adsorption Isotherm SDS on extra fine $CaCO_3$

Adsorption Isotherm SDS on CaCO3 (Exp6)

						CTAC titrant =		0.00864 M			
Run	Stock mL	Dilution (DI)	[SDS] added (micM)	CaCO3 wt(g)	SDS analyte supernatant (mL)	initial reading (mL)	final reading (mL)	total mL CTAC	[CTAC] = [SDS] bulk (micM)	[SDS]ad (micM)	[SDS]ad (micmols/g)
11	25	25	23500	1.0603	2	31.75	37.05	5.3	22896	604	12.53230218
10	20	30	18800	1.1277	10	9.9	31.75	21.85	18878.4	-78.4	-1.52948479
9	18	32	16920	1.0148	1	37.1	39	1.9	16416	504	10.92629089
8	16	34	15040	1.0677	10	11.5	28	16.5	14256	784	16.15435047
7	14	36	13160	1.1916	10	22.3	36.2	13.9	12009.6	1150.4	21.23934206
6	12	38	11280	1.0789	10	10.7	22.2	11.5	9936	1344	27.40569098
5	10	40	9400	1.0569	10	31.1	40	8.9	7689.6	1710.4	35.60298988
4	8	42	7520	1.126	10	24.3	31.05	6.75	5832	1688	32.98046181
3	6	44	5640	1.0542	10	19	24.25	5.25	4536	1104	23.03927149
2	4	46	3760	1.086	10	13.4	17	3.6	3110.4	649.6	13.15948435
1	2	48	1880	1.0385	10	10.7	12.75	2.05	1771.2	108.8	2.304862783
0	0	50	0	1.0324	10	0	0	0	0	0	0

Adsorption Isotherm SDS on CaCO3 (Exp7)

						CTAC titrant =		0.005132 M			
Run	Stock mL	Dilution (DI)	[SDS] added (micM)	CaCO3 wt(g)	SDS analyte supernatant (mL)	initial reading (mL)	final reading (mL)	total mL CTAC	[CTAC] = [SDS] bulk (micM)	[SDS]ad (micM)	[SDS]ad (micmols/g)
11	25	25	23500	1.0711	2	31.85	40.75	8.85	22709.1	790.9	16.24479507
10	20	30	18800	1.068	2	24.6	31.8	7.15	18346.9	453.1	9.333520599
9	18	32	16920	1.0197	2	18.3	24.65	6.3	16165.8	754.2	16.27184466
8	16	34	15040	1.0758	2	37.9	43.4	5.45	13984.7	1055.3	21.5807771
7a	14	36	13160	1.0081	2	40.8	45.5	4.65	11931.9	1228.1	26.801111
7	14	36	13160	1.0081	2	33.35	37.85	4.45	11418.7	1741.3	38.00079357
6a	12	38	11280	1.0251	2	34	38.05	4	10264	1016	21.80470198
6	12	38	11280	1.0251	2	29.5	33.35	3.8	9750.8	1529.2	32.81865184
5	10	40	9400	1.0637	2	26.4	29.25	2.8	7184.8	2215.2	45.81592554
4	8	42	7520	1.0124	5	20.75	26.4	5.6	5747.84	1772.16	38.50999605
3	6	44	5640	1.0639	5	39.45	43.75	4.25	4362.2	1277.8	26.42316007
2	4	46	3760	1.0135	10	33.5	39.45	5.9	3027.88	732.12	15.89209669
1	2	48	1880	1.0034	10	30.1	33.4	3.25	1667.9	212.1	4.650388678
0	0	50	0	1.0324	10	10	10.05	0.05	25.66	-25.66	-0.54680356

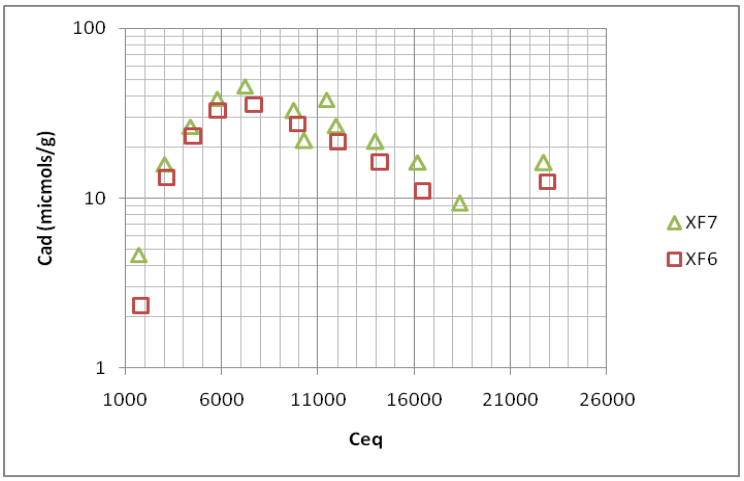

B4: Adsolubilization data Styrene with SDS on coarse $CaCO_3$

Adsolubilization Coarse CaCO3 Expt2:

SDS	5.7E-19	m2/molecule	57	A2/molecule	**Solution**	36	mL		
CMC	0.0081	mol/L	8.1	mM	**Solid wt**	4	g		
Stock SDS	102279	µM			**[SDS]ad/g**	13	µmols/g		
[SDS]	6444.44	µM			**[SDS]ad**	1444.444	µM		
Sat'd Styr-h2O	0.003	mol/L			**[SDS]eq**	5000	µM		

	MW	
SDS	288.38	g/mol
styrene	104.15	g/mol
AIBN	164.2	g/mol

[SDS] = 6534.49

						λ = 281 nm								
						initial reading	final reading				in 36 mL soln			
Run	**3000µM sat'd styr (mL)**	**SDS stk soln (mL)**	**Dilution (mL)**	**[Styr] added (µM)**	**C CaCO3 wt(g)**	**frm cal. Data Ai**	**dil.**	**Af**	**([ ]f - blank) [Styr]bulk (micM)**	**[]i - []f [Styr]ad (micM)**	**[Styr]ad (micmols/g)**	**Xadm**	**Xaq**	**K= Xadm/Xaq**
9	33.7	2.3	0	2808.3333	4.0438	2.022	0.2307692	0.288	1727.7778	1080.5556	9.6196647	4.28E-01	9.69E-01	4.42E-01
8	30	2.3	3.7	2500	4.0608	1.8	0.2307692	0.276	1655.5556	844.44444	7.4862096	3.69E-01	9.68E-01	3.81E-01
7	28	2.3	5.7	2333.3333	4.0616	1.68	0.2307692	0.253	1517.1296	816.2037	7.2344232	3.61E-01	9.65E-01	3.74E-01
6	25	2.3	8.7	2083.3333	4.0458	1.5	0.2307692	0.238	1426.8519	656.48148	5.8414487	3.12E-01	9.63E-01	3.25E-01
5	22	2.3	11.7	1833.3333	4.0447	1.32	0.2307692	0.201	1204.1667	629.16667	5.5999209	3.03E-01	9.56E-01	3.17E-01
4	20	2.3	13.7	1666.6667	4.0468	1.2	0.5	0.332	916.66667	750	6.6719383	3.42E-01	9.43E-01	3.62E-01
3	15	2.3	18.7	1250	4.0588	0.9	0.5	0.266	733.33333	516.66667	4.5826353	2.63E-01	9.30E-01	2.83E-01
2	10	2.3	23.7	833.33333	4.0385	0.6	1	0.482	663.88889	169.44444	1.5104618	1.05E-01	9.23E-01	1.14E-01
1	5	2.3	28.7	416.66667	4.0111	0.3	1	0.24	327.77778	88.888889	0.7977861	5.80E-02	8.55E-01	6.78E-02
0	0	2.3	33.7	0	4.0313	0	1	0.004	5.5555556	-5.555556	0	-3.86E-03	9.10E-02	-4.24E-02
SUM	188.7	23	148.3											

[SDS]add = 6534.49 µM
[SDS]eq = 5090.05 µM
calibration curve: [] in µM
A = 0.00072 *[]

Adsolubilization Coarse CaCO3 Expt3:

SDS	5.7E-19	m2/molecule	57	A2/molecule	**Solution**	36	mL		
CMC	0.0081	mol/L	8.1	mM	**Solid wt**	4	g		
Stock SDS	105307	µM			**[SDS]ad/g**	13.5	µmols/g		
[SDS]	6500	µM			**[SDS]ad**	1500	µM		
Sat'd Styr-h2O	0.003	mol/L			**[SDS]eq**	5000	µM		

	MW	
SDS	288.38	g/mol
styrene	104.15	g/mol
AIBN	164.2	g/mol

[SDS] = 6727.9

						λ = 281 nm								
						initial reading	final reading				in 36 mL soln			
Run	**3000µM sat'd styr (mL)**	**SDS stk soln (mL)**	**Dilution (mL)**	**[Styr] added (µM)**	**C CaCO3 wt(g)**	**frm cal. Data Ai**	**dil.**	**Af**	**([ ]f - blank) [Styr]bulk (micM)**	**[]i - []f [Styr]ad (micM)**	**[Styr]ad (micmols/g)**	**Xadm**	**Xaq**	**K= Xadm/Xaq**
9	33.7	2.3	0	2808.333	4.044	2.022	0.23077	0.288	1.73E+03	1080.5556	9.6196647	4.19E-01	9.69E-01	4.32E-01
8	30	2.3	3.7	2500	4.061	1.8	0.23077	0.242	1.45E+03	1049.0741	9.3003021	4.12E-01	9.63E-01	4.27E-01
7	28	2.3	5.7	2333.333	4.062	1.68	0.23077	0.225	1.35E+03	984.72222	8.7280875	3.96E-01	9.60E-01	4.13E-01
6	25	2.3	8.7	2083.333	4.046	1.5	0.23077	0.211	1.26E+03	818.98148	7.2873927	3.53E-01	9.58E-01	3.69E-01
5	22	2.3	11.7	1833.333	4.045	1.32	0.23077	0.203	1.22E+03	617.12963	5.4927848	2.91E-01	9.56E-01	3.05E-01
4	20	2.3	13.7	1666.667	4.047	1.2	0.5	0.319	8.81E+02	786.11111	6.9931798	3.44E-01	9.41E-01	3.66E-01
3	15	2.3	18.7	1250	4.059	0.9	0.5	0.198	5.44E+02	705.55556	6.2580073	3.20E-01	9.07E-01	3.53E-01
2	10	2.3	23.7	833.3333	4.039	0.6	1	0.469	645.83333	187.5	1.6714127	1.11E-01	9.21E-01	1.21E-01
1	5	2.3	28.7	416.6667	4.011	0.3	1	0.284	388.88889	27.777778	0.2493082	1.82E-02	8.75E-01	2.08E-02
0	0	2.3	33.7	0	4.031	0	1	0.004	5.5555556	-5.555556	0	-3.72E-03	9.10E-02	-4.09E-02
SUM	188.7	23	148.3											

[SDS]add = 6727.95 µM
[SDS]eq = 5227.95 µM
calibration curve: [] in µM
A = 0.00072 *[]

B5: Adsolubilization isotherm and admicellar partition styrene with SDS on coarse $CaCO_3$

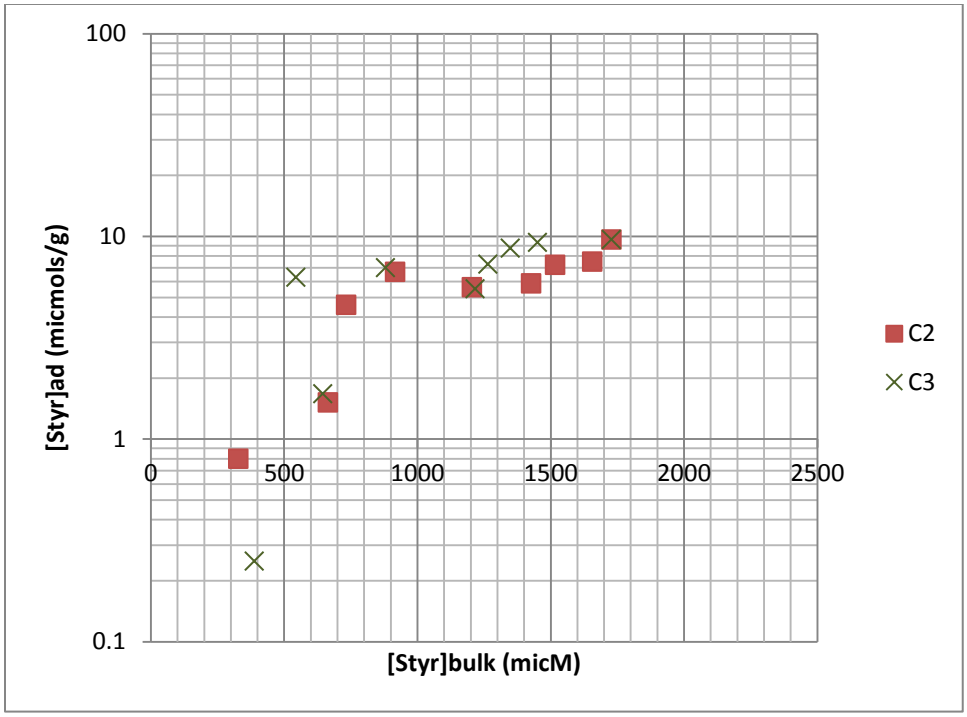

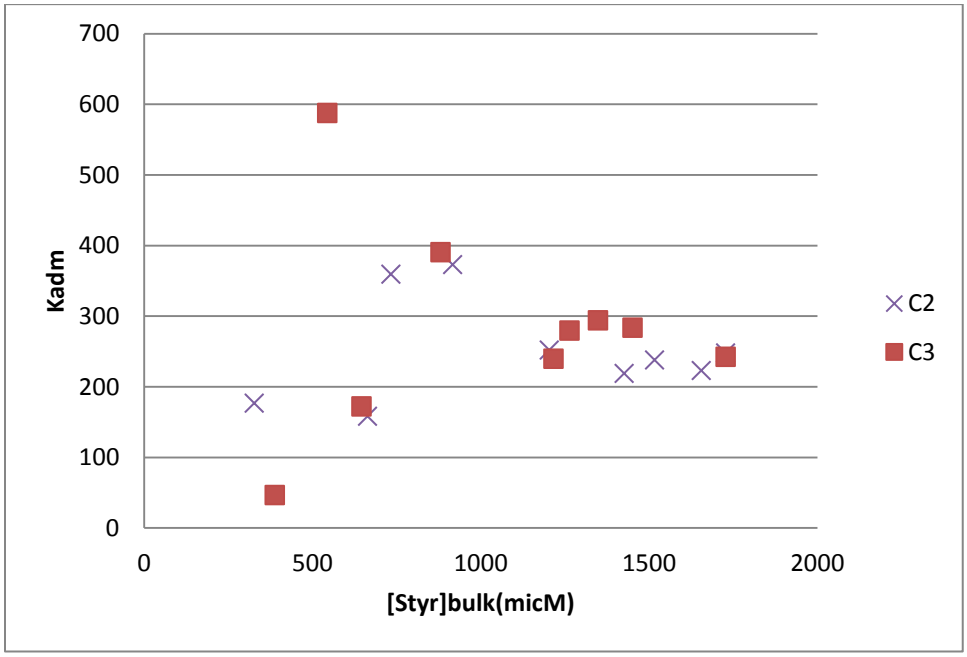

B6: Adsolubilization data Styrene with SDS on Fine $CaCO_3$

Adsolubilization Fine CaCO3 Expt2:

SDS	5.7E-19	m2/molecule		57	A2/molecule		**Solution**	38	mL					**MW**	
CMC	0.0081	mol/L		8.1	mM		**Solid wt**	2	g				SDS	288.38	g/mol
Stock SDS	50370	µM					**[SDS]ad/g**	65	µmols/g				styrene	104.15	g/mol
[SDS]	9421.05	µM	135mL stock in 1010mL				**[SDS]ad**	3421.053	µM				AIBN	164.2	g/mol
Sat'd Styr-h2O	0.003	mol/L					**[SDS]eq**	6000	µM						

							λ = 281 nm								
	[SDS] =	9278.68				initial reading	final reading				in 38 mL soln				
Run	**3000µM sat'd styr (mL)**	**SDS stk soln (mL)**	**Dilution (mL)**	**[Styr] added (µM)**	**F CaCO3 wt(g)**	**frm cal. Data Ai**	**dil.**	**Af**	**([ ]f - blank) [Styr]bulk (micM)**	**[]i - []f [Styr]ad (micM)**	**[Styr]ad (micmols/g)**	**Xadm**	**Xaq**	**K= Xadm/Xaq**
10	31	7	0	2447.3684	2	1.9089474	0.2307692	0.344	1905.3971	541.97131	10.297455	0.136757	9.72E-01	1.41E-01
9	23	7	8	1815.7895	2	1.4163158	0.2307692	0.202	1116.5082	699.28125	13.286344	0.169715	9.53E-01	1.78E-01
8	13	7	18	1026.3158	2	0.8005263	0.5	0.215	545.56805	480.74774	9.134207	0.123212	9.08E-01	1.36E-01
7	6	7	25	473.68421	2	0.3694737	1	0.291	367.36292	106.32129	2.0201045	0.030142	8.69E-01	3.47E-02
6	4	7	27	315.78947	2	0.2463158	1	0.216	271.20908	44.580397	0.8470275	0.012864	8.30E-01	1.55E-02
5	2	7	29	157.89474	2	0.1231579	1	0.109	134.02959	23.865147	0.4534378	0.006928	7.07E-01	9.80E-03
4	0	7	31	0	2	0	1	0	0	0	0	0	0.00E+00	#DIV/0!
SUM	79		138											

[SDS]add =	9278.68	µM
[SDS]eq =	5857.63	µM
calibration curve: [] in µM		
A =	0.00078	*[]

Adsolubilization Fine CaCO3 Expt4: Date:

SDS	5.7E-19	m2/molecule		57	A2/molecule		**Solution**	39	mL					**MW**	
CMC	0.0081	mol/L		8.1	mM		**Solid wt**	1	g				SDS	288.38	g/mol
Stock SDS	100000	µM					**[SDS]ad/g**	65	µmols/g				styrene	104.15	g/mol
[SDS]	7666.6667	µM	135mL stock in 1010mL				**[SDS]ad**	1666.667	µM				AIBN	164.2	g/mol
Sat'd Styr-h2O	0.003	mol/L					**[SDS]eq**	6000	µM						

							λ = 281 nm								
	[SDS] =	7894.74				initial reading	final reading								
Run	**3000µM sat'd styr (mL)**	**SDS stk soln (mL)**	**Dilution (mL)**	**[Styr] added (µM)**	**F CaCO3 wt(g)**	**frm cal. Data Ai**	**dil.**	**Af**	**([ ]f - blank) [Styr]bulk (micM)**	**[]i - []f [Styr]ad (micM)**	**[Styr]ad (micmols/g)**	Xadm	Xaq	K= Xadm/Xaq
7	36.5	3	0	2772.1519	1	1.8018987	0.2307692	0.316	2.10E+03	670.10062	26.46897	0.286764	9.74E-01	2.94E-01
6	30	3	6	2307.6923	1	1.5	0.2307692	0.278	1.85E+03	458.97436	17.9	0.215923	9.71E-01	2.22E-01
5	25	3	11	1923.0769	1	1.25	0.2307692	0.207	1.38E+03	547.69231	21.36	0.247337	9.61E-01	2.57E-01
4	20	3	16	1538.4615	1	1	0.5	0.338	1.04E+03	503.07692	19.62	0.23186	9.49E-01	2.44E-01
3	15	3	21	1153.8462	1	0.75	0.5	0.259	7.92E+02	361.53846	14.1	0.178255	9.35E-01	1.91E-01
2	10	3	26	769.23077	1	0.5	1	0.459	701.53846	67.692308	2.64	0.03903	9.27E-01	4.21E-02
1	5	3	31	384.61538	1	0.25	1	0.24	364.61538	20	0.78	0.011858	8.68E-01	1.37E-02
0	0	3	36	0	1	0	1	0.003	4.6153846	-4.615385	0	-0.00278	7.68E-02	-3.62E-02
SUM	141.5	24	147											

[SDS]add	7894.7368	µM
[SDS]eq =	6228.0702	µM
calibration curve: [] in µM		
A =	0.00065	*[]

B7: Adsolubilization isotherm and admicellar partition styrene with SDS on Fine $CaCO_3$

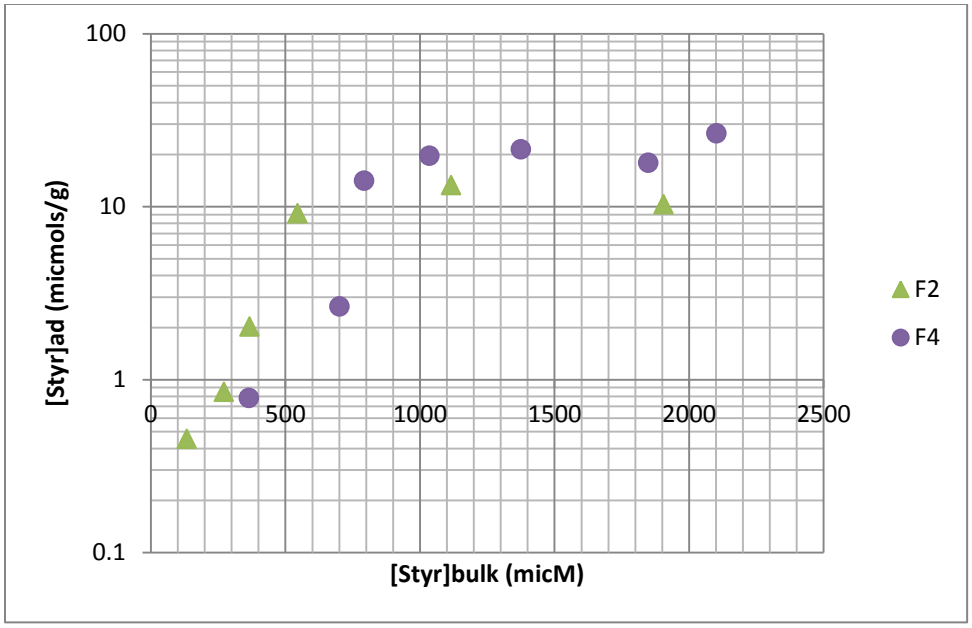

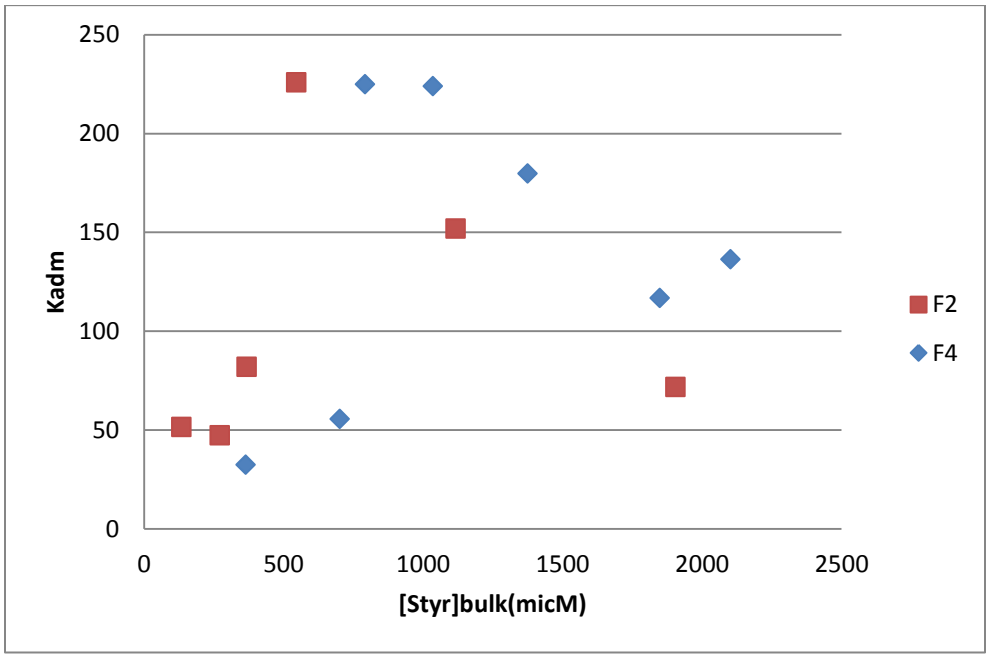

B8: Adsolubilization data Styrene with SDS on Extra fine $CaCO_3$

Adsolubilization EXtrafine CaCO3 Expt2:

SDS	5.7E-19	m2/molecule	57	A2/molecule	**Solution**	39	mL	
CMC	0.0081	mol/L	8.1	mM	**Solid wt**	1	g	
Stock SDS	50900	µM			**[SDS]ad/g**	35	µmols/g	
[SDS]	6397.44	µM			**[SDS]ad**	897.4359	µM	
Sat'd Styr-h2O	0.003	mol/L			**[SDS]eq**	5500	µM	

	MW	
SDS	288.38	g/mol
styrene	104.15	g/mol
AIBN	164.2	g/mol

λ = 281 nm

[SDS] = 6525.64

Run	3000µM sat'd styr (mL)	SDS stk soln (mL)	Dilution (mL)	[Styr] added (µM)	XF CaCO3 wt(g)	initial reading: frm cal. Data Ai	final reading: dil.	final reading: Af	([ ]f - blank) [Styr]bulk (micM)	[]i - []f [Styr]ad (micM)	in 39 mL soln: [Styr]ad (micmols/g)	Xadm	Xaq	K= Xadm/Xaq
7	34	5	0	2615.38	1	1.6476923	0.2307692	0.273	1873.0159	742.36874	28.95238	0.452718	9.71E-01	4.66E-01
6	30	5	4	2307.69	1	1.4538462	0.2307692	0.232	1591.0053	716.68702	27.95079	0.44401	9.66E-01	4.59E-01
5	25	5	9	1923.08	1	1.2115385	0.2307692	0.2	1370.8995	552.17745	21.53492	0.380914	9.61E-01	3.96E-01
4	20	5	14	1538.46	1	0.9692308	0.5	0.319	1007.9365	530.52503	20.69048	0.371526	9.48E-01	3.92E-01
3	15	5	19	1153.85	1	0.7269231	0.5	0.223	703.1746	450.67155	17.57619	0.334299	9.27E-01	3.61E-01
2	10	5	24	769.231	1	0.4846154	1	0.448	706.34921	62.881563	2.452381	0.06548	9.27E-01	7.06E-02
1	5	5	29	384.615	1	0.2423077	1	0.226	353.96825	30.647131	1.195238	0.033022	8.64E-01	3.82E-02
0	0	5	34	0	1	0	1	0.003	4.7619048	-4.761905	0	-0.00533	7.90E-02	-6.75E-02
SUM	139	40	133											

[SDS]add = 6525.64 µM
[SDS]eq = 5628.21 µM
calibration curve: [] in µM
A = 0.00063 *[]

Adsolubilization EXtrafine CaCO3 Expt3:

SDS	5.7E-19	m2/molecule	57	A2/molecule	**Solution**	39	mL	
CMC	0.0081	mol/L	8.1	mM	**Solid wt**	1	g	
Stock SDS	100000	µM			**[SDS]ad/g**	35	µmols/g	
[SDS]	6397.44	µM			**[SDS]ad**	897.4359	µM	
Sat'd Styr-h2O	0.003	mol/L			**[SDS]eq**	5500	µM	

	MW	
SDS	288.38	g/mol
styrene	104.15	g/mol
AIBN	164.2	g/mol

λ = 281 nm

[SDS] = 6410.26

Run	3000µM sat'd styr (mL)	SDS stk soln (mL)	Dilution (mL)	[Styr] added (µM)	XF CaCO3 wt(g)	initial reading: frm cal. Data Ai	final reading: dil.	final reading: Af	([ ]f - blank) [Styr]bulk (micM)	[]i - []f [Styr]ad (micM)	in 39 mL soln: [Styr]ad (micmols/g)	Xadm	Xaq	K= Xadm/Xaq
7	36.5	2.5	0	2807.692	1	1.8811538	0.23077	0.327	2.11E+03	697.24455	27.192537	0.437232	9.74E-01	4.49E-01
6	30	2.5	6.5	2307.692	1	1.5461538	0.23077	0.223	1.44E+03	869.88136	33.925373	0.492204	9.63E-01	5.11E-01
5	25	2.5	11.5	1923.077	1	1.2884615	0.28571	0.244	1.27E+03	652.92767	25.464179	0.421145	9.58E-01	4.40E-01
4	20	2.5	16.5	1538.462	1	1.0307692	0.5	0.311	9.24E+02	614.58094	23.968657	0.406464	9.43E-01	4.31E-01
3	15	2.5	21.5	1153.846	1	0.7730769	0.5	0.236	7.00E+02	453.84615	17.7	0.335863	9.27E-01	3.62E-01
2	10	2.5	26.5	769.2308	1	0.5153846	1	0.42	622.38806	146.84271	5.7268657	0.140616	9.18E-01	1.53E-01
1	5	2.5	31.5	384.6154	1	0.2576923	1	0.269	397.01493	-12.39954	-0.4835821	-0.01401	8.77E-01	-1.60E-02
0	0	2.5	36.5	0	1	0	1	0.003	4.4776119	-4.477612	0	-0.00501	7.47E-02	-6.72E-02
SUM	141.5	20	150.5											

[SDS]add = 6410.26 µM
[SDS]eq = 5512.82 µM
calibration curve: [] in µM
A = 0.00067 *[]

B9: Adsolubilization isotherm and admicellar partition styrene with SDS on Extra fine $CaCO_3$

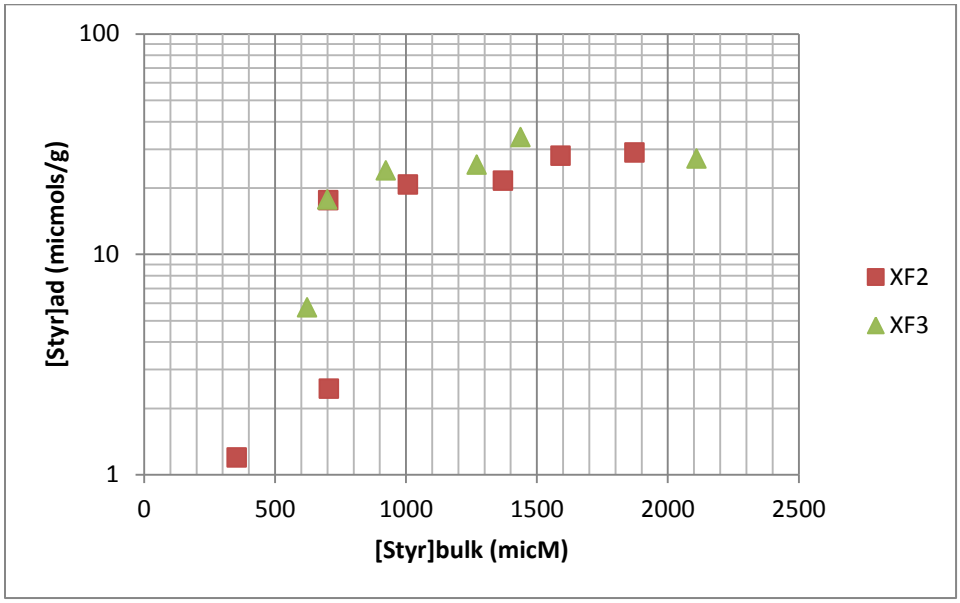

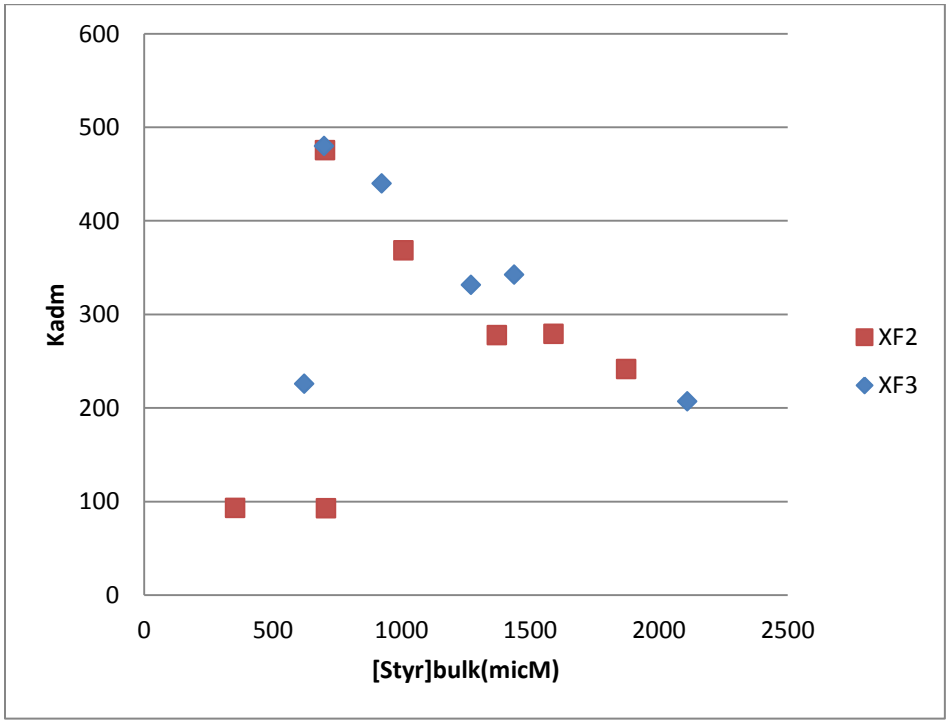

B10: Admicellar Polymerization of $CaCO_3$

Experiment Data	Date:070710				Date:072610		Date: 110910(HH)					
	XF-S6000(1:10)		XF-S6000 (1:1)		F-S6000 (1:10)		C		F		XF	
Solution	212.40	mL	21.05	mL	200.80	mL	20.02	mL	20.04	mL	19.96	mL
Solid wt	212.00	g	21.30	g	204.40	g	20.00	g	20.01	g	20.00	g
[SDS]eq	**5977.40**	µM	**5848.46**	µM	**6963.94**	µM	**4992.99**	µM	**5946.83**	µM	**5505.41**	µM
n[SDS]eq	1269.60	µmol	123.11	µmol	1398.36	µmol	99.96	µmol	119.17	µmol	109.89	µmol
[SDS]ad/g	38.50	µmols/g	38.50	µmols/g	70.00	µmols/g	13.00	µmols/g	65.00	µmols/g	35.00	µmols/g
n[SDS]ad	8162.00	µmol	820.05	µmol	14308.00	µmol	260.04	µmol	1300.83	µmol	700.11	µmol
[SDS]	44404.90	µM	44805.70	µM	78218.92	µM	17982.02	µM	70858.28	µM	40581.16	µM
n[SDS]total	**9431.60**	µmol	**943.16**	µmol	**15706.36**	µmol	**360.00**	µmol	**1420.00**	µmol	**810.00**	µmol
Stk SDS	170.00	mL	17.00	mL	4.53	g	3.60	mL	14.20	mL	8.10	mL
[styrene]	16454.61	µM	24904.70	µM	34810.35	µM	8728.67	µM	17439.92	µM	26264.72	µM
n[styrene]	**3494.96**	µmol	**524.24**	µmol	**6989.92**	µmol	**174.75**	µmol	**349.50**	µmol	**524.24**	µmol
wt styr	0.36	g	0.05	g	0.73	g	0.02	g	0.04	g	0.05	g
mL styr	0.40	mL	0.06	mL	0.80	mL	0.02	mL	0.04	mL	0.06	mL
Initiator(AIBN/VA	**365.41**	µmol	**548.11**	µmol	**669.91**	µmol	**20.71**	µmol	**38.37**	µmol	**56.03**	µmol
	1720.38	µM	26038.58	µM	3336.23	µM	1034.29	µM	1914.56	µM	2807.08	µM
	0.06	g	0.09	g	0.11	g	0.0034	g	0.0063	g	0.0092	g
Dilution	42.00	mL	3.90	mL	200.00	mL	16.40	mL	5.80	mL	11.80	mL
surf,ad : styrene	**2.34**		**1.56**		**2.05**		**1.49**		**3.72**		**1.34**	
INI:Styr	**0.10**		**1.05**		**0.10**		**0.12**		**0.11**		**0.11**	

	Date:070710	Date:072610	Date: 110910(HH)
	HH'(1:10) or (1:1): 2 or 1.5sds per styr		HH

wt loss
%wt loss

Experiment Data	Date: 031711(HHrt)								Date: 042111(MH)					
	C		Ccontrol		F		XF		C		F		XF	
Solution	20.02	mL	20.00	mL	20.04	mL	19.96	mL	19.84	mL	19.96	mL	19.76	mL
Solid wt	20.03	g	20.02	g	20.06	g	19.88	g	20.07	g	20.01	g	20.01	g
[SDS]eq	**4977.86**	µM	**4985.70**	µM	**5798.93**	µM	**5718.99**	µM	**3508.60**	µM	**2497.49**	µM	**2012.96**	µM
n[SDS]eq	99.66	µmol	99.71	µmol	116.21	µmol	114.15	µmol	69.61	µmol	49.85	µmol	39.78	µmol
[SDS]ad/g	13.00	µmols/g	13.00	µmols/g	65.00	µmols/g	35.00	µmols/g	5.50	µmols/g	20.00	µmols/g	16.00	µmols/g
n[SDS]ad	260.34	µmol	260.29	µmol	1303.79	µmol	695.85	µmol	110.39	µmol	400.15	µmol	320.22	µmol
[SDS]	17982.02	µM	18000.00	µM	70858.28	µM	40581.16	µM	9072.58	µM	22545.09	µM	18218.62	µM
n[SDS]total	**360.00**	µmol	**360.00**	µmol	**1420.00**	µmol	**810.00**	µmol	**180.00**	µmol	**450.00**	µmol	**360.00**	µmol
Stk SDS	3.60	mL	3.60	mL	14.20	mL	8.10	mL	2.00	mL	5.00	mL	4.00	mL
[styrene]	8728.67	µM	0.00	µM	17439.92	µM	26264.72	µM	17615.72	µM	26264.72	µM	26530.56	µM
n[styrene]	**174.75**	µmol	**0.00**	µmol	**349.50**	µmol	**524.24**	µmol	**349.50**	µmol	**524.24**	µmol	**524.24**	µmol
wt styr	0.02	g	0.00	g	0.04	g	0.05	g	0.04	g	0.05	g	0.05	g
mL styr	0.02	mL	0.00	mL	0.04	mL	0.06	mL	0.04	mL	0.06	mL	0.06	mL
Initiator(AIBN/VA	**11.44**	µmol	**0.00**	µmol	**21.65**	µmol	**29.38**	µmol	**36.60**	µmol	**48.80**	µmol	**48.80**	µmol
	571.60	µM	0.00	µM	1080.32	µM	1472.03	µM	1844.72	µM	2444.84	µM	2469.59	µM
	0.0037	g	0.0000	g	0.0070	g	0.0095	g	0.3000	mL	0.4000	mL	0.4000	mL
Dilution	16.40	mL	16.40	mL	5.80	mL	11.80	mL	17.50	mL	14.50	mL	15.30	mL
surf,ad : styrene	**1.49**		**#DIV/0!**		**3.73**		**1.33**		**0.32**		**0.76**		**0.61**	
INI:Styr	**0.07**		**#DIV/0!**		**0.06**		**0.06**		**0.10**		**0.09**		**0.09**	

	Date: 031711(HHrt)	Date: 042111(MH)
	HH, Rt VA044	MH, ads adsol 3 hrs, AIBN stk in etOH ads3hrs, poly 3hrs

wt loss	19.22	19.25	19.21	19.04	18.43	17.90	18.15
%wt loss	4.03%	3.86%	4.23%	4.23%	8.18%	10.53%	9.31%

Experiment Data	Date: 051511(MM)						Date:051511(ML)				Date:051511(HM)				Date:051511(HL)	
	C		F		XF		F		XF		F		XF		XF	
Solution	19.96	mL	19.98	mL	19.98	mL	19.98	mL	19.98	mL	19.98	mL	20.16	mL	20.02	mL
Solid wt	20.01	g	20.01	g	20.01	g	20.00	g	20.02	g	20.02	g	20.01	g	20.00	g
[SDS]eq	**3053.11**	µM	**2941.74**	µM	**2894.81**	µM	**2950.45**	µM	**2885.45**	µM	**5582.13**	µM	**5443.68**	µM	**5490.66**	µM
n[SDS]eq	60.94	µmol	58.78	µmol	57.84	µmol	58.95	µmol	57.65	µmol	111.53	µmol	109.74	µmol	109.92	µmol
[SDS]ad/g	5.50	µmols/g	20.00	µmols/g	16.00	µmols/g	20.00	µmols/g	16.00	µmols/g	65.00	µmols/g	35.00	µmols/g	35.00	µmols/g
n[SDS]ad	110.06	µmol	400.22	µmol	320.16	µmol	400.05	µmol	320.35	µmol	1301.47	µmol	700.26	µmol	700.08	µmol
[SDS]	8567.13	µM	22972.97	µM	18918.92	µM	22972.97	µM	18918.92	µM	70720.72	µM	40178.57	µM	40459.54	µM
n[SDS]total	**171.00**	µmol	**459.00**	µmol	**378.00**	µmol	**459.00**	µmol	**378.00**	µmol	**1413.00**	µmol	**810.00**	µmol	**810.00**	µmol
Stk SDS	1.90	mL	5.10	mL	4.20	mL	5.10	mL	4.20	mL	15.70	mL	9.00	mL	9.00	mL
[styrene]	8754.91	µM	17492.29	µM	17492.29	µM	8746.14	µM	8746.14	µM	8746.14	µM	17336.11	µM	8728.67	µM
n[styrene]	**174.75**	µmol	**349.50**	µmol	**349.50**	µmol	**174.75**	µmol	**174.75**	µmol	**174.75**	µmol	**349.50**	µmol	**174.75**	µmol
wt styr	0.02	g	0.04	g	0.04	g	0.02	g	0.02	g	0.02	g	0.04	g	0.02	g
mL styr	0.02	mL	0.04	mL	0.04	mL	0.02	mL	0.02	mL	0.02	mL	0.04	mL	0.02	mL
Initiator(AIBN/VA	**17.08**	µmol	**29.28**	µmol	**29.28**	µmol	**19.52**	µmol	**19.52**	µmol	**19.52**	µmol	**39.04**	µmol	**12.20**	µmol
	855.69	µM	1465.44	µM	1465.44	µM	976.96	µM	976.96	µM	976.96	µM	1936.47	µM	609.38	µM
	0.1400	mL	0.2400	mL	0.2400	mL	0.1600	mL	0.1600	mL	0.1600	mL	0.3200	mL	0.1000	mL
Dilution	17.90	mL	14.60	mL	15.50	mL	14.70	mL	15.60	mL	4.10	mL	10.80	mL	10.90	mL
surf,ad : styrene	**0.63**		**1.15**		**0.92**		**2.29**		**1.83**		**7.45**		**2.00**		**4.01**	
INI:Styr	**0.10**		**0.08**		**0.08**		**0.11**		**0.11**		**0.11**		**0.11**		**0.07**	

	Date: 051511(MM)			Date:051511(ML)		Date:051511(HM)		Date:051511(HL)
	MM, ads adsol 3 hrs, AIBN stk in etOH ads3hrs, poly 3hrs			ML		HM		HL
wt loss	17.56	18.60	18.04	17.90	18.15	18.60	18.04	18.04
%wt loss	12.25%	7.05%	9.85%	10.51%	9.35%	7.10%	9.83%	9.81%

	MW			Stock		
SDS	288.38	g/mol		55480	µM	
				100000	µM	
				90000	µM	Date:041411
styrene	104.15	g/mol				
AIBN	164.2	g/mol		149766.5449	µM	
				121997.5639	µM	(0.5 g in 25mL)
VA044	323.33	g/mol		76057.48513	µM	

Appendix C

C1: SDS monolayer calculation

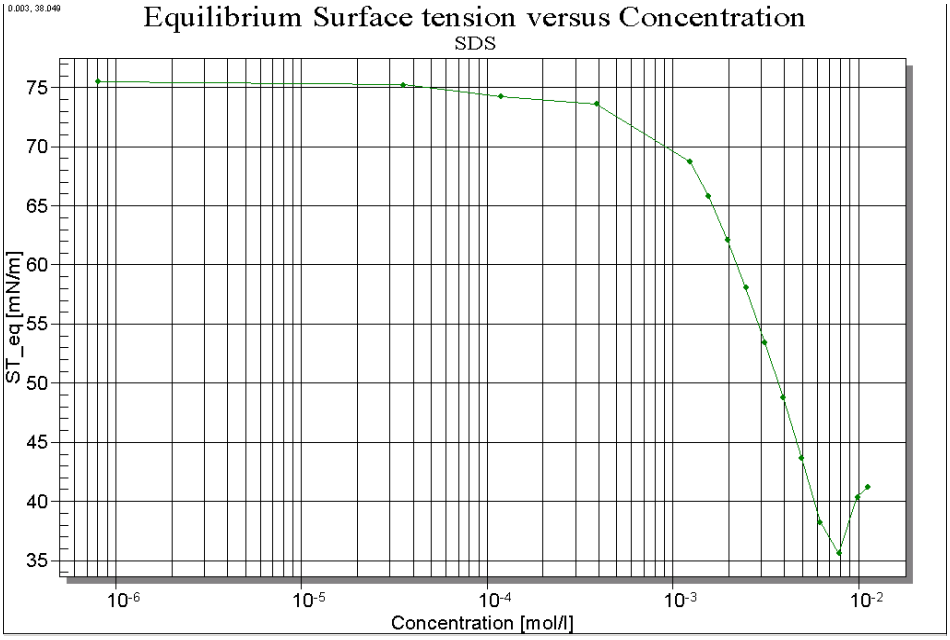

	satd F		Index	purified lab SDS	SigAl SDS	satd XF	satd F	satd C	SigAl SDS sept27
ST^o (mN/m)	77.71			75.53	77.16	77.56	77.71	77.76	76.86
Base line (mN/m)	32.38			36.93	32.98	35.39	32.38	33.26	33.8
Slope(mN/m/decade)	-52.45			-51.02	-37.24	-44.15	-52.45	-51.78	-41.02
CMC (mol/L)	0.004062			6.69E-03	5.35E-03	0.003577	0.004062	0.004165	0.005203
						with swamping			
Gibbs eq (1:1) ionic surfactant	$\Gamma = -1/(4.606RT) *(\delta\gamma/\delta\log C_1)$					$\Gamma = -1/(2.303RT) *(\delta\gamma/\delta\log C_1)$			
	$a^s_1 = 10^{23}/N\Gamma_1$					$a^s_1 = 10^{23}/N\Gamma_1$			
Γ =	0.0046	mol/1000m^2				0.0092	mol/1000m^2		
a^s_1 =	36.11	Å^2 /molecule				18.05	Å^2 /molecule		

	Xtra Fine	Fine	Medium	Coarse		Xtra Fine	Fine	Medium	Coarse
m2/g (BET)	1.126	0.593	0.44	0.256		1.126	0.593	0.44	0.256
µmol/g (monolayer)	5.177768887	2.726836	2.023284	1.177184		10.35554	5.453671	4.046569	2.354367
bilayer	10.35553777	5.453671	4.046569	2.354367		20.71108	10.90734	8.093138	4.708735
sat'd SDS m2/g (BET)	1.047	0.547		0.256		1.047	0.547		0.256
µmol/g (monolayer)	4.814497358	2.51531	0	1.177184		9.628995	5.030621	0	2.354367
bilayer	9.628994716	5.030621	0	2.354367		19.25799	10.06124	0	4.708735
m2/g (Malvern)	1.74	1	0.48	0.22		1.74	1	0.48	0.22
µmol/g (monolayer)	8.001170394	4.598374	2.207219	1.011642		16.00234	9.196748	4.414439	2.023284
bilayer	16.00234079	9.196748	4.414439	2.023284		32.00468	18.3935	8.828878	4.046569
% PSD diff	54.53%	68.63%	9.09%	-14.06%					
(Adsorption isotherm)									
SDS sat'd adsorption, µmol/g	35	65		13		35	65		13
%diff (N2 BET analysis)	70.41%	91.61%		81.89%		40.83%	83.22%		63.78%
%diff (Laser diffraction)	54.28%	85.85%		84.44%		8.56%	71.70%		68.87%
%diff (SDS sat'd)	72.49%	92.26%		81.89%		44.98%	84.52%		63.78%
x(N2 BET analysis)	3.379834129	11.91858		5.521653		1.689917	5.959288		2.760827
x (Laser diffraction)	2.187180017	7.067716		6.425196		1.09359	3.533858		3.212598
x (SDS sat'd)	3.634855043	12.92087		5.521653		1.817428	6.460435		2.760827

C2: BET particle size analysis of coarse $CaCO_3$

Quantachrome NovaWin2 - Data Acquisition and Reduction
for NOVA instruments
©1994-2007, Quantachrome Instruments
version 9.0

Quantachrome INSTRUMENTS
Optimizing particle performance

Analysis				Report			
Operator:	OJO	Date:	2011/07/21	Operator:		Date:	7/22/2011
Sample ID:	07_21_11	Filename:		C:\QCdata\Physisorb\CaCO3 (Coarse) 7_21_11.qps			
Sample Desc:	Surface Area/Pore volume	Comment:		Degassed @ 300 deg C for 3 hrs			
Sample weight:	7.9694 g	Sample Volume:		3.16734 cc			
Outgas Time:	3.0 hrs	OutgasTemp:		300.0 C			
Analysis gas:	Nitrogen	Bath Temp:		77.3 K			
Press. Tolerance:	0.100/0.100 (ads/des)	Equil time:		240/240 sec (ads/des)	Equil timeout:		480/480 sec (ads/des)
Analysis Time:	178.3 min	End of run:		2011/07/21 0:00:00	Instrument:		Nova Station A
Cell ID:	5						

Multi-Point BET

Data Reduction Parameters Data

Adsorbate	Nitrogen	Temperature	77.350K		
	Molec. Wt.: 28.013 g	Cross Section:	16.200 A²	Liquid Density:	0.808 g/cc

Multi-Point BET Data

Relative Pressure [P/Po]	Volume @ STP [cc/g]	1 / [W((Po/P) - 1)]	Relative Pressure [P/Po]	Volume @ STP [cc/g]	1 / [W((Po/P) - 1)]
4.77924e-02	0.0595	6.7515e+02	2.40684e-01	0.0870	2.9164e+03
9.66224e-02	0.0670	1.2780e+03	2.88032e-01	0.0935	3.4631e+03
1.44838e-01	0.0737	1.8398e+03	3.35634e-01	0.1002	4.0355e+03
1.92864e-01	0.0800	2.3898e+03			

BET summary

Slope =	11569.519
Intercept =	1.457e+02
Correlation coefficient, r =	0.999900
C constant=	80.415
Surface Area =	0.297 m²/g

C3: BET particle size analysis of fine $CaCO_3$

Quantachrome NovaWin2 - Data Acquisition and Reduction
for NOVA instruments
©1994-2007, Quantachrome Instruments
version 9.0

Quantachrome INSTRUMENTS
Optimizing particle performance

Analysis				Report			
Operator:	OJO	Date:	2011/07/27	Operator:		Date:	7/27/2011
Sample ID:	07_27_11	Filename:		C:\QCdata\Physisorb\CaCO3_Fine_7_27_11.qps			
Sample Desc:	Surface Area/Pore volume	Comment:		Degassed @ 300 deg C for 3 hrs			
Sample weight:	4.927 g	Sample Volume:		1.95036 cc			
Outgas Time:	3.0 hrs	OutgasTemp:		300.0 C			
Analysis gas:	Nitrogen	Bath Temp:		77.3 K			
Press. Tolerance:	0.100/0.100 (ads/des)	Equil time:		240/240 sec (ads/des)	Equil timeout:		480/480 sec (ads/des)
Analysis Time:	176.9 min	End of run:		2011/07/27 0:00:00	Instrument:		Nova Station A
Cell ID:	5						

Multi-Point BET

Data Reduction Parameters Data

Adsorbate	Nitrogen	Temperature	77.350K		
	Molec. Wt.: 28.013 g	Cross Section:	16.200 A²	Liquid Density:	0.808 g/cc

Multi-Point BET Data

Relative Pressure [P/Po]	Volume @ STP [cc/g]	1 / [W((Po/P) - 1)]	Relative Pressure [P/Po]	Volume @ STP [cc/g]	1 / [W((Po/P) - 1)]
4.69666e-02	0.1425	2.7661e+02	2.40310e-01	0.1844	1.3729e+03
9.60930e-02	0.1534	5.5441e+02	2.87735e-01	0.1959	1.6498e+03
1.44683e-01	0.1633	8.2870e+02	3.34984e-01	0.2092	1.9268e+03
1.92793e-01	0.1735	1.1012e+03			

BET summary

Slope =	5722.537
Intercept =	3.120e+00
Correlation coefficient, r =	0.999969
C constant=	1835.270
Surface Area =	0.608 m²/g

C4: BET particle size analysis of extra fine $CaCO_3$

Quantachrome NovaWin2 - Data Acquisition and Reduction
for NOVA instruments
©1994-2007, Quantachrome Instruments
version 9.0

Quantachrome INSTRUMENTS
Optimizing particle performance

Analysis				Report			
Operator:	OJO	**Date:**	2011/07/28	**Operator:**		**Date:**	7/29/2011
Sample ID:	07_28_11	**Filename:**		C:\QCdata\Physisorb\CaCO3_XFine_7_28_11.qps			
Sample Desc:	Surface Area/Pore volume	**Comment:**		Degassed @ 300 deg C for 3 hrs			
Sample weight:	3.8792 g	**Sample Volume:**		1.55235 cc			
Outgas Time:	3.0 hrs	**OutgasTemp:**		300.0 C			
Analysis gas:	Nitrogen	**Bath Temp:**		77.3 K			
Press. Tolerance:	0.100/0.100 (ads/des)	**Equil time:**		240/240 sec (ads/des)	**Equil timeout:**		480/480 sec (ads/des)
Analysis Time:	166.2 min	**End of run:**		2011/07/28 0:00:00	**Instrument:**		Nova Station A
Cell ID:	5						

Multi-Point BET

Data Reduction Parameters Data

Adsorbate	**Nitrogen**	**Temperature**	77.350K		
	Molec. Wt.: 28.013 g	**Cross Section:**	16.200 A²	**Liquid Density:**	0.808 g/cc

Multi-Point BET Data

Relative Pressure [P/Po]	Volume @ STP [cc/g]	1 / [W((Po/P) - 1)]	Relative Pressure [P/Po]	Volume @ STP [cc/g]	1 / [W((Po/P) - 1)]
4.82512e-02	0.2501	1.6219e+02	2.39202e-01	0.3295	7.6351e+02
9.61000e-02	0.2733	3.1130e+02	2.86691e-01	0.3507	9.1685e+02
1.44217e-01	0.2897	4.6535e+02	3.33968e-01	0.3731	1.0752e+03
1.92137e-01	0.3069	6.1996e+02			

BET summary

Slope =	3186.213
Intercept =	6.149e+00
Correlation coefficient, r =	0.999950
C constant=	519.202
Surface Area =	1.091 m²/g

manufactured silica fume has max. surface area of around 380 m²/g

C5: Laser diffraction (Malvern zetasizer) particle size analysis of coarse $CaCO_3$

BCI
No.27, Jalan P/21, Selaman Industrial Park, Sec 10, 43650 Bandar Baru Bangi . Selangor Darul Ehsan
Tel : 603-8922 1822 Fax : 603-8922 3088
Email : sales@bcichemical.com.my

Result: Sieve ASTM E11:61 Report

CaCO3 Coarse

Sample Name: AdiCARB 150 (C)
C124 (HKK) - 230310 [SAM]

SOP Name:

Measured: Saturday, April 03, 2010 11:14:15 AM

Measured by: Administrator

Analysed: Saturday, April 03, 2010 11:14:16 AM

Sample bulk lot ref:

Result Source: Averaged

Particle Name: CaCO3 (calcite)	**Accessory Name:** Hydro 2000MU (A)	**Analysis model:** General purpose	**Sensitivity:** Normal
Particle RI: 1.572	**Absorption:** 0.1	**Size range:** 0.020 to 2000.000 um	**Obscuration:** 15.29 %
Dispersant Name: Water	**Dispersant RI:** 1.330	**Weighted Residual:** 1.870 %	**Result Emulation:** Off
Concentration: 0.0661 %Vol	**Span :** 2.460	**Uniformity:** 0.743	**Result units:** Volume
Specific Surface Area: 0.218 m²/g	**Surface Weighted Mean D[3,2]:** 27.580 um	**Vol. Weighted Mean D[4,3]:** 133.726 um	**Density:** 1.000 g/cm³

d(0.1): 26.279 um d (0.5) : 105.002 um d(0.9): 284.635 um

Mesh No	Aperture µm	Volume In %	Vol Below %
10	2000	0.00	100.00
12	1700	0.00	100.00
14	1400	0.00	100.00
16	1180	0.00	100.00
18	1000	0.00	100.00
20	850	0.00	100.00
25	710	0.00	100.00
30	600	0.00	100.00
35	500	0.68	99.32

Mesh No	Aperture µm	Volume In %	Vol Below %
35	500	1.62	99.32
40	425	2.82	97.70
45	355	3.58	94.89
50	300	4.93	91.31
60	250	5.41	86.38
70	212	6.24	80.97
80	180	7.83	74.74
100	150	8.51	66.91
120	125		58.40

Mesh No	Aperture µm	Volume In %	Vol Below %
120	125	7.95	58.40
140	106	7.75	50.46
170	90	8.04	42.70
200	75	6.74	34.66
230	63	5.56	27.92
270	53	4.21	22.35
325	45	3.37	18.14
400	38		14.77

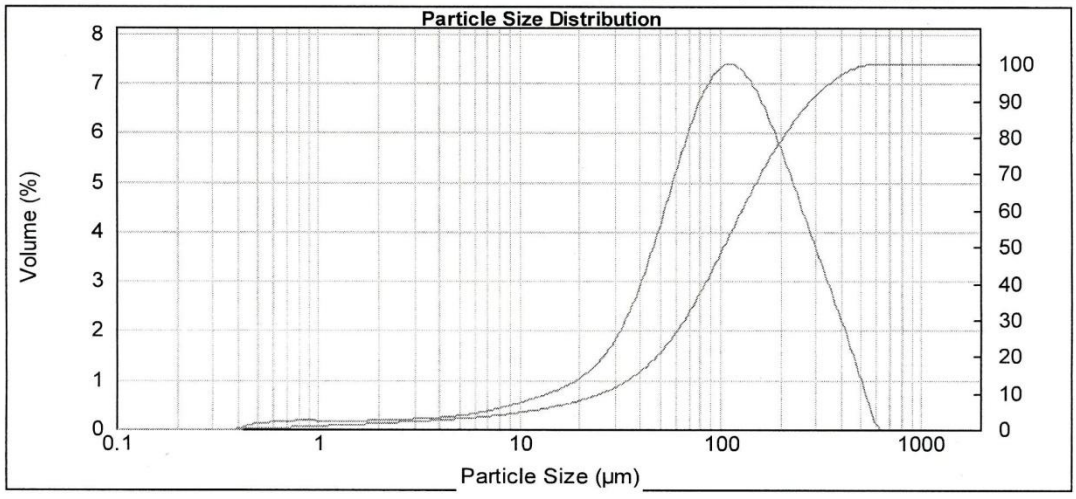

Operator notes: *Add 5 drops of 15% Sodium Hexametaphosphate solution.*

Malvern Instruments Ltd. Mastersizer 2000 Ver. 5.40 File name: 20100403 Calcium Carbonat

C6: Laser diffraction (Malvern zetasizer) particle size analysis of fine $CaCO_3$

No.27, Jalan P/21, Selaman Industrial Park, Sec 10, 43650 Bandar Baru Bangi . Selangor Darul Ehsan
Tel : 603-8922 1822 Fax : 603-8922 3088
Email : sales@bcichemical.com.my

Result: Sieve ASTM E11:61 Report

$CaCO_3$ Fine

Sample Name: AdiCARB 25 (F) C133 (KPM) - 230310 [SAM]

SOP Name:

Measured: Saturday, April 03, 2010 10:28:48 AM

Measured by: Administrator

Analysed: Saturday, April 03, 2010 10:28:49 AM

Sample bulk lot ref:

Result Source: Averaged

Particle Name: CaCO3 (calcite)	**Accessory Name:** Hydro 2000MU (A)	**Analysis model:** General purpose	**Sensitivity:** Normal
Particle RI: 1.572	**Absorption:** 0.1	**Size range:** 0.020 to 2000.000 um	**Obscuration:** 17.30 %
Dispersant Name: Water	**Dispersant RI:** 1.330	**Weighted Residual:** 1.988 %	**Result Emulation:** Off
Concentration: 0.0168 %Vol	**Span :** 2.442	**Uniformity:** 0.761	**Result units:** Volume
Specific Surface Area: 0.997 m²/g	**Surface Weighted Mean D[3,2]:** 6.019 um	**Vol. Weighted Mean D[4,3]:** 30.592 um	**Density:** 1.000 g/cm³

d(0.1): 2.305 um **d (0.5) :** 26.181 um **d(0.9):** 66.246 um

Mesh No	Aperture µm	Volume In %	Vol Below %
10	2000	0.00	100.00
12	1700	0.00	100.00
14	1400	0.00	100.00
16	1180	0.00	100.00
18	1000	0.00	100.00
20	850	0.00	100.00
25	710	0.00	100.00
30	600	0.00	100.00
35	500		100.00

Mesh No	Aperture µm	Volume In %	Vol Below %
35	500	0.00	100.00
40	425	0.00	100.00
45	355	0.00	100.00
50	300	0.00	100.00
60	250	0.00	100.00
70	212	0.00	100.00
80	180	0.00	100.00
100	150	0.00	100.00
120	125		100.00

Mesh No	Aperture µm	Volume In %	Vol Below %
120	125	0.32	100.00
140	106	2.07	99.68
170	90	3.90	97.61
200	75	5.44	93.71
230	63	6.80	88.27
270	53	7.33	81.47
325	45	7.94	74.14
400	38		66.20

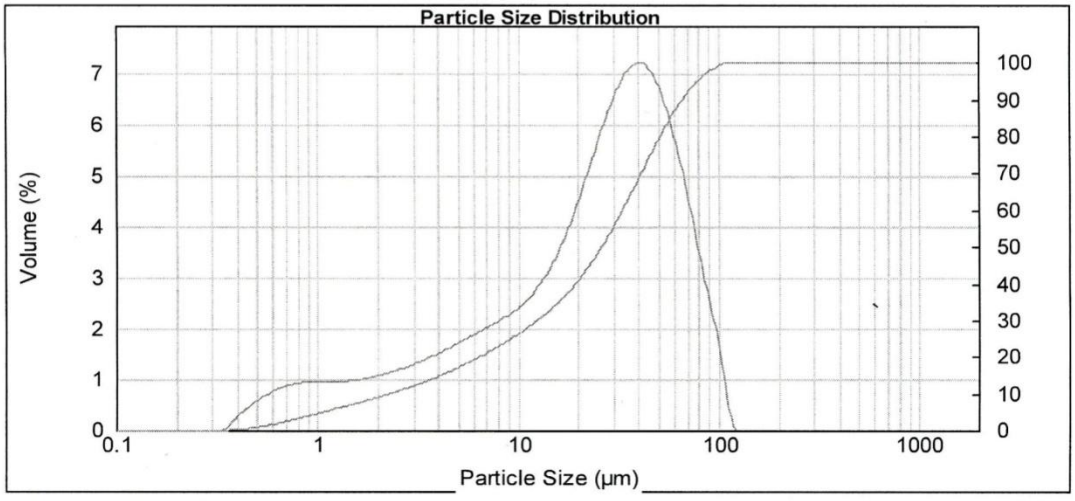

Operator notes: *Add 5 drops of 15% Sodium Hexametaphosphate solution.*

Malvern Instruments Ltd Mastersizer 2000 Ver. 5.40 File name: 20100403 Calcium Carbonate

C7: Laser diffraction (Malvern zetasizer) particle size analysis of extra fine$CaCO_3$

BCI
No.27, Jalan P/21, Selaman Industrial Park, Sec 10, 43650 Bandar Baru Bangi . Selangor Darul Ehsan
Tel : 603-8922 1822 Fax : 603-8922 3088
Email : sales@bcichemical.com.my

Result: Sieve ASTM E11:61 Report

$CaCO_3$ Extra Fine

Sample Name: AdiCARB 5 (XF) C232 (OM) - 230310 [SAM]
SOP Name:
Measured: Saturday, April 03, 2010 10:17:11 AM
Measured by: Administrator
Analysed: Saturday, April 03, 2010 10:17:13 AM
Sample bulk lot ref:
Result Source: Averaged

Particle Name: CaCO3 (calcite)	**Accessory Name:** Hydro 2000MU (A)	**Analysis model:** General purpose	**Sensitivity:** Normal
Particle RI: 1.572	**Absorption:** 0.1	**Size range:** 0.020 to 2000.000 um	**Obscuration:** 17.96 %
Dispersant Name: Water	**Dispersant RI:** 1.330	**Weighted Residual:** 1.887 %	**Result Emulation:** Off
Concentration: 0.0098 %Vol	**Span :** 1.976	**Uniformity:** 0.605	**Result units:** Volume
Specific Surface Area: 1.74 m²/g	**Surface Weighted Mean D[3,2]:** 3.450 um	**Vol. Weighted Mean D[4,3]:** 8.953 um	**Density:** 1.000 g/cm³

d(0.1): 1.220 um d (0.5) : 8.274 um d(0.9): 17.569 um

Mesh No	Aperture µm	Volume In %	Vol Below %
10	2000	0.00	100.00
12	1700	0.00	100.00
14	1400	0.00	100.00
16	1180	0.00	100.00
18	1000	0.00	100.00
20	850	0.00	100.00
25	710	0.00	100.00
30	600	0.00	100.00
35	500	0.00	100.00

Mesh No	Aperture µm	Volume In %	Vol Below %
35	500	0.00	100.00
40	425	0.00	100.00
45	355	0.00	100.00
50	300	0.00	100.00
60	250	0.00	100.00
70	212	0.00	100.00
80	180	0.00	100.00
100	150	0.00	100.00
120	125	0.00	100.00

Mesh No	Aperture µm	Volume In %	Vol Below %
120	125	0.00	100.00
140	106	0.00	100.00
170	90	0.00	100.00
200	75	0.00	100.00
230	63	0.00	100.00
270	53	0.00	100.00
325	45	0.00	100.00
400	38		100.00

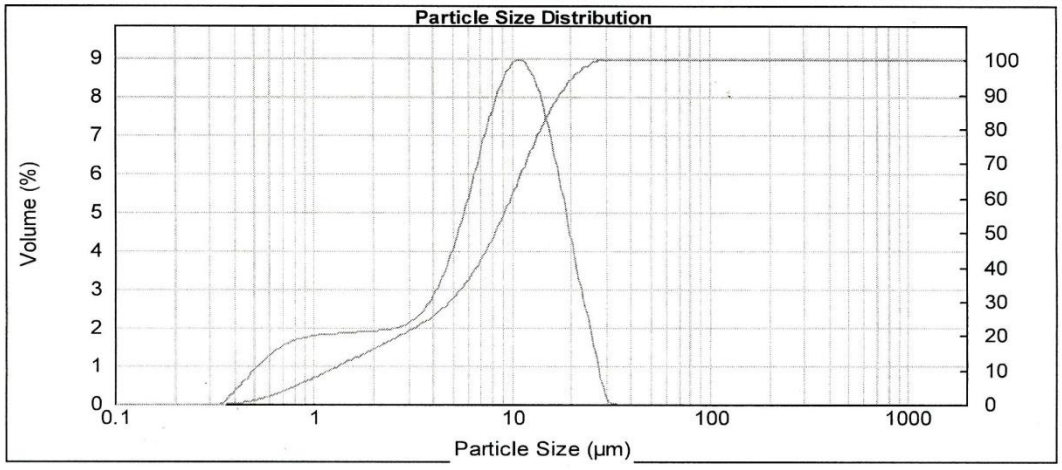

Operator notes: *Add 5 drops of 15% Sodium Hexametaphosphate solution.*

Malvern Instruments Ltd. Mastersizer 2000 Ver. 5.40 File name: 20100403 Calcium Carbonate.me

VITA

I, Poh Lee Cheah finished with a bachelor degree in Analytical Chemistry from University of Science Malaysia in 2008. I started my career as a research officer at BCI Chemical Sdn. Bhd. I was in the R&D team specializing in formulating laundry detergents and testing of specialty chemicals used in oil and gas industry.

In early 2009, I was introduced to my current advisor, Dr. John O'Haver through my superior Dr. Chun Hwa See at BCI. We found a high possibility to collaborate with each other and also an opportunity for me to further enhanced my academic and research development. I enrolled into graduate program at Chemical Engineering at University of Mississippi in Fall 2009. In the first 2 years of program has provided me the fundamental understanding in Chemical Engineering. After 3 years of the program, I am writing this thesis write-up to conclude my research work for my master's degree.

I am looking to continue my doctorate degree in exploring area of surfactant science and related work. I am hoping to build both my academic and research path in the future.